INFORMATION TO USERS

This manuscript has been reproduced from the microfilm master. UMI films the text directly from the original or copy submitted. Thus, some thesis and dissertation copies are in typewriter face, while others may be from any type of computer printer.

The quality of this reproduction is dependent upon the quality of the copy submitted. Broken or indistinct print, colored or poor quality illustrations and photographs, print bleedthrough, substandard margins, and improper alignment can adversely affect reproduction.

In the unlikely event that the author did not send UMI a complete manuscript and there are missing pages, these will be noted. Also, if unauthorized copyright material had to be removed, a note will indicate the deletion.

Oversize materials (e.g., maps, drawings, charts) are reproduced by sectioning the original, beginning at the upper left-hand corner and continuing from left to right in equal sections with small overlaps.

Photographs included in the original manuscript have been reproduced xerographically in this copy. Higher quality 6" x 9" black and white photographic prints are available for any photographs or illustrations appearing in this copy for an additional charge. Contact UMI directly to order.

UMI®

University of Alberta

Thymocyte Motility is Mediated by β_1 Integrins and RHAMM

by

Sheryl Lynn Gares　©

A thesis submitted to the Faculty of Graduate Studies and Research in partial fulfillment

of the requirements for the Degree of Doctor of Philosophy

in

Medical Sciences - Oncology

University of Alberta, Edmonton, AB

Fall 2000

The author has granted a non-exclusive licence allowing the National Library of Canada to reproduce, loan, distribute or sell copies of this thesis in microform, paper or electronic formats.

The author retains ownership of the copyright in this thesis. Neither the thesis nor substantial extracts from it may be printed or otherwise reproduced without the author's permission.

L'auteur a accordé une licence non exclusive permettant à la Bibliothèque nationale du Canada de reproduire, prêter, distribuer ou vendre des copies de cette thèse sous la forme de microfiche/film, de reproduction sur papier ou sur format électronique.

L'auteur conserve la propriété du droit d'auteur qui protège cette thèse. Ni la thèse ni des extraits substantiels de celle-ci ne doivent être imprimés ou autrement reproduits sans son autorisation.

0-612-59590-0

Canada

University of Alberta
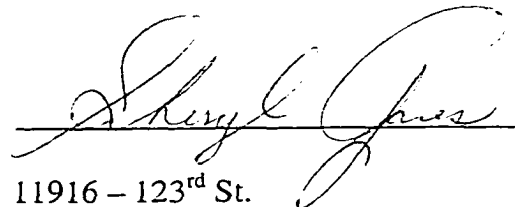
Library Release Form

Name of Author: Sheryl L. Gares

Title of Thesis: Thymoycte Motility is Mediated by β_1 Integrins and RHAMM

Degree: Doctor of Philosophy

Year this Degree Granted: 2000

Permission is hereby granted to the University of Alberta Library to reproduce single copies of this thesis and to lend or sell such copies for private, scholarly, or scientific research purposes only.

The author reserves all other publication and other rights in association with the copyright in the thesis, and except as hereinbefore provided, neither the thesis nor any substantial portion thereof may be printed or otherwise reproduced in any material form whatever without the author's prior written permission.
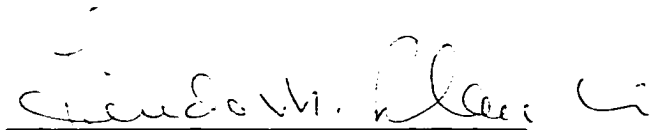
11916 – 123rd St.
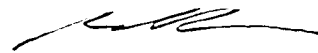
Edmonton, AB T4L 0G8

Oct 3, 2000

University of Alberta

Faculty of Graduate Studies and Research
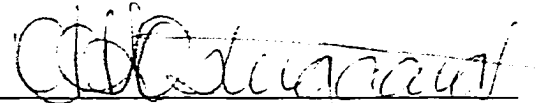
The undersigned certify that they have read, and recommend to the Faculty of Graduate studies and Research for acceptance, a thesis entitled *Thymocyte Motility is Mediated by β_1 Integrins and RHAMM* submitted by Sheryl Lynn Gares in partial fulfillment of the requirements for the degree of Doctor of Philosophy in Medical Sciences - Oncology

Dr. Linda M. Pilarski
Supervisor

Dr. Andrew R. Shaw
Supervisory committee member

Dr. Hanne Ostergaard
Supervisory committee member

Dr. Michael Hendzel
Internal examiner

Dr. Paul Kubes
External examiner

Dr Roseline Godbout
Examining committee chair

Sept 27, 2000

ABSTRACT

As human thymocytes differentiate they either remain anchored to thymic stromal cells and extracellular matrix (ECM) components or, while at other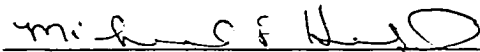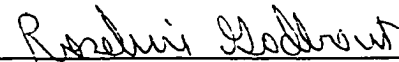 stages of differentiation, thymocytes are migratory. Thus, both adhesion and motility receptors are required by thymocytes. To examine the function of the fibronectin (Fn)-binding integrins $\alpha_4\beta_1$ and $\alpha_5\beta_1$ on *ex vivo* thymocytes, timelapse microscopy was used to record cell behavior and both adhesion to and motility on Fn assessed. $\alpha_4\beta_1$ integrins mediated adhesion to Fn for non-migratory thymocytes while interactions of both $\alpha_4\beta_1$ and $\alpha_5\beta_1$ integrins with Fn were required by motile cells along with the receptor for hyaluronan (HA) mediated motility (RHAMM). This suggested Fn-binding β_1 integrins might interact with Fn at low avidity to provide traction for migratory thymocytes. Consistent with this hypothesis, thymocytes stimulated with a β_1 integrin activating mAb were significantly more adhesive to Fn and motility was concomitantly decreased. This suggested low avidity binding of β_1 integrins promoted locomotion for thymocytes.

To investigate how HA interactions with RHAMM promoted motility, the expression of RHAMM was examined. Most human thymocytes expressed intracellular RHAMM and a smaller proportion expressed cell surface RHAMM. HA redistributed intracellular RHAMM to the cell surface and the redistributed RHAMM mediated motility. The two distribution patterns suggested thymocytes expressed two RHAMM isoforms. Consistent with this hypothesis, thymocytes expressed full length isoforms of RHAMM (RHAMM^{FL}), a splice variant of RHAMM (RHAMM^{-48}), but did not express a third RHAMM splice variant (RHAMM^{-147}). To determine if RHAMM splice variants had different cellular distribution patterns than RHAMM^{FL}, COS cells were transfected

with plasmids expressing green fluorescent protein (GFP) fused to RHAMM. GFP-RHAMM[FL] and GFP-RHAMM[-147] were intracellular proteins that co-localized with the microtubule cytoskeleton. GFP-RHAMM[-48] was distributed intracellularly throughout the cytoplasm or in association with cell membranes. Thus, all three RHAMM isoforms were expressed intracellularly by an adherent cell line, whereas thymocytes, which are migratory cells, expressed cell surface RHAMM and intracellular RHAMM. These experiments indicated only migratory cells expressed cell surface RHAMM and redistribution of intracellular RHAMM might be required for surface expression. This implicates redistribution of intracellular RHAMM as a mechanism to stimulate motility.

DEDICATION

This thesis is dedicated to Bradley Petford who imparted in me self-realization, happiness

and strength

ACKNOWLEDGEMENTS

This degree was initiated during a productive and happy period of my life and continued, with difficulty, through a most tragic and painful period experience. That I found the strength to see this project through to completion is wholly due to the powerful impact one individual has had on my life. Therefore, my first acknowledgement is to Bradley Petford, who will always be with me.

I extend sincere thanks to my supervisor, Dr Linda Pilarski, who very graciously accepted me into her laboratory and allowed me the latitude to find my way. Linda has been a most imaginative and enthusiastic supervisor and her support created a research environment that was stimulating even through the darkest days of trying to understand RHAMM. I've had a true learning experience on many levels. I also wish to extend thanks to the members of my supervisory committee, Dr Andew Shaw and Dr Hanne Ostergaard for their insights into the mysterious workings of RHAMM.

Juanita Wisniak has been an invaluable colleague and friend during this project. I acknowledge her professionalism, talent and hard work that were invaluable to complete some of the difficult experiments reported in this thesis. I also thank Juanita for her friendship and encouragement. Her presence has made the years spent on my thesis a real pleasure. I thank the students and technicians of the Pilarski laboratory. These individuals contributed to the completion of this project with their friendship and support.

Lastly, but most importantly, I thank Dennis Weetman, Phoenix and Dr Anne Allen whose personal support and generosity of spirit saw me through this period. I don't think I could have seen the project through without these three beings and their absolute belief in me.

TABLE OF CONTENTS

LIST OF FIGURES

LIST OF ABBREVIATIONS

aa .... amino acid

BSA .... bovine serum albumen

DP .... double positive

ECM .... extracellular matrix

ERK .... ezrin-radixin-moesin

FAs .... focal adhesions

FBS .... fetal bovine serum

FITC .... fluorescein isothiocyanate

*f*MLP .... formylated-methionine-leucine-phenylalanine

Fn .... fibronectin

GEF .... guanine nucleotide exchange factor

GFP .... green fluorescent protein

gpi .... glycosylphosphatidylinositol

GST .... glutathione-S-transferase

GTPase .... guanosine triphosphatase

HA .... hyaluronan

HRP .... horseradish peroxidase

IF .... immunofluorescence

LSM .... laser scanning microscope

MAb .... monoclonal antibody

MHC .... major histocompatibility complex

MLC .... myosin light chain

MMTV	murine mammary tumor virus
MN	multinegative
MTs	microtubules
MTOC	microtubule organizing center
Pak1	p21-activated kinase 1
PBS	phosphate buffered saline
PE	phycoerythrin
PKC	protein kinase C
PLC	phospholipase C
PLL	poly-L-lysine
PMN	polymorphonuclear cell
PTK	protein tyrosine kinase
RHAMM	receptor for hyaluronan mediated motility
ROCK	Rho-associated coiled-coil forming kinase
RT-PCR	reverse transcriptase polymerase chain reaction
SCID	severe combined immunodeficiency
SDF-1	stem cell-derived factor-1
SP	single positive
TCR	T cell receptor
TEC	thymic epithelial cell
TNC	thymic nurse cell

1 INTRODUCTION

1.1 How Cells Locomote

To function as mediators of immune responses leukocytes must have the ability to become locomotory when alerted to sites of infection or trauma within an organism. Numerous types of receptors, including adhesion, cytokine and chemokine receptors enable leukocytes to adapt to changes in the microenvironment by transducing signals following ligand binding (Damsky & Werb, 1992; Lafrenie & Yamada, 1996; Sánchez-Madrid & del Pozo, 1999). Signal transduction activates the intracellular and extracellular components required to mediate migratory behavior. Examination of these processes has revealed that locomotory behavior requires the activation and coordination of a large and complex array of components.

1.1.1   Assessment of cell locomotion

Comparison of many highly divergent cell types indicates many of the basic mechanisms used to mediate locomotion are similar among cells (Stossel, 1993; Lauffenburger & Horwitz, 1996; Mitchison & Cramer, 1996). First a cell must become polarized and this generally occurs in response to an external stimulus. Morphologically polarization is apparent when the cell extends protrusions that create a 'leading edge'. Second, the leading edge forms attachments to the substrate providing the cell with traction. Finally, the cell pulls itself forward requiring contraction and de-adhesion of the trailing edge of the cell. Repetition of this simple series of steps enables a cell to crawl forward. However, the cellular components involved in this process are numerous and their activity must be coordinately controlled to enable directional motility (Nabi, 1999; Sánchez-Madrid & del Pozo, 1999; Small et al., 1999a; 1999b; Waterman-Storer &

Salmon, 1999; Chen et al., 2000). Compared with adhesive cells like fibroblasts, leukocytes are migratory cells and might coordinate cell processes differently to accommodate rapid locomotion.

Leukocytes assume locomotory behavior to extravasate between cells lining blood vessels and to migrate through extracellular matrix (ECM) to reach sites of inflammation (Springer, 1994). Lymphocytes and thymocytes also migrate through lymphoid organs during their development. To understand how these processes are initiated and regulated, *in vitro* and *in vivo* assays have been developed to analyze cell migration. Migratory leukocytes have a particularly distinct appearance, so morphological analysis has been used as an indirect measure of motile behavior (del Pozo et al., 1995; Harris & Miyaska, 1995; Cox et al., 1997). However, cell motility is more often measured directly rather than relying only on morphological observations. Random motility, directional locomotion and/or velocity refer to different aspects of cell locomotion that can be quantitated (Wilkinson, 1998). Random motility generally refers to spontaneous or stimulated locomotion in the absence of a chemotactic gradient. Directional locomotion refers to uniform directional movement usually toward a chemotactic factor and velocity or chemokinesis is a measure of distance traveled in a defined time period.

Leukocytes normally traffic through the body in the circulatory system. To migrate into tissue or lymphoid organs, they must first attach to endothelial cells lining blood vessels then extravasate between the adjacent cells to gain access to the underlying basement membrane and ECM (Springer, 1994). To study the receptor interactions and chemokines that stimulate this process, chemotaxis and transmigration assays have been developed. Chemotaxis and transmigration assays generally use Boyden-like chambers in

which leukocytes are placed into an upper chamber containing a porous filter that is coated with ECM components or a layer of endothelial cells. A lower chamber contains the chemotactic stimulus. Cells migrating through the filters into the lower chamber are considered chemotactic and are quantitated by direct microscopic counting or by labeling cells then using radiometric or spectrophotometric methods as an indirect measure of cell number (Azzarà, 1997). This type of *in vitro* model is commonly used to assess the potential contribution of adhesion or chemokine receptors expressed by neutrophils and monocytes that stimulate or mediate extravasation or migration through interstitial spaces (Campbell et al., 1996; Weber et al., 1996). This method can accommodate large sample numbers and is amenable to experimental manipulation such as treating cells with antibodies or pharmacologic agents. However, cross-sectional analyses of relatively thick cellulose ester filters frequently indicate a portion of migratory cells don't migrate through the entire depth of the filter, so the number of chemotactic cells is underestimated (Azzarà, 1997). It is also impossible to determine if inhibitors or antibodies block adhesion to the substrate or migration through the filter, since the outcome will be the same in either case.

Another drawback of modified Boyden chambers is that *ex vivo* lymphocytes are weakly adherent to thin polycarbonate filters and migrate poorly through the small pores of the filters (Ratner, 1992). Three-dimensional type I collagen gels or gels combined with other ECM components support lymphocyte migration more effectively and have been used to study lymphocyte motility (Southern et al., 1995; Friedl et al., 1995; Ratner et al., 1997). Migration into three-dimensional collagen gels is quantitated by microscopic examination. The distance of the 'migration front' or the number of cells

migrating a particular distance is determined. A criticism of this approach is the lack of homogeneity of cells at the migration front (Azzarà, 1997). For example, the leading front is set to the point at which an arbitrarily determined number of cells have migrated in response to a stimulus. The distance traveled by this fraction of cells is measured and presented as an indication of the behavior of cells in the entire population. The relevance of the criticism is emphasized when assessing the effects of pharmacologic agents on leukocytes. A patient with a syndrome that attenuates normal polymorphonuclear (PMN) chemotaxis was treated with lithium carbonate (Azzarà, 1997). Using the leading front method to assess chemotaxis indicates this therapy increases PMN chemotaxis to normal levels. However, assessment of multiple planes of the filter actually indicates the majority of cells are still poorly chemotactic.

Video timelapse microscopy is commonly used to assess random motility and chemotaxis. This approach provides a direct method to assess migratory responses of leukocytes because cells can be tracked over time by viewing the recorded images. Since cells are directly observed, random motility, persistence and velocity can be quantitated using this method. Surfaces are coated with different ECM components or endothelial cells to determine if cells bind to and migrate on these substrates. To study chemotactic responses, a stimulus is added directly to the chamber with a micropipette and migration toward the point of addition assessed by viewing the recorded images (Zigmond et al., 1981; Servant et al., 2000). Alternatively, Dunn chemotaxis chambers (or variations of this design) can be used. These chambers are designed to accommodate the addition of chemotactic factors through a filling slit which simplifies addition of the stimulus and orientation of the field (Allen et al., 1998; Entschladen et al., 2000). Leukocytes

migrating toward quadrants encompassing the filling slit are considered chemotactic. To reduce the qualitative aspect of discerning chemotaxis from random migration, calculation of the angle of the migration path using a virtual axis can be done to yield a numeric value (Allen et al., 1998). Based on a mathematical model, directionality can then be statistically determined.

Other experimental designs include pre-treating cells with pharmacologic reagents or antibodies and assessing the ability of these reagents to change cell behavior. Increases or decreases in motility or chemotaxis implicate the receptor or molecular component in the motile process. The contribution of intracellular components to polarization and motility of living cells has also been examined using video timelapse recording in conjunction with fluorescence microscopy (Parent & Devreotes, 1999; Servant et al., 2000). Cells transfected with constructs containing the gene encoding green fluorescent protein (GFP) fused to the gene of interest were tracked and redistribution of the GFP-tagged intracellular component was directly observed.

A constraint of video timelapse methods is that conventional microscopic analysis requires cells be on a relatively flat surface. This means that a two-dimensional approach must be used to study a process that, *in vivo,* is three-dimensional. Since *in vitro* experiments are meant to give us insight into *in vivo* processes, the question arises; is the mechanism of motility essentially the same for cells migrating across surfaces compared with migration through three-dimensional tissues? Collagen gels are transparent, so can be used in conjunction with video timelapse microscopy to examine leukocyte migration through a three-dimensional matrix (Entschladen et al., 1997; Friedl et al., 1998). Random motility of neutrophils migrating in collagen gels alloyed with different ECM

components indicates mesh size affects velocity (Kuntz & Saltzman, 1997). When the mechanical and structural properties of different alloys appear similar, cell velocity is affected by gel composition and velocity is inversely related to the strength of adhesion assessed using two-dimensional adhesion assays. This suggests that the way receptors function as cells migrate across two-dimensional substrates is related to the manner in which these receptors function in three-dimensional matrices and, by extrapolation, in tissues. This study validates the use of two-dimensional systems to study cell behavior.

The *in vivo* environment has been emulated even more closely by designing an *in vitro* model of neutrophil chemotaxis through three-dimensional amniotic tissues (Mandeville et al., 1997). Fluorophore-injected neutrophils were tracked by scanning through the tissue matrix at each time point followed by image reconstruction. Comparison of neutrophils chemotaxing across two-dimensional filters and through tissue indicates the overall shape and distribution of F-actin and cell surface receptors is similar. However, neutrophils migrating through tissue extend lateral pseudopods into tissue openings that presumably generate force to drive forward locomotion. Migration is interdependent on tissue architecture and the direction of the chemotactic gradient, since directionality is not wholly dictated by the chemotactic stimulus. This indicates the importance of cell contact with matrix components in guiding cell migration. A problem with this particular method is the potential for cellular damage as a result of exposure to high-energy excitation sources. In general, tracking cells through three-dimensional matrices is a powerful method to examine locomotion, since this approach emulates the *in vivo* microenvironment.

Intravital microscopy is another powerful tool that can be used to study leukocyte extravasation and migration through ECM *in vivo* (Werr et al., 1998; 2000). The mesenteric microvasculature provides a good anatomic region for analysis, since portions of the intestine can be exposed for microscopic analysis. The permeability of intestinal tissue allows addition of chemotactic stimulants or antibodies to stimulate or inhibit migration. Digital images are recorded enabling quantitative assessment of velocity and migration. The obvious advantage of this design is the direct examination of an *in vivo* process without the need to try to recreate complex tissues. Disadvantages are inherent to this approach as well. It is a relatively complex surgical procedure, animal models must be used, a mixed cell population is examined and it is extremely labor intensive.

Motility assays allow questions to be asked about the function of receptors and stimulants in cell adhesion and migration and the way intracellular constituents are reorganized to accommodate locomotion. Since we are ultimately trying to understand how cells operate *in vivo*, *in vitro* methods must be critically evaluated with respect to the relevance of the data generated. When leukocytes crawl through filters does this accurately reflect the processes they use to extravasate through endothelial-lined venules? Does lateral migration across a two-dimensional substrate reflect the receptor interactions that occur as cells migrate through complex three-dimensional ECM? The increasing complexity of migration assays indicates these concerns are being addressed.

1.1.2 <u>Actin filament assembly and protrusion formation</u>

Before becoming locomotory, a cell becomes polarized. Polarization establishes a domain within the cell that is morphologically and functionally distinct from the rest of the cell (Lauffenburger & Horwitz, 1996; Nabi, 1999). Protrusions form in response to

stimuli and the localized reorganization of F-actin and redistribution of other components create a polarized area in the cell that becomes the leading edge. Small cylindrical filopodia and flat, broad lamellipodia are structures that characterize the leading front. Polarized leukocytes have a leading edge characterized by an extended pseudopod and a distinct trailing edge called the nuropod that appears like a slim pseudopod (Sánchez-Madrid & del Pozo, 1999).

Morphological polarity is related to directional locomotion for leukocytes. PMNs stimulated with the chemotactic peptide *f*MLP polarize in the direction of the chemoattractant and timelapse microscopic analysis indicates they also migrate in this direction (Zigmond et al., 1981). Polarity is relatively stable, since PMNs resume moving along their original migratory path in the absence of a chemotactic gradient even after a temporary cessation of locomotion induced by removal of the stimulus. Reversing the chemotactic gradient causes cells to reverse direction rather than reverse their polarity. If *f*MLP is removed for a sufficiently long period to allow cells to round up before addition of fresh *f*MLP, morphological and functional polarity are lost. This indicates polarity is stable, but reversible, thus, is a dynamic process. Since morphological polarity predicates the direction of locomotion, components present in the leading edge are likely to be directly implicated in mediating motility. Extensive efforts have been made to identify these components and determine their function.

Asymmetric redistribution of chemokine receptors has been suggested as a mechanism whereby leukocytes can initiate or maintain directional motility (Nieto et al., 1997). Chemokine receptors redistribute to the leading edge of chemokine-stimulated T lymphoblasts, but redistribution is dependent on integrin-mediated adhesion. In contrast,

directional sensing by the amoeboid form of the slime mold *Dictyostelium* is achieved by maintaining a non-polarized distribution of chemosensory receptors on the cell surface, even in the presence of a chemoattractant gradient (Parent & Devreotes, 1999). Chemoattractants do stimulate translocation of GFP-tagged intracellular proteins containing pleckstrin homology domains in *Dictyostelium* and in neutrophil cell lines (Servant et al., 2000). The redistribution is asymmetric, occurs within seconds of adding the stimulus and is toward the highest concentration of chemoattractant. This is evidence that redistribution of intracellular components either initiates the formation of or maintains a polarized domain in cells.

The dynamic assembly and disassembly of F-actin provides motile cells with a structural component able to rapidly adapt to shape changes of a motile cell. Actin filaments (F-actin) are polymers of G-actin monomers and filaments self-associate to form a double-stranded helix. Actin-binding myosin fragments bind to the helix and give the filament the appearance of having a barbed end (plus end) and a pointed end (minus end), thus F-actin has polarity (Stossel, 1993; Chen, 2000). ATP-bound G-actin monomers attach to plus ends preferentially and hydrolyze ATP after binding. ADP-actin is preferentially released from the minus end of the F-actin filament. Therefore, at steady state, addition to the plus end equals removal from the minus end and there is no net growth of actin filaments. However, cellular signaling cascades can alter the balance to favor either filament lengthening or shortening. Because it is inherently dynamic, the assembly-disassembly of F-actin has been proposed to be a driving force of cell locomotion (Condeelis et al., 1992; Stossel, 1993; Lauffenburger & Horwitz, 1996; Mitchison & Cramer; 1996).

The actin cytoskeleton is a relatively rigid, cross-linked structure (gelled state), but disassembly of actin filaments produces a more flexible structure (sol state). Electron microscopic images of macrophages prepared to preserve the ultrastructure of the actin cytoskeleton demonstrate the leading edge of a polarized macrophage contains a cross-linked F-actin network, thus the actin cytoskeleton is associated with the polarized region of the cell (Stossel, 1993). F-actin is also predominantly localized to the leading front of T cells migrating through three-dimensional collagen matrices (Ratner et al., 1997). This suggests actin redistribution initiates or accompanies cell polarization. Mathematical analysis of phalloidin-stained fMLP-stimulated PMNs over time indicates asymmetric distribution of F-actin precedes the development of polarized cell morphology (Coates et al., 1992), indicating F-actin redistribution might regulate polarization.

Actin redistribution and membrane protrusions are associated, but what is the mechanical driving force? Assembly of F-actin in lipid vesicles causes vesicle deformation suggesting actin polymerization in cells can generate protrusive forces and there are models to propose how this occurs (Lauffenburger & Horwitz, 1996). The 'solation-expansion' hypothesis suggests localized signals cause regional disruption of the cortical actin cytoskeleton by uncapping and severing actin filaments creating a solated region in the actin cytoskeleton (Condeelis et al., 1992; Stossel, 1993; Mitchison & Cramer, 1996). Solation of actin presumably disrupts membrane-cytoskeletal cross-links as well, increasing membrane flexibility. As solated actin filaments are lengthened and reorganized into a network they return to the gel state creating an osmotic gradient and the forming gel becomes hydrated and swells. Localized osmotic swelling generates

sufficient mechanical force to push against the membrane and form a protrusion. F-actin reassembly and cross-linking may further enlarge and stabilize the protrusion.

The 'Brownian ratchet' or thermal ratchet model suggests F-actin in the fluid phase 'fluctuates due to Brownian motion' (Stossel, 1993; Mitchison & Cramer, 1996). The fluctuation produces sufficient space for G-actin monomers to bind to filaments proximal to the membrane. Sustained filament growth forces the membrane to protrude. This mechanism requires actin filaments be cross-linked, as in lamellipodia, or bundled, as in filopodia, to generate sufficient rigidity to force membrane protrusions.

The third model suggests membrane-bound motor proteins such as myosin I, move antegrade to newly polymerizing actin filaments and 'push' out the membrane. This requires that motor proteins attach to a solid structure to generate the force necessary to cause membrane protrusion (Mitchison & Cramer, 1996). Actin polymerization then fills in the space produced by membrane protrusion. Each of these models favors the localized reorganization of actin as the means to generate protrusive forces rather than the transmission of force from the cell body.

Each model dictates that actin filaments must be bundled or cross-linked to give the re-assembling structure sufficient mechanical strength to cause membrane protrusion; therefore, G-actin and F-actin binding proteins and the factors that control their activity are of interest as regulators of membrane protrusion formation (Cunningham 1992; Chen et al., 2000). Although actin and myosin filaments might provide the structural components to polarize the cell, upstream events must initiate the localized rearrangement of the cytoskeleton. In a *Dictyostelium* model, chemosensory receptors and their associated G proteins remain uniformly distributed around the cell periphery (Parent &

Devreotes, 1999), but chemokine receptors are redistributed to the cell front of lymphocytes (Nieto et al., 1997). Receptor redistribution would likely occur after signals generated by initial agonist binding. Therefore, activation of factors after agonist binding occurs and before actin reorganization must mediate the localized intracellular response that polarizes the cell. The Rho family of GTPases, Rac, Rho and Cdc42, have generated much interest because they appear to play a central role in cellular activities that link surface receptor-mediated signaling and reorganization of the actin cytoskeleton (Hall, 1998). In fibroblasts, activation of Rho is associated with the formation of actin stress fibers and focal adhesions (FAs). The reciprocal experiment indicates inactivation of Rho leads to the rapid dissolution of FAs and stress fibers (Nobes & Hall, 1995); therefore, Rho activity might be associated with sessile behavior. Rac activity is associated with focal complex formation, F-actin cross-linking and lamellipodia formation while Cdc42 activity is associated with F-actin bundling and formation of filopodia. Therefore, these two GTPases are associated with rearrangements of the actin cytoskeleton that correlate with locomotory behavior.

1.1.3   Rho family GTPases and leukocyte motility

Much of what is known about the activities of Rho family GTPases comes from investigating their effects on cell spreading using adherent cell lines such as fibroblasts. This work suggests Cdc42, Rac and Rho are interdependent and act sequentially, but are spatially restricted from one another (Nobes & Hall, 1995; Hall, 1998, Small et al., 1999a). Cdc42 activity establishes cell polarity then Rac is activated, lamellipodia are extended and focal complexes are formed. As the cell stretches forward, these contact sites come into proximity with Rho and activated Rho stimulates the formation of FAs

and stress fibers that anchor the cell. In highly locomotory cells such as leukocytes that do not adhere strongly or form FAs, how do these GTPases function?

To investigate the morphological and functional effects of Rac, Rho and Cdc42 on leukocytes, constitutively active or dominant negative mutants of each Rho family GTPase has been microinjected into cells or inserted into plasmids used to transfect cell lines (Cox et al., 1997; Allen et al., 1998; D'Souza-Schorey, 1998; Weber et al., 1998; del Pozo et al., 1999). Random and directional motility in response to a CSF-1 gradient was assessed for a murine macrophage cell line, Bac, microinjected with each of the mutated proteins while cellular morphology and distribution of F-actin were assessed using confocal microscopy (Allen et al., 1998). CSF-1 stimulates Bac cells to become polarized and chemotactic. Injection of constitutively active Cdc42 inhibits the CSF-1-stimulated chemotactic response and decreases random migration speed. Morphologically, macrophages remain relatively rounded with long filopodia around the entire cell periphery. F-actin is distributed around the periphery and in filopodial protrusions (Allen et al., 1998). In contrast, macrophages injected with dominant negative Cdc42 are highly motile, but not chemotactic and do not form filopodia. Cells remain relatively rounded with broad lamellipodial-type extensions and F-actin is distributed to protrusions around the periphery. Since cells remain motile in the absence of Cdc42 activity, but not chemotactic, Cdc42 activity must be associated with intracellular events that direct the cell toward a chemotactic stimulus. Constitutive activity of Cdc42 correlates with an inability to establish a morphologically polarized cellular region and subsequent chemotactic behavior. However, the mechanisms that

mediate cell motility appear to be independent of Cdc42 activity, since cells expressing inactive Cdc42 are still motile.

Injection of constitutively active Rac causes extensive membrane ruffling and F-actin distribution around the entire cell periphery indicating active lamellipodial formation. However, the cells are not chemotactic and are poorly migratory in response to CSF-1. In a model using Jurkat cells transfected with T7-tagged constitutively active Rac, Rac activity increases adhesion to Fn and cell spreading (D'Souza-Schorey et al., 1998). Thus, decreased locomotion might be a result of increasing adhesion in a non-polarized manner. Injection of dominant negative Rac inhibits membrane ruffling and migration, but does not affect the formation of filopodia in monocytes (Allen et al., 1998). This is consistent with the previously defined role of Cdc42 and Rac in filopodia and lamellipodia formation, respectively (Nobes & Hall, 1995). Macrophages injected with constitutively active Rho appear and behave similarly to cells injected with dominant negative Rac. The cells are non-motile and only extend filopodial-like protrusions. Injecting cells with C3 transferase to inhibit Rho causes the cells to spread and become highly deformed, but they remain non-polarized and non-migratory.

Constitutive activity of Cdc42 or Rac appears to enhance protrusive activity and F-actin assembly, but does not enhance chemotaxis or random motility. This indicates F-actin assembly and protrusion formation are not sufficient to mediate locomotion and suggests polarization is also required. It has been suggested a polarized shape is unlikely to occur without asymmetric F-actin distribution (Coates et al., 1992). In a fibroblast cell line, activation of a downstream target of Rac is dependent on the activation and translocation of Rac from the cytosol to the cytoplasmic membrane (del Pozo et al.,

2000). This suggests activated Rac is normally localized to an area of the cell that leads to the reorganization of actin in that region. Rac might also promote adhesion in localized cellular domains.

Constitutively active Rho decreases motility and protrusion formation consistent with its role in promoting strong adhesive interactions of cells with substrate. Morphologically, Bac cells appear small, rounded and project actin-rich filopodia or stress fibers. However, inhibition of Rho activity does not promote motility, even though cells exhibit numerous filopodial and lamellipodial projections. This suggests Rho activity is required by highly locomotory cells. Inactivation of Rho ablates chemokine-stimulated triggered binding of macrophages and neutrophils (Laudanna et al., 1996; Weber et al., 1998) suggesting that adhesive contacts are required by migrating cells and both Rac and Rho function to stimulate integrin-mediated adhesion. Rac and Rho also facilitate adhesion of $\alpha_4\beta_7$ to MAdCAM-1 in a murine T lymphoma cell line (Zhang et al., 1999).

Using different monocyte cell lines transfected either with constitutively active or dominant negative Cdc42 (Weber et al., 1998) or with dominant negative Cdc42 or Rac (Cox et al., 1997), produces morphological or functional defects similar to the observations of Allen et al. (1998). In the latter report, phagocytic activity was also decreased implicating Cdc42 and Rac in Fcγ receptor-mediated endocytosis (Cox et al., 1997). A different approach was used to study the effects of constitutively active or dominant negative forms of Rho, Rac and Cdc42 in T cell lines that spontaneously polarize on fibronectin (Fn)-coated surfaces (del Pozo et al., 1999). Plasmids containing mutant forms of each GTPase fused to GFP were used to transfect T cell lines. ICAM-1

and ICAM-3 redistribute to uropods of polarized T cells (del Pozo et al., 1995; 1997; Serrador at al., 1997), so redistribution of ICAM-3 was used as an indicator of cell polarization. Consistent with the data using monocyte/macrophage cell lines, constitutively active Rho inhibits deformation of transfected cells while active Rac and Cdc42 cause extreme cell deformation or protrusion activity. However, ICAM-3 does not redistribute to the uropod in cells transfected with these constitutively active GTPases. Cells transfected with wild-type forms of Rho, Rac or Cdc42 redistribute ICAM-3 to the uropod, indicating the GFP tag does not impair cell polarization. This suggests that locomotory defects in cells expressing hyperactive forms of each GTPase might be due to an inability to polarize.

Cells transfected with the dominant negative forms of Rho-, Rac- or Cdc42-GFP appear morphologically similar to each other and redistribute ICAM-3 and the ezrin-radixin-moesin (ERM) protein moesin to the uropod, thus these transfectants polarize normally (del Pozo et al., 1999). Both cell deformation and ICAM-3 redistribution are Fn-dependent, since transfected cells remain non-polarized on poly-L-lysine (PLL)-coated plates. Constitutive activity of all three GTPases decrease stem cell-derived factor-1 (SDF-1)-stimulated chemotaxis of transfected cells as does expression of dominant negative Cdc42. This is consistent with previous reports using macrophage cell lines (Allen et al., 1998; Weber et al., 1998). However, in contrast to the inhibitory effects of microinjected dominant negative Rac and inactivated Rho on macrophage chemotaxis (Allen et al., 1998), T cells transfected with dominant negative Rac or Rho do not significantly decrease chemotactic responses to SDF-1 (del Pozo et al., 1999). Injection of dominant negative Rho, Rac and Cdc42 might result in sufficiently high expression

levels to effectively sequester their respective GTP exchange factors from endogenous GTPases, whereas endogenous activity may still occur in transfected cell lines due to lower expression levels of transfected genes.

The observations using transfected T cell lines are consistent with the requirement that cells must polarize to locomote and that normal activity levels of Cdc42 are required for chemotactic responses. All of these groups demonstrate Cdc42 and Rac hyperactivity promote actin reorganization and cell deformation, but inhibit chemotaxis. The data suggest localized Cdc42, Rac or Rho activity is required to initiate or maintain cell polarity and subsequent chemotaxis. In a model system examining chemokine-stimulated cell polarization of a neutrophil cell line transfected with a gene encoding a pleckstrin homology domain of the AKT protein kinase fused to GFP (PHAKT-GFP), intracellular PHAKT-GFP fusion proteins translocate to the cell membrane nearest the chemotactic stimulus (Servant et al., 2000). Inhibition of actin polymerization by sequestering actin monomers by treatment of cells with latrunculin B did not inhibit polarized translocation of PHAKT-GFP toward the chemotactic stimulus. This suggests cellular asymmetry is established before actin reassembly occurs and that GTPase activity and subsequent actin reassembly must be localized to maintain the asymmetry.

1.1.4   Microtubules and cell polarity

Microtubules (MTs) are also polymeric macromolecules comprised of monomeric subunits of α and β tubulin. The tubulin subunits form heterodimers that polymerize into strands called protofilaments. Thirteen protofilaments associate such that adjacent strands are staggered with respect to the α and β subunits and the sheet of associated protofilaments coils to form a hollow ring structure. MTs are also polarized structures

with a plus and minus end and have dynamic instability, but hydrolyze GTP during assembly rather than ATP.

Early studies indicated an intact MT cytoskeleton was required to maintain persistence and directional motility of fibroblasts (Vasiliev, 1991) and leukocytes (Anderson et al., 1984). However, another group reported human PMNs treated with the MT depolymerizing agent colchicine maintained their polarized morphology toward a chemotactic gradient suggesting an intact MT cytoskeleton was not required for the polarization or locomotion of leukocytes (Zigmond et al, 1981). Subsequently, it was shown that highly locomotory fish epidermal keratocytes do not appear to require a MT cytoskeleton for directional locomotion (Euteneuer & Schliwa, 1984). Portions of locomoting cells can 'break away' and these fragments maintain directional motility in the complete absence of the MT cytoskeleton and the MT organizing center (MTOC). Thus, it was concluded the MT cytoskeleton did not function to mediate motility for highly locomotory cells like leukocytes and fish keratocytes.

In cell types that do require an intact MT cytoskeleton to migrate, MTs appear to initiate or maintain polarity. Fibroblasts treated with colchicine form protrusions around the entire cell periphery, but a leading front is not established and cells are unable to migrate (Nabi, 1999). This suggests an intact MT cytoskeleton is not required for protrusion formation, but implicates MTs in cell polarization. The MT network delivers vesicles containing both newly synthesized proteins and proteins from the endocytic path. Directing cellular traffic to a particular site could favor establishment of a leading edge, thus influencing cell polarity.

MTs appear to be directed to protrusions by the actin cytoskeleton. Analysis of motile fibroblasts injected with fluoresceinated tubulin and vinculin followed by examination using timelapse fluorescence microscopy indicates that as growing MTs extend toward the cell periphery they make multiple physical contacts with sites containing vinculin (Kaverina et al., 1998). These sites, identified morphologically as FAs, protect the MT from depolymerization by mild nocodazole treatment suggesting MTs are stabilized at these sites. MTs also extend to focal complexes in lamellipodia. The authors propose MTs are guided toward adhesions by actin filaments, possibly by actin-binding sites contained in proteins with MT binding sites, such as MT-associated protein (MAP). They suggest interaction of MTs with actin at sites of FAs relaxes the contact site by decreasing the contractility of stress fibers, allowing the cell to change shape or polarize (Small et al., 1999a). They also speculate that MTs either provide or sequester components that influence adhesion or protrusion formation.

Pharmacologic agents that prevent depolymerization of MTs, such as taxol, also inhibit cell migration suggesting both the assembly and disassembly of MTs is required for MTs to function for motile cells (Waterman-Storer and Salmon, 1999). These authors suggest that in migratory cells F-actin reorganization and MT polymerization and depolymerization are interdependent processes. Their observations suggest the growing ends of MTs are at the cell membrane and a proportion of free minus ends are in the cell body of migratory fibroblasts. They propose the polarized assembly and disassembly of MTs regulate the activity of Rho family GTPases that in turn promote actin reorganization in protrusions and FAs. For example, inactive Rac-GDP binds to tubulin monomers while active Rac-GTP does not bind tubulin, so MT disassembly sequesters

inactive Rac. As tubulin subunits are added to growing MT ends a guanine nucleotide exchange factor (GEF) called GEF-H1, that localizes to MTs, is brought into proximity to tubulin-bound Rac-GDP then Rac binds GTP and is released from tubulin. Since MT assembly is predominantly at the cell periphery, activated Rac is brought proximal to polarized or polarizing regions of the cell where it functions in F-actin assembly in the extending lamellipodium. This model proposes the MT cytoskeleton acts as an organizing matrix to coordinate the activity and localization of Rho family GTPases. Recent evidence does indicate a downstream target of Rac is not activated unless active GTP-Rac is redistributed from the cytosol to the cell membrane (del Pozo et al., 2000). It has also been demonstrated that Rho is translocated to the cell membrane (Takaishi et al., 1995).

Depolymerization of MTs increases the formation of stress fibers and cell contractility. Specific Rho inhibitors negate this effect indicating MT disassembly correlates with Rho activation (Waterman-Storer & Salmon, 1999). The nucleotide exchange factor GEF-H1 is also a potential candidate for Rho activation. Another molecule called Trio has two GEF domains. When GEF domain 1 is expressed by transfected fibroblasts, they resemble cells transfected with constitutively active Rac (Seipel et al., 1999). Transfected cells are highly protrusive and F-actin is redistributed to ruffled membranes, consistent with the function of this domain as an activator of Rac. Fibroblasts transfected with GEF domain 2, which activates Rho, resemble Rho-transfected cells. Interestingly, GEF domain 1 transfectants, but not Rac transfectants, are able to transmigrate. Since GEF-H1 and Trio potentially activate both Rac and Rho in cells, coordinating Rac and Rho activity appears to require spatial separation or sequential

activation. The spatial separation of MT assembly-disassembly could enable the same GEF to activate Rac and Rho in different cellular locations.

These models focus on the role of MTs in spreading or migrating fibroblasts. MTs appear to function in vesicle delivery, cell relaxation and coordinating activity of Rho GTPases and these activities might initiate or maintain polarization. Rho GTPases are also important mediators of leukocyte motility, but there are contradictory reports on the need for an intact MT cytoskeleton in migrating leukocytes (Zigmond et al., 1981; Anderson et al, 1984). The MTOC reorients while T cells interact with antigen presenting cells and Cdc42 activity is associated with polarization (Stowers et al., 1995). The MTOC of T cells orient toward the APC and this might function to deliver vesicles to the point of contact of the T cell with the APC. Although these experiments were not designed to examine the function of the MTs during locomotion, it suggests the MT cytoskeleton functions in cell polarization and this is also a critical step in the initiation of migration.

1.1.5 Microtubules are redistributed by migratory leukocytes

Leukocytes do not form FAs or stress fibers, but most observations indicate F-actin is concentrated at the leading edge of migrating leukocytes along with components of focal complexes like FAK and talin (Ratner et al., 1997; Serrador et al., 1997; Friedl et al., 1998; Eddy et al., 2000). Unique to migrating leukocytes compared with other eukaryotic cells is the uropod at the trailing edge of the cell. Examination of the distribution of MTs in locomoting T lymphocytes and neutrophils indicates MTs are redistributed to the uropod or cell rear (Ratner et al., 1997; Volkov et al., 1998; Entschladen et al., 2000). T lymphoblasts migrating through three-dimensional collagen

gels form a uropod behind the MTOC and as the uropod grows, MTs become localized to this cellular domain into a tight sheaf (Ratner et al., 1997). Taxol-treated cells still redistribute MTs to the uropod as they locomote indicating MTs need not be disassembled to localize to the uropod. In comparison with chemokine-stimulated T cells, fMLP-stimulated neutrophils migrating through collagen gels redistribute MTs to the rear of the cell, but complete restriction to the uropod is not apparent (Entschladen et al., 2000). This contrasts markedly with the distribution of the MT cytoskeleton of migratory fibroblasts in which MTs remain radially extended (Kaverina et al., 1998; Waterman-Storer & Salmon, 1999). It also suggests MT assembly and disassembly might not be required for lymphocyte migration. Consistent with this, T lymphoblasts treated with the depolymerizing agents colchicine or nocodazole still form uropods and locomote through collagen gels suggesting intact MTs are not required for structural support of the cell or uropod (del Pozo et al., 1995; Ratner et al., 1997). However, when T lymphoblasts locomote through a highly cross-linked matrix with small pores, pre-treating lymphoblasts with colchicine or nocodazole significantly increases the number of migrating cells and the distance migrated (Ratner et al., 1997). Another group also reported colcemid, but not taxol enhances T cell migration through collagen gels (Nikolai et al., 1999). This indicates MT disassembly does promote lymphocyte migration under certain circumstances.

The redistribution of MTs to the uropod might be a unique adaptation of lymphocytes, since they require a mechanism that enables extreme cell deformation as they extravasate and invade tissues with very restricted spaces (Ratner et al., 1997). Redistribution of this rigid structure might increase cell flexibility and enable

polarization. These experiments do not indicate whether MTs are normally disassembled before or during redistribution to the uropod, only that lymphocytes are able to redistribute the MT cytoskeleton in the absence of disassembly. The enhancement of migration observed in particular 'microenvironments' when MTs are disassembled implies MT disassembly could be a mechanism used by lymphocytes to promote migration through constricted spaces. MT disruption in monocyte cell lines activates the entire Ras-dependent signal transduction cascade resulting in extracellular-regulated kinase (ERK) activation and translocation to the nucleus (Schmid-Alliana et al., 1998). They suggest cellular shape changes alone might stimulate tubulin-based signal transduction.

An integrin-mediated signaling path that involves PKC activity is associated with redistribution of MTs to the uropod. The PKC isoenzymes $\beta(I)$ and δ redistribute along with MTs and the MTOC to the uropod of a T cell line in response to PMA and cross-linking of LFA-1 (Volkov et al., 1998). A PKC-β-deficient clone of the HUT-78 T lymphoma cell line adheres to substrate, but is non-motile and does not polarize the MT cytoskeleton upon LFA-1 cross-linking, implicating PKC phosphorylation activity in stimulating the locomotion of T lymphoma cells. PKC inhibitors also decrease locomotion of the parental HUT-78 cells. Biochemical analysis indicates an increase of α tubulin in the cytoskeletal fraction of HUT-78 cells compared with the cytosolic fraction when cell surface LFA-1 is cross-linked. This suggests MT assembly in a lymphoma cell line is stimulated by the same signals that polarize cells and promote migration. LFA-1 mediates cell to cell contact of leukocytes with ICAM-1 on endothelial cells lining blood vessels (Springer, 1994). MT assembly might enhance transient cell spreading resulting

in increased adhesion before the MT cytoskeleton is drawn into the uropod as leukocytes begin to extravasate. Interestingly, HUT-78 cells only migrate through collagen gels if treated with MT depolymerizing agents (Ratner et al., 1997). Perhaps MT disassembly activates signal transduction cascades that initiate migration. MT disruption in monocytes is associated with PTK signaling and ERK translocation (Schmid-Alliana et al., 1998).

PMA also enhances the migration of *ex vivo* T cells through three-dimensional collagen gels and PKC inhibitors ablate PMA-enhanced locomotion, but not spontaneous locomotion (Entschladen et al., 1997). However, PKC inhibitors have little effect on SDF-1-induced locomotion. Under these circumstances phosphotyrosine kinase (PTK) activity is critical for motility (Entschladen et al., 2000). In contrast, *f*MLP-stimulated neutrophil migration is modestly decreased by PTK inhibition, but rapidly declines when PKC is inhibited. Morphological assessment of migration of these cells through collagen gels shows the orientation of MTs and the MTOC is the same in spontaneously locomoting T cells as in chemotaxing T cells. Neutrophils, which have lower tubulin content than T cells, have a more diffuse distribution pattern of MTs, but MTs are also redistributed to the cell rear of *f*MLP-stimulated migratory cells. Although this work indicates different agonists activate different signal transduction paths, MT redistribution patterns are similar.

There is little direct evidence indicating leukocyte motility requires MT assembly or disassembly. MTs might be sequestered to the uropod simply to maintain the integrity of the MT cytoskeleton and still enable cell deformation (Ratner et al., 1997). Several other components are found in the uropod and some appear to have an active function

while others might be sequestered to inhibit normal function. The motor protein myosin II redistributes to the neck of the uropod of RANTES-stimulated T cells (Serrador et al., 1997). In *f*MLP-stimulated neutrophils myosin II is localized to the cell front and the uropod (Eddy et al., 2000). However, the activated form of myosin II is predominantly localized to the uropod. Using the myosin inhibitor butanedione monoxime prevents uropod formation suggesting myosin-based contractile forces might be required to form the uropod (del Pozo et al., 1995). Some classes of myosin interact with MTs (Mermall et al., 1998) and perhaps this is how MTs are redistributed.

Myosin II-mediated contraction is also associated with migratory activity. Inhibiting activation of downstream targets of Rho, Rho-associated coiled-coil forming kinases (ROCKs) prevents phosphorylation and activation of myosin light chain (MLC) resulting in significant inhibition of chemotaxis (Niggli, 1999). Although drug-treated neutrophils appear morphologically polarized, they no longer have a uropod in comparison with untreated cells. Another group has shown impairment of myosin II activation inhibits neutrophil chemotaxis and uropod retraction, but only when neutrophils are locomoting on adhesive substrates (Eddy et al., 2000). Although Rho activity is required to promote triggered adhesion of neutrophils (Laudanna et al., 1996), it is also associated with the generation of contractile forces that likely de-adhere migrating cells. If Rho activity is enhanced by MT depolymerization, localization of MTs to the leukocyte uropod might also localize activated myosin II to the uropod.

The ERM proteins are intracellular proteins that link cell surface ECM and intercellular adhesion receptors to the actin cytoskeleton (Bretscher, 1999) and these proteins might coordinate redistribution of proteins to the uropod. Human T cell lines

cross-linked with anti-CD43 or anti-ICAM-3 mAbs or stimulated with the chemokine RANTES redistribute moesin, ezrin and radixin to the uropod (del Pozo et al., 1995; Serrador et al., 1997; 1998). The adhesion molecules ICAM-1, ICAM-3, CD43 and CD44 also redistribute to the uropod of stimulated T cells. Immunoprecipitation and immunoblotting indicate moesin physically interacts with ICAM-3 and to a lesser extent with CD44 when T cells are stimulated with chemotactic factors. Anti-CD43 stimulates interaction of CD43 with both ezrin and moesin. Therefore, the physical association of these adhesion receptors with ERM proteins correlates with polarization of cells.

Since activated ERM proteins normally interact with the actin cytoskeleton, how do they function in the uropod of leukocytes where F-actin is weakly or not localized? In adherent cell types, Rho-GDP dissociation inhibitor and the Rho GEF Dbl can bind activated moesin and radixin, respectively (Bretscher, 1999). Binding to the ERM proteins in each case leads to the subsequent release and/or activation of Rho. Redistribution of ERM proteins to the uropod might localize active Rho to the uropod of leukocytes where it functions to activate myosin II, that in turn functions to polarize cells or drive motility by producing contractile forces (Mitchison & Cramer, 1996).

T cell lines transfected with dominant negative forms of Rac and Rho fused to GFP have increased distribution of these two GTPases at the rear of the cell (del Pozo et al., 1999). Cdc42-GFP is often exclusively distributed to the uropod of transfected cell lines. These experiments cannot address whether only inactive GTPases are specifically redistributed or sequestered to posterior regions of cells because constitutively active forms of each GTPase inhibit polarization. The authors speculate localization of inactive Rho GTPases function in rear release of cells. Since Rho and Rac activity increase

integrin-mediated cell adhesion (Laudanna et al., 1996; D'Souza-Schorey et al., 1998) this is a plausible model.

The uropod functions in motility, since if it is not present or is unable to retract, cells are unable to migrate. The distribution of MTs in locomoting T cells and neutrophils is distinct from locomoting fibroblasts suggesting the MT cytoskeleton might function in unique ways for leukocytes. Drug-induced MT disassembly enhances motility of lymphocytes in circumstances that require cells locomote through very restricted spaces. MT depolymerization decreases expression of L-selectin and adhesion of neutrophils to endothelial cells (Cronstein et al., 1995). The expression of L-selectin relative to β_2 integrin expression also decreases on neutrophils isolated from individuals who ingest colchicine. Loss of L-selectin correlates with migratory behavior, so colchicine treatment might promote *in vitro* migration by altering surface expression of adhesion receptors.

1.1.6   Traction and contraction

F-actin assembly and perhaps myosin motors generate forces to drive locomotion, but cells also require traction forces to promote motility. Myosin II appears critical for maintenance of cell velocity and this is related to traction. Two myosin II-based models have been proposed to explain how traction force might be generated (Mitchison & Cramer, 1996). The contraction model proposes that myosin II binds to adjacent actin filaments of opposing polarities in the cell body. Myosin movements pull on the filaments in equal and opposite directions creating tension. Additional forces including strong adhesive interactions at the cell front relative to the trailing edge and/or polarized assembly of F-actin generate a net force that drives directional motility.

In the transport model, myosin-based forces are the main driving force to pull the cell forward. Myosin movements must be unidirectional to generate a net force in one direction, so this model dictates that adjacent F-actin filaments proximal to the substrate be aligned with their plus ends oriented in the same direction. Actin filaments attach to the substrate via focal complexes and act as 'tracks' for myosin to move along. In this model adhesion receptors are also required, but need not be spatially polarized with respect to the strength of adhesion.

An experiment to determine which mechanism is likely to be used by migrating cells is to examine the polarity of actin filaments in the cell body. Electron microscopic examination of actin filament arrangement in migrating heart fibroblasts indicates actin filaments in the cell body are arranged with opposing polarities (Cramer et al., 1997). This observation is consistent with the requirements of the contractile model. However, integrin tracks left on the substrate behind migrating fibroblasts suggest these integrins have been 'ripped' from the cell surface as the cell locomotes (Lauffenburger & Horwitz, 1996). This observation could be interpreted to mean adhesive strength of integrins at the trailing edge is not decreased and this is consistent with a transport model. Thus, evidence supports key features of both models. Both models suggest myosin II and F-actin co-localization should occur in migrating cells. However, the asymmetric arrangement of F-actin at the cell front (Ratner et al., 1997; Serrador et al., 1997) and activated myosin II in the uropod of leukocytes (Serrador et al., 1997; Eddy et al., 2000) suggest these cells use a mechanism different than either the contractile or the transport model. Rapidly locomoting, poorly adhesive cells like leukocytes might rely entirely on the protrusive forces generated at the cell front to drive locomotion, since they do not

have to overcome strong adhesive forces like those present in adherent cell types (Mitchison & Cramer, 1996). Although adhesive interactions with substrate might be weak as leukocytes migrate, they will presumably be required at least at the cell front. Integrins mediate adhesion, but are also associated with motile behavior and cytoskeletal reorganization (Williams & Solomkin, 1999), thus are of particular interest as mediators of traction for migratory leukocytes.

Integrins are cell surface heterodimers that mediate anchorage for adherent cells and provide traction during migration. The extracellular domains adhere to ECM components or cell surface receptors on adjacent cells while intracellular domains are indirectly linked to the actin cytoskeleton via focal complex components (Damsky & Werb, 1992). When highly adhesive cells are induced to become migratory, small integrin-mediated contact sites form at the leading edge (Lauffenburger & Horwitz, 1996). The focal contacts remain stationary as the locomoting cell moves over them and become larger as the distance from the leading edge increases. In fibroblasts transfected with a GFP-β_1 integrin chimera, focal contacts or adhesions in cells induced to locomote by wounding the monolayer have stationary GFP-β_1 integrin-containing FAs (Smilenov et al., 1999). In contrast, stationary cells contain highly mobile FAs that move along actin filaments in a myosin-dependent manner. The authors suggest traction requires immobile adhesive contacts be maintained between the cell and substrate as cells migrate. The mobility of FAs in stationary cells provide no traction, thus maintain sessile behavior. FAs at the rear of migrating fibroblasts disappear or become mobile suggesting the rear region of the cell is not involved in traction.

Leukocytes do not form morphological structures consistent with conventional FAs or stress fibers, but the strength of integrin binding can be altered to promote strong adhesion or weak adhesion. Integrins can be 'triggered' to undergo conformational changes that increase the affinity of ligand binding and integrins can be clustered to increase avidity (Faull et al., 1994; Stewart & Hogg, 1996). These characteristics make integrins adaptable to the changing needs of migrating cells. Triggered adhesion of integrins can be induced by agonist binding apart from integrins and their ligands (inside-out signaling) and include chemoattractants and chemokines (Williams & Solomkin, 1999). A lymphoid cell line transfected with the chemoattractant receptors, fPR or IL8-R demonstrates triggered binding to VCAM-1 via $\alpha4\beta1$ upon stimulation with fMLP or IL8 (Laudanna et al., 1996). Triggered adhesion correlates with increased Rho activity as indicated by the increase of Rho-GTP. The Rho inhibitor C3 transferase significantly decreases triggered binding indicating Rho activity stimulates an increase in integrin affinity or avidity. Human neutrophils also demonstrate triggered binding to fibrinogen that is inhibited by C3 transferase. This demonstrates chemoattractants and chemokines stimulate triggered adhesion of integrins via Rho. Rho activation might be a common step of all signal transduction paths for inside-out signaling to integrins (Williams & Solomkin, 1999).

Since integrins are indirectly linked to the actin cytoskeleton and activated Rho GTPases trigger actin cytoskeletal organization, how do these constituents interact? Initial work in fibroblasts indicated integrin clustering and focal complex assembly require both integrin binding to ECM and activation of Rac and Rho (Hotchin & Hall, 1995). However, more recent work indicates focal complexes can form independently of Rho

family GTPase activity. Fibroblasts transfected with dominant negative forms of Cdc42, Rac or Rho then grown on Fn were examined microscopically over time to assess the formation of focal contacts and actin distribution (Clark et al., 1998). Each transfected cell line is capable of assembling focal complexes, but in less abundance than in untransfected cells. This suggests integrin-mediated signaling cascades promote focal complex assembly in the absence of the coordinated activity of all three GTPases, but robust FA formation and actin reorganization requires Rho family GTPase activity.

Examination of the effect of the inactive GTPases on targets of integrin signaling, FAK, paxillin, ERK2, src and Akt indicate Rho and Cdc42 activity converge with integrin-mediated signal transduction paths. A lack of Rho activity correlates with decreased phosphorylation of FAK, paxillin and ERK2. Expression of dominant negative Cdc42 correlates with inhibition of ERK2 phosphorylation and kinase activity and decreased phosphorylation and kinase activity of Akt. This suggests that signals that activate Cdc42 and Rho, like growth factors, phospholipids and chemokines (Hall, 1998), might synergize with integrin-mediated signaling by acting on the same downstream targets. Integrin-mediated signaling might also coordinate GTPase activity. Adhesion to Fn correlates with translocation of active Rac-GTP to the cell membrane from the cytosol and the activation of a target of Rac, p21-activated kinase1 (PAK1) (del Pozo et al., 2000). When cells are kept in suspension, Rac can become activated, but PAK1 remains inactive. Insertion of a transmembrane domain into Rac leads to stimulation of PAK1 activity even when cells are in suspension, whereas ablation of Rac's membrane localization domain inhibits adhesion-mediated activation of PAK1. This suggests that in fibroblasts, integrin-mediated adhesion coordinates Rac activity by stimulating Rac

redistribution to the cell membrane, possibly to areas where integrins are localized. Activated Rho has also been shown to translocate to the cell membrane of fibroblasts where it co-localizes with ERM proteins (Takaishi et al., 1995) and Cdc42 translocates to the cell membrane of spreading monocytes (Aepfelbacher et al., 1994). This spatial coordination of GTPases, perhaps mediated by integrins, could lead to localized focal complex assembly and actin reorganization during cell polarization or spreading.

Both inactivity and sustained activity of Cdc42, Rac and Rho impairs or inhibits chemotaxis of monocytes and the migratory defect correlates with the inability to reorganize actin asymmetrically and polarize (Allen et al., 1998; Weber et al., 1998). However, T cell lines transfected with dominant negative GFP chimeras of Rho, Rac and Cdc42 form uropods on Fn-coated, but not on PLL-coated surfaces (del Pozo et al., 1999). Thus, Fn enables cells to assume a migratory morphology in the absence of coordinated activity of all three Rho GTPases. T cells expressing constitutively active Rac-GFP also form uropods on Fn-coated surfaces, but not on PLL, indicating adhesion can overcome the non-polarizing effects of hyperactive Rac or inactive Cdc42, Rac or Rho. The authors suggest GTPases direct integrin distribution, but integrin-based signaling might be required to direct Rho family GTPase activities so actin and focal complex assembly are appropriately localized. Examination of focal complexes in macrophages indicate injection of dominant negative Cdc42 or Rac correlates with rapid dispersion of phosphotyrosine activity and vinculin from focal complexes, but β_1 integrins remain clustered (Allen et al., 1997).

In a model exploring the contribution of integrins to endothelial attachment and extravasation by chemokine-stimulated monocytes, the relative avidity of these

interactions was examined. *Ex vivo* human monocytes use α_4 integrin- and LFA-1-mediated attachment to mediate chemokine-stimulated migration across and through endothelial monolayers (Weber et al., 1996; Weber & Springer, 1998). Intermediate concentrations of ligand coated onto surfaces or expressed on endothelial cells correlates with optimal locomotion rates. This suggests the relative avidity of interactions of integrins and their ligands affects lo-comotion. When chemokine-stimulated migration on VCAM-1-coated surfaces is assessed over time, the majority of monocytes migrate rapidly, slow down then resume the original range of velocities over a thirty minute time period (Weber & Springer, 1998). This data has been interpreted to indicate chemokine stimulation transiently increases the avidity of integrin binding that manifests as a temporary decrease in cell velocity.

Consistent with data from a fibroblast model indicating that integrin binding should be weak or moderate to support migratory behavior (Palacek et al., 1997), forcing β_1 integrins into a high affinity binding conformation using activating mAbs decreases the spontaneous and chemokine-sti mulated migration of monocytes (Weber & Springer, 1998) and the spontaneous locomotion of T cells through collagen gels (Friedl et al., 1998). In the latter report, confocal analysis of T cells in the collagen gel indicates high affinity binding conformations of β_1 integrin inhibit cell deformation and β_1 integrins remain evenly distributed around the cell periphery. These are direct demonstrations that strong adhesion inhibits locomotion and implies weaker adhesive contacts are required to mediate motility.

1.1.7 Distribution patterns of integrins on leukocytes

Localization of adhesive contacts to the leading edge predicts a mechanism of motility used by highly locomotory cells that might not require conventional traction forces (Mitchison & Cramer, 1996). One would then predict leukocytes migrating on type I collagen would distribute $\alpha_2\beta_1$ integrin to the cell front. However, T cells migrating through three-dimensional collagen gels distribute β_1 integrins to the cell rear and uropod (Ratner et al., 1997; Friedl et al., 1998). Chemokines stimulate the redistribution of several other receptors including CD43, CD44, ICAM-1 and especially ICAM-3 to the uropod of T lymphoblasts (del Pozo et al., 1995; Serrador et al., 1997; 1998). Uropod formation is stimulated by chemokines and by cell binding to integrin ligands including ICAM-1, VCAM-1 and Fn. Uropod formation is also dependent on integrin-based adhesion, since chemokine-stimulated T cells attached to PLL do not polarize (del Pozo et al., 1995).

The redistribution of adhesion receptors to the uropod might also promote de-adhesion. Optically sectioned confocal images compiled after T cells migrated across Fn-coated surfaces indicate the uropod is not at substrate level (del Pozo et al. 1997; Serrador et al., 1997), suggesting receptors localized to the uropod are not mediating adhesion to substrate. However, the uropods of T cells migrating through collagen gels appear to make numerous contacts with collagen fibers (Friedl et al., 1998) and the uropods of neutrophils migrating across Fn appear to contact the substrate (Pierini et al., 2000), indicating that in some situations, receptors distributed to the uropod are proximal to substrate. Examination of the distribution of LFA-1 and $\alpha_4\beta_1$ on T lymphoblasts adhering to TNFα-stimulated endothelial cells indicates neither LFA-1 nor $\alpha_4\beta_1$ integrins

localize to the uropod, but remain distributed across T cell surfaces where they likely interact with ICAM-1 and VCAM-1 expressed by TNF-α-stimulated endothelial cells (del Pozo et al., 1995). This contrasts with the uropodal distribution of β_1 integrins on T cells migrating through collagen gels.

The distribution of integrins and their participation in locomotion has also been studied using models of neutrophil recruitment. After extravasation, PMNs in human, rat and mouse models upregulate expression of the collagen receptor, $\alpha_2\beta_1$ integrin and the Fn receptors, $\alpha_4\beta_1$ integrin and $\alpha_5\beta_1$ integrin (Reinhardt et al., 1997a; Werr et al., 1998; 2000). *In vivo* analysis of extravasated PMNs using intravital microscopy indicates the α_4 integrin subunit is predominantly localized to the uropod of polarized cells and anti-α_4 mAbs do not significantly affect migration velocity in this *in vivo* model (Werr et al., 1998). In contrast, extravasated PMNs stimulated *in vitro* with *f*MLP migrate across type I collagen-coated surfaces and distribute α_2 integrin subunits predominantly at the cell front. Type I collagen-specific peptides and anti-α_2 or anti-β_1 integrin mAbs inhibit *ex vivo* chemotaxis of human PMNs and *in vivo* migration of rat PMNs indicating $\alpha_2\beta_1$ integrin functions in motility (Werr et al., 2000). In these models, integrin heterodimers apparently involved with adhesion/motility are at the cell front whereas integrins not involved are localized to the uropod. This suggests the asymmetric distribution of integrins on locomoting neutrophils is functional.

Another group examining the distribution of integrins as neutrophils migrate on different ECM components has made similar observations. Neutrophils adhere to vitronectin using $\alpha_v\beta_3$ integrin and this heterodimer is predominantly distributed at the cell front as well as in endocytic vesicles of *f*MLP-stimulated cells (Lawson & Maxfield,

1995). *f*MLP-stimulated neutrophils migrating on Fn have pronounced distribution of α_5 integrin subunits at the cell front and in endocytic vesicles, whereas β_2 integrins are predominantly at the cell rear (Pierini et al., 2000). Suppressing the Ca^{2+} flux in cells using Quin2/AM significantly decreases *f*MLP-stimulated migration on vitronectin or Fn. Microscopic examination of Quin2/AM-treated cells indicates neutrophils are highly polarized on Fn, but α_5 subunits are distributed to the unusually elongated uropod and very little α_5 integrin is localized to the cell front or in intracellular vesicles. Reducing the strength of adhesion using function blocking antibodies to $\alpha_5\beta_1$ or $\alpha_v\beta_3$ integrins restores *f*MLP-stimulated motility of Quin2/AM-treated neutrophils on Fn or vitronectin, respectively. This suggests inhibition of the Ca^{2+} flux interferes with downregulation of strong integrin adhesion at the posterior region of the cell and uropod detachment (Pierini et al., 2000). The distribution patterns of $\alpha_5\beta_1$ and $\alpha_v\beta_3$ integrins led the authors to postulate that integrins localized to the cell front mediate strong adhesion. As cells locomote, integrins in contact with substrate become localized to the rear of the cell where they de-adhere by a Ca^{2+}-dependent mechanism. De-adhering integrins are endocytosed and recycled back to the cell front consistent with the model of membrane receptor recycling described by Bretscher (Bretscher, 1996; Bretscher & Aguado-Velasco, 1998). This mechanism allows a 'gradient of adhesiveness' to be maintained along the cell axis (Lawson & Maxfield, 1995; Pierini et al., 2000) consistent with the type of adhesion required by a contractile model of traction force.

The distribution of β_1 integrins in T cells migrating through collagen gels contrasts with the distribution patterns of functioning integrins in neutrophils. $\alpha_2\beta_1$ integrin would be expected to mediate adhesion to type I collagen and mAbs to α_2

significantly inhibit migration of T cells in collagen gels (Friedl et al., 1995), but β_1 integrin subunits are almost exclusively distributed to the distal portion of the uropod of migrating T cells rather than at the cell front (Friedl et al., 1998). Adhesion to type I collagen mediated by the β_2 integrin, LFA-1 has been documented for PMNs (Garnotel et al., 1995) and β_2 integrins are localized to the cell front of the T lymphocytes (Friedl et al., 1998). However, T cells treated with a variety of different function-blocking anti-β_1 or anti-β_2 mAbs remain polarized and migratory implying neither β_1 nor β_2 integrins mediate traction as T cells migrate through collagen gels.

Integrins mediating strong adhesion are likely associated with focal complexes, so the distribution of F-actin and FAK (Friedl et al., 1998) or F-actin, α-actinin and talin (Pierini et al., 2000) were examined. Both groups find that the majority of focal complex components are localized to the cell front suggesting that, at least in neutrophils, integrins mediating adhesion are likely associated with focal complexes at the cell front. This data is in agreement with a report in which *ex vivo* neutrophils chemotaxing through three-dimensional amniotic tissue were examined. Confocal analysis of *f*MLP-stimulated neutrophils migrating through the tissue matrix indicates α_v, α_5 integrin subunits and α-actinin co-localize with F-actin at the leading edge (Mandeville et al., 1997). This suggests integrin-based focal complexes are formed by neutrophils migrating across two-dimensional substrates and through complex three-dimensional tissue matrices.

In contrast to the frontal distribution of FAK, F-actin in unstimulated migratory T cells is arranged cortically and in lateral filopodia contacting collagen fibrils (Friedl et al., 1998). However, previous observations using a similar system indicated F-actin was distributed entirely to the cell front of T cells (Ratner et al., 1997). Since FAK, β_1

integrin and F-actin are spatially separated in T cells, this implies β_1 integrin-mediated focal complexes are not formed (Friedl et al., 1998). The authors interpret their data to mean β_1 integrins are not involved in mediating traction as T cells migrate through three-dimensional collagen matrices. They conclude interactions of the lateral protrusions with collagen fibrils might generate sufficient biophysical force to support T cell migration in the absence of specific integrin-mediated adhesion. $fMLP$-stimulated neutrophils migrating through three-dimensional amniotic tissue also have lateral protrusions that appear to 'push' cells through the matrix (Mandeville et al., 1997). However, these cells distribute α_v and α_5 integrin subunits to the leading edge and to lateral protrusions along with F-actin and α-actinin suggesting integrin-based adhesion might be used in combination with biophysical force under certain circumstances.

Non-motile Quin2/AM-treated cells distribute F-actin, α-actinin and talin to both the leading edge *and* the extended uropod (Eddy et al., 2000; Pierini et al., 2000). This suggests that as cells locomote, a Ca^{2+}-dependent cellular mechanism dissociates focal complexes as they become proximal to the posterior region of the cell. This presumably weakens the strength of adhesion to the substrate allowing release of the cell rear. Myosin II-based contractile forces function in de-adhesion, since myosin II inhibitors produce morphological and functional effects similar to Ca^{2+} buffering (Eddy et al., 2000). Calcineurin also functions in de-adhesion of $\alpha_v\beta_3$ integrins from vitronectin (Lawson & Maxfield, 1995), but inhibition of calcineurin does not affect α_5 integrin-mediated migration on Fn (Pierini et al., 2000).

To determine if integrin de-adhesion is followed by endocytosis of integrins, the endocytic path was tracked using a fluorochrome-labeled lipid analogue, C_6-NBD-gal.

Intracellular α_5 integrin co-localizes with endocytic vesicles that redistribute toward the cell front of migratory cells. However, exocytosis of α_5 integrin chains at the leading edge is not demonstrated. The cumulative evidence suggests β_1 and β_3 integrins likely play a role in attachment at the cell front that provides traction for locomoting neutrophils. The inability of Ca^{2+}-buffered cells to detach, the redistribution of α_5 or $\alpha_v\beta_3$ integrins to the uropod and the reduced level of intracellular integrins suggest β_1 and β_3 integrins remain attached to substrate as Ca^{2+}-buffered cells attempt to locomote. These integrins mediate strong attachment at the cell front of locomoting cells where they form focal complexes. As cells migrate over the contact sites, integrins become localized to the cell rear where adhesion strength is weakened concomitant with myosin II-based contraction. $\alpha_5\beta_1$ or $\alpha_v\beta_3$ integrins are then endocytosed and presumably cycled back to the cell front.

A critical difference between the neutrophil and lymphocyte models is that Friedl et al. (1998) use *ex vivo* unstimulated peripheral blood lymphocytes while the neutrophil models use extravasated and/or chemoattractant-stimulated neutrophils. Unstimulated T lymphocytes from circulating blood might be so weakly adhesive they do not require strong forces to de-adhere integrins when biophysical forces can be used to migrate through the fibrous structure of a collagen gel. When leukocytes bind to endothelial cells lining blood vessel walls and extravasate they upregulate expression and adhesiveness of integrins such as LFA-1 and β_1 integrins (Springer, 1994; Reinhardt et al., 1997a). Thus, they might require a mechanism that enables de-adhesion mediated by these strongly adhesive integrins. Inhibition of myosin II does not inhibit chemotaxis or tail retraction when *f*MLP-stimulated neutrophils migrate across substrates like human serum to which

they adhere weakly and talin and F-actin remain localized to the cell front (Eddy et al., 2000). This suggests that the mechanism proposed by Pierini et al., (2000) might only function when leukocytes must overcome relatively strong adhesive interactions to migrate.

Cross-talk between different integrins can also affect the strength of adhesion and promote motility. Receptor occupancy of $\alpha_v\beta_3$ integrins enhance $\alpha_4\beta_1$ or $\alpha_5\beta_1$ integrin-mediated migration of T lymphocytes (Imhof et al., 1997) and LFA-1-mediated migration of monocyte cell lines (Weerasinghe et al., 1998) presumably by decreasing the strength of binding to VCAM-1 or ICAM-1, respectively. Binding to immobilized ICAM-1 or forcing LFA-1 on T lymphoblasts into an active conformation decreases $\alpha_4\beta_1$- and $\alpha_5\beta_1$- mediated adhesion to Fn and correlates with an increase in $\alpha_5\beta_1$ integrin-mediated migration on Fn (Porter & Hogg, 1997). Function-blocking mAbs to α_4 integrin subunits also increase $\alpha_5\beta_1$-mediated migration. These observations parallel those in monocytes showing there is a sequential activation of $\alpha_4\beta_1$ and $\alpha_5\beta_1$ in response to chemokine stimulation (Weber et al., 1996). Integrins such as $\alpha_4\beta_1$ and LFA-1 do not recycle (Bretscher, 1992), so decreasing the affinity or avidity of these integrins by inside-out signaling might promote de-adhesion as leukocytes begin to extravasate.

1.2 The Human Thymus and Thymocyte Development

Development of a diverse peripheral T cell repertoire able to respond to a broad array of potential pathogens, yet tolerant to self depends upon a complex, orchestrated series of events that occur in the thymus (Kisielow & von Boehmer, 1995; Rodewald & Fehling, 1998; Killeen at al., 1998; Res & Spits, 1999; Sebzda et al., 1999). Generation

and modeling of the T cell repertoire begin as thymocyte precursors arrive from the bone marrow, begin to rearrange T cell receptor (TCR) genes and proliferate. Successful TCR gene rearrangement is the first critical step in the development of a functional T cell. Once $TCR_{\alpha\beta}$ genes are rearranged and expressed along with CD3, CD4 and CD8, thymocytes undergo positive and negative selection before emigrating the thymus to populate the peripheral immune system. The outcome of positive and negative selection (survival or death) is dependent on signals generated when $TCR_{\alpha\beta}$ heterodimers interact with MHC molecules on thymic stromal cells. It is well recognized that the TCR, MHC class I and II, CD4 and CD8 molecules play a critical role in these interactions (Chan et al., 1998; Ellmeier et al., 1999; Sebzda at al., 1999). However, interactions of developing thymocytes with thymic stromal elements also rely upon contacts being made between additional receptors expressed on thymocytes and stromal cells during sessile phases of differentiation (Haynes, 1986; Ritter & Boyd, 1993; Savino et al., 1993; Lagrota-Cândido et al., 1996; Halvorson et al., 1998; Amsen & Kruisbeek, 1998). Although the path taken by thymocytes as they undergo differentiation and selection is still unclear, migration must occur within the thymic lobule as thymocytes differentiate; therefore, motility receptors are also required as cells differentiate. β_1 integrins mediate adhesion and motility for human thymocytes (Salomon et al., 1994; Crisa et al., 1996; Salomon et al., 1997; Gares et al, 1998). The receptor for hyaluronan (HA)-mediated motility (RHAMM) also mediates thymocyte motility and might function in conjunction with β_1 integrins (Pilarski et al., 1993; Gares et al., 1998; Gares & Pilarski, 1999). Recently chemokines and chemokine receptors have been found to be expressed in the thymus and to stimulate thymocyte chemotaxis (Dairaghi et al., 1998; Zaitseva et al., 1998; Franz-

Bacon et al., 1999; Suzuki et al., 1999; Zaballos et al., 1999). This suggests the regulation of adhesion and motility is also vital to thymocyte differentiation.

1.2.1   Thymus architecture and thymocyte ontogeny

The thymus is a multi-lobulated organ with lobules divided from one another by a subcapsule containing connective tissue and blood vessels. In humans, the thymus is organized and thymocyte differentiation begins between the $16^{th} - 20^{th}$ weeks of gestation (Haynes, 1984). Phenotypic analysis of thymocytes and stromal cells indicate the thymic microenvironment within each lobule consists of discrete regions (Haynes, 1984; 1986; Boyd & Hugo, 1991). The outermost region is the subcapsular cortex and contains immature thymocytes or thymocyte progenitors. Thymic epithelial cells (TECs) in this region have a phenotype similar to medullary TECs, but distinct from cortical TECs. The cortex is heavily populated with immature, double positive, (DP; $CD4^+8^+$) thymocytes, nurse cells, macrophages and cortical TECs. The majority of cells in the corticomedullary junction and medulla are macrophages, dendritic cells, medullary TECs and single positive, (SP; $CD4^+8^-$ and $CD4^-8^+$) thymocytes. The medulla also contains multinegative (MN; $CD3^-4^-8^-$) thymocytes expressing phenotypic markers consistent with a generative thymocyte lineage (Pilarski, 1993a). As thymocytes differentiate they acquire and downregulate expression of a variety of cell surface receptors (Shortman & Wu, 1996; Res & Spits, 1999). Expression of particular arrays of cell surface molecules correlates with different stages of TCR gene rearrangement and expression. Thus, surface phenotype is a convenient tool to track lineage progression and localize differentiation and selection events to regions within the thymus. Although most thymocyte research has been done using murine systems, humanized SCID mouse models and fetal tissue organ

cultures (FTOC) have been developed to examine human thymocyte ontogeny "*in vivo*" (Res & Spits, 1999). Histological analysis of the ontogeny of thymic stromal elements and thymocytes has also been done using *ex-vivo* fetal and neonatal human tissue (Haynes, 1984; 1986).

In both mouse and human models, the site of entry of thymocyte progenitors has not been definitively determined and may be the cortico-medullary junction or the subcapsular region (Haynes, 1984; Boyd & Hugo, 1991; van Ewijk et al., 1994). However, during fetal development, the thymus does not contain an inner medullary region until the onset of thymocyte differentiation (Haynes, 1986) suggesting early in ontogeny stem cell entry might be in the sub-cortical region. Bone marrow-derived progenitors that arrive via the blood to colonize the human thymus appear to be differentiated stem cells with the phenotype $CD2^{lo}7^+34^+44^+45RA^+10^+$ (Terstappen et al., 1992; Kraft et al., 1993; Galy et al., 1993; Blom et al., 1999). Clonal assays indicate these thymic progenitors have the capacity to differentiate into T, NK or dendritic cells, thus might be lymphoid progenitor cells. Isolation of bone marrow cells with this phenotype can also give rise to B cells under appropriate *in vitro* conditions, suggesting they are in fact lymphoid committed progenitors (Res & Spits, 1999).

As differentiation proceeds, thymocyte precursors begin to express CD5 then CD1a and downregulate expression of CD34 and CD44. CD1a expression correlates with expression of the pre-TCR$_\alpha$ (pTα) receptor and RAG-1 and rearrangement of the TCR δ, γ and β genes is detectable, thus CD1a is a marker that defines progenitors committed to the T cell lineage. The subcapsular cortex is the chief site of detectable lymphopoiesis in the thymus (Haynes, 1984) suggesting progenitors might enter the

thymus in this region. However, progenitors lacking CD1a expression are localized to the thymic medulla suggesting an earlier progenitor might arrive in this region and undergo differentiation (Pilarski, 1993a). The presence of dendritic cells in the medulla and corticomedullary junction and the capacity of $CD1a^-5^-34^+45RA^+10^+$ progenitors to differentiate into a dendritic lineage suggests that, once the thymus is compartmentalized in humans, early differentiation occurs in the medulla favoring that progenitor entry is at the cortico-medullary junction. Thymocytes or pro-thymocytes might then migrate to the subcortical region, proliferate and mature to the DP stage. The thymic hormones, thymopoietin and thymosin α_1 are secreted by epithelial cells in the medulla and subcapsular cortex (Haynes, 1986). These hormones stimulate a variety of functions including the induction of terminal deoxynucleotidyl transferase (Tdt) that is required for TCR gene rearrangement (Dardenne & Savino, 1994). The presence of these hormones in the subcapsular cortex and the medulla suggest differentiation of progenitors to committed T cell precursors could be stimulated at either site.

As differentiation proceeds, pro-thymocytes begin to express CD4, CD8 then CD3 and the TCR (Shortman & Wu, 1996; Res & Spits, 1999). Once TCRs are expressed at the cell surface, positive and negative selection occurs as TCRs on DP thymocytes interact with MHC molecules expressed on thymic stromal cells. Low affinity or avidity interactions are thought to support positive selection of thymocytes while high avidity interactions presumably lead to negative selection and apoptosis (Sebdza et al., 1999). There is abundant evidence in murine models that positive selection of DP thymocytes likely occurs in the cortex and is mediated by cortical TECs (Amsen & Kruisbeek, 1998). A model system that provided evidence for this used transgenic mice that selectively

expressed MHC class II I-E molecules on cortical, medullary or both cortical and medullary TECs (Benoist & Mathis, 1989). All TCRs that utilize the $V_\beta 6$ gene segment interact with I-E^k MHC molecules potentially allowing a substantial proportion of the thymocyte population to be positively selected. Phenotypic analysis indicates an increased proportion of peripheral CD4$^+$ T cells express a TCR utilizing $V_\beta 6$ only in mice expressing the selecting MHC molecules on cortical TECs. This suggests positive selection requires expression of selecting MHC class II molecules on cortical epithelium.

In another murine model, positive selection of thymocytes bearing anti-HY specific transgenic TCRs only occurs in bone marrow chimeras when recipient mice express MHC molecules that match the MHC restriction of the transgenic TCR expressed by transplanted thymocytes (von Boehmer, 1990). This indicates the donor bone marrow is unable to reconstitute the thymic microenvironment with cells that mediate positive selection and suggests the radiation resistant epithelial cells of the recipient mice are required for this process. Subsequent work using mice expressing different transgenic TCRs or superantigens combined with selective MHC expression of cortical TECs, medullary TECs or bone marrow-derived cells also indicate positive selection is most efficient when cortical TECs express the selecting MHC molecules (Amsen & Kruisbeek, 1998). For murine systems, the cumulative evidence strongly favors the hypothesis that positive selection of DP thymocytes occurs in the cortex. This suggests progenitor thymocytes migrate from the cortico-medullary junction to the subcapsular cortex as they differentiate then back through the cortex to undergo positive selection. .

Bone marrow-derived cells have been shown to be required for negative selection of autoreactive thymocytes in male mice bearing transgenic TCRs specific for male HY

antigen (von Boehmer, 1990). Although there have been demonstrations of both thymic epithelial and bone marrow-derived cells inducing tolerance, dendritic cells are most efficient at mediating negative selection (Amsen & Kruisbeek, 1998). Dendritic cells are localized to the medulla and cortico-medullary junction implying negative selection occurs in this region. Consistent with this, examination of mice expressing TCRs with specificity for pigeon cytochrome C crossed with mice that express endogenous cytochrome C on epithelial and hematopoietic cells indicates deletion of these autoreactive thymocytes occurs at the corticomedullary junction and in the medulla (Oehen et al., 1996). However, deletion of anti-HY transgenic thymocytes has also been observed in the cortex suggesting cortical TECs in some models can mediate negative selection (von Boehmer, 1990). In contrast with this model, mice lacking thymic dendritic cells and medullary TECs fail to mediate deletion of potentially autoreactive thymocytes (Lauffer et al., 1996). T cells expressing TCRs that utilize V_β segments that bind strongly to endogenous mouse mammary tumor virus (MMTV) superantigens are found in the periphery indicating a failure to delete potentially autoreactive cells. Since only cortical TECs express MHC molecules in the thymus of these mice, this supports the idea that medullary cells are required for negative selection.

Histological examination of the thymic stroma of various transgenic mouse models used to examine positive and negative selection indicate organizational defects of the medulla of these mice (Brabb et al., 1997). Mice that express transgenic TCRs on thymocytes against a background expected to promote positive selection of thymocytes do not have a centrally organized medulla. Phenotypic analysis indicates dendritic cells and medullary TECs are present in foci scattered throughout the cortex. Examination of

the thymic stroma using mice that express transgenic TCRs against a background that should induce deletion of these cells reveals even greater scattering of medullary foci throughout the cortex. Thus, deletion of autoreactive thymocytes in the cortical region does not mean cortical TECs are actually mediating deletion.

Labeling DNA strand breaks in apoptosing cells can be done by the TUNEL method and this provides an *in situ* method to examine the outcome of positive and negative selection. Analysis of thymus tissue sections from MHC-deficient mice indicates apoptosing cells are confined to the cortex and are as frequent as apoptotic cells in thymic tissue from normal mice (Surh & Sprent, 1994). This experimental approach assumes that in the absence of positive selection, thymocytes will die by neglect. Since apoptotic thymocytes are confined to the cortex, the data can be interpreted to indicate positive selection occurs in the cortex. A similar approach was used to determine the anatomic site of negative selection. Mice expressing certain endogenous MMTV antigens and MHC class II I-E molecules delete all TCRs that have utilized $V_\beta 5$ gene segments. I-E$^+$ or I-E$^-$ mice were crossed with $V_\beta 5$ transgenic mice then thymus sections were examined. Tissue sections from I-E$^+$ mice, but not I-E$^-$ mice, indicate apoptotic thymocytes are now detectable in the medulla and cortico-medullary junction. Although this suggests negative selection occurs in this region of the thymus, it does not exclude negative selection could occur in the cortex followed by thymocyte migration and apoptosis in the medulla.

Differentiating thymocytes make physical contact with different types of stromal cells in a sequential manner. Using mice congenic for cell surface Thy-1, donor thymocytes in bone marrow chimeras can be tracked as they differentiate (Kyewski,

1987). Donor thymocytes are found physically associated in a temporal manner first with thymic macrophages then thymic nurse cells and finally with dendritic cells. Since these stromal cells have distinct anatomical sites within the thymus, this data suggests thymocytes migrate through the thymus. Additional evidence suggesting thymocytes track through the cortex into the medulla as they undergo positive and negative selection is based on observations that thymic epithelium requires physical interaction or proximity with thymocytes to develop and mature. Cyclosporin A treatment inhibits progression of cortical DP thymocytes to the SP stage and immunohistochemical analysis of the thymus indicates the medulla and medullary stromal cells are virtually absent in these mice while the cortex appears normal (Ritter & Boyd, 1993). SCID mice and RAG1 or RAG2 knockout mice have small medullary regions that are sparsely populated with stromal cells. This anatomical defect can be reversed by injection of bone marrow containing precursor cells suggesting thymocyte development stimulates stromal development (van Ewijk et al., 1994). Histological analysis of thymus tissue from TCR_{α}-deficient mice and SCID mice crossed with $TCR_{\alpha\beta}$ or TCR_{β} transgenic mice indicates $TCR_{\alpha\beta}$ expression restores normal thymus architecture to SCID mice. TCR_{α}-deficient mice produce DP thymocytes, but lack SP thymocytes and this phenotype correlates with a lack of medullary stromal cell development. Blocking thymocyte differentiation at an early stage by creating human $CD3\varepsilon$ receptor transgenic mice or IL2-deficient mice inhibits or decreases the development of DP thymocytes and causes abnormal cortical and medullary architecture (Hollander et al., 1995; Reya et al., 1998). This correlative evidence suggests thymocytes at different stages of maturation stimulate the generation and/or organization of different thymic stromal compartments. Since specific maturational subsets are

required for the development of different stromal regions, this implies thymocytes must migrate through these regions and again emphasizes the requirement of thymocytes to be migratory cells.

1.2.2 ECM components in the thymus

The thymic microenvironment contains several different ECM components in addition to stromal cells and thymocytes. Although interactions between thymocytes and stromal cells are critical for thymocyte selection and are mediated by MHC, TCR, CD4 and CD8 molecules, contacts between ECM and thymocyte ECM receptors are also important to promote adhesive contacts during sessile phases of development and to mediate motility when thymocytes migrate through the thymus. Immunohistochemical analysis of the thymus of human neonates indicates the septae separating thymic lobules contain types I and III collagen (Berrih et al., 1985; Watt et al., 1992). The basement membranes adjacent to interlobular septae and intralobular perivascular spaces contain type IV collagen, Fn and laminin and these components extend into the subcapsular cortex. In contrast with other organs, basement membrane ECM components are also distributed within thymic lobules. Connective fibers at the cortico-medullary junction contain an abundance of Fn and the three types of collagen. The medulla contains extracellular Fn and laminin and laminin also appears to be intracellularly expressed in medullary TECs. Characterization of murine and human laminin expression by PCR and ELISA indicate thymic TECs actually express merosin, but not laminin (Chang et al., 1993). Laminin and merosin share two light chains, but each has a unique third chain that characterizes the two similar ECM proteins. Previous studies likely utilized antibody reagents that cross-react with laminin and merosin.

The appearance of ECM components in the thymus rudiment occurs soon after bone marrow-derived cells seed the thymus and thymic stromal cells begin to differentiate (Haynes, 1984; Patel et al., 1995). Fn is detectable in the human fetal thymus along the thymic capsule and proximal to stromal cells within the developing thymus by the 8th week of gestation. At later stages of development as the medulla becomes apparent, Fn is distributed through the medulla and around Hassel's bodies. HA has a similar distribution pattern as Fn, but is not detectable until the 16th week of gestation when thymocyte differentiation is underway. *In vitro* cultures of thymic epithelial cultures secrete types I and IV collagen, laminin and Fn suggesting the thymic ECM is produced, at least in part, by intrathymic TECs (Berrih et al., 1985).

Stromal cell differentiation and compartmentalization of the thymus seems dependent on the arrival of bone marrow derived progenitors and their differentiation into thymocytes (Ritter & Boyd, 1993; van Ewijk et al., 1994). Examination of the ontogeny of the murine thymus indicates the distribution patterns of ECM components are also related to the kinetics of thymus compartmentalization (Lannnes-Vieira et al., 1991), thus ECM proteins might participate, at least indirectly, in thymocyte differentiation. At day 13 of gestation type I collagen is restricted to the thymic capsule, while laminin (presumably merosin) is distributed in the capsule and around a few stromal cell clusters. Type IV collagen and Fn are distributed throughout the developing thymus. The thymus is not yet compartmentalized at this stage of ontogeny. By day 17 laminin is also distributed through the thymus and all three components are now distributed to basement membranes and intralobular perivascular spaces. At day 19 the thymus is compartmentalized and intralobular Fn, laminin and type IV collagen are predominantly

distributed to the medullary region. Interestingly, TCR_β-deficient mice and RAG knockout mice have increased thymic expression of ECM proteins whereas CD4 and $\beta 2$-microglobulin knockout mice have decreased distribution of medullary ECM components (Savino et al., 1998). This suggests the thymic ECM is also influenced by thymocyte ontogeny.

The distribution patterns of Fn and type IV collagen through the thymus rudiment suggest these components might guide the migration of bone marrow precursors from the blood vessels within the thymic capsule into the developing thymic cortex (Lannes-Vieira et al., 1991). It has been postulated ECM proteins act as a "conveyer belt" to guide the migration path of thymocytes through the thymus as differentiation proceeds (Savino, 1996). The ECM components could guide progenitors as they migrate deep into the cortex to initiate medullary development by providing ligand for cell surface adhesion/motility receptors to bind. ECM also lines the septae and might guide thymocyte precursors to or from the subcapsular cortex as they undergo differentiation and proliferation. Injection of neonatal mice with anti-Fn antibodies promotes downregulation of the CD3 complex (Savino et al., 1993), whereas immobilized Fn enhances the CD3-dependent proliferation of DN fetal thymocytes (Halvorson et al., 1998). Soluble antibodies to α_4 or α_5 integrins inhibit thymocyte proliferation indicating β_1 integrins are co-stimulatory molecules for differentiating thymocytes. ECM proteins might also stimulate the adhesion and proliferation of stromal cells in the thymus.

Cortical expression of collagens, laminin, Fn and HA is weak or absent in the thymus of neonates, except in the subcapsular cortex. Hydrocortisone treatment of mice or normal aging of mice and humans stimulates the appearance of cortical ECM proteins,

particularly Fn (Berrih et al., 1985; Lannes-Vieira et al., 1991). The distribution of these ECM components to the cortical region is associated with thymic atrophy. *In vitro*, murine thymocytes with a cortical phenotype appear to bind epithelial cell monolayers via cell-associated Fn (Utsumi et al., 1991) suggesting ECM components might be present in the cortex in association with stromal cells. Immunoelectron microscopy verifies that Fn is distributed adjacent to thymic nurse cells (TNCs) in proximity with thymocytes (Savino et al., 1993), but at concentrations apparently undetectable by immunohistochemical methods (Berrih et al., 1985). Using antibodies that specifically recognize splice variants of Fn verifies the human cortex contains little Fn, but the CS1 domain recognized by $\alpha_4\beta_1$ integrin is detectable, although it is still more abundant in the medulla (Crisa et al., 1996). TECs in the cortex and cortico-medullary junction express the $\alpha4\beta1$ ligand VCAM-1 suggesting intercellular binding might be mediated directly by cellular receptors (Salomon et al., 1997).

IFNγ enhances the expression of MHC molecules on TNCs as well as stimulating the secretion of type IV collagen and the expression of α_5 and α_6 integrin subunits (Lagrota-Cândido et al. 1996). IFNγ is secreted by thymocytes and at low concentration enhances the adhesion of thymocytes to epithelial cell lines. Antibodies to Fn, laminin, type IV collagen, α_5 or α_6 integrins significantly decrease adhesion suggesting these receptors and ECM proteins function in mediating cellular interactions in the cortical region of the neonatal thymus. This group suggests the ECM components link thymocytes with stromal cells when receptors on adjacent cells jointly bind soluble ECM components (Savino et al., 1993). ICAM-1 expression is also upregulated by IFNγ as

well as IL1 and TNF, thus thymocytes might also interact with stromal cells via LFA-1

and ICAM-1 (Singer et al., 1990).

1.2.3 Integrin-mediated adhesion and motility in thymocyte ontogeny

Bone marrow-derived progenitors seed the thymus by emigrating from blood

vessels into the developing thymus. Stem cell colonization of the thymic rudiment occurs

prior to development of the thymic vasculature, so progenitors exit pharyngeal vessels

and migrate through mesenchymal tissue that forms the thymic capsule to reach the

developing epithelial component of the thymus (Anderson et al., 1996). There is virtually

no data available that identifies the receptors required for emigration into the thymus, but

presumably the mechanism is similar to the multistep paradigm that describes how

peripheral blood leukocytes home to lymphoid organs and sites of inflammation

(Springer, 1994). Progenitors must express cell surface molecules that mediate rolling

and tethering to cells lining pharyngeal vessels. L-selectin and $\alpha_4\beta_7$ integrins mediate

lymphocyte homing to peripheral lymph nodes and mucosal lymphoid tissues (Dunon et

al., 1996) and pro-thymocytes express these receptors (Dianzani & Malavasi, 1995;

Andrews et al., 1996). The vascular endothelium of the human fetal thymus expresses an

L-selectin ligand called MECA-79 that potentially mediates rolling of progenitors in

thymic blood vessels. MECA-79 also binds to carbohydrate determinants expressed by

high endothelial venule CD34 and GlyCAM-1 (Springer, 1994), thus in the developing

thymus CD34 expressed by progenitors might mediate homing by binding MECA-79.

$\alpha_4\beta_7$ integrin in conjunction with L-selectin mediates rolling upon interaction with

MAdCAM-1, but it is not known if the thymic vasculature expresses MAdCAM-1

(Dunon et al., 1996). $\alpha_4\beta_7$ integrins, similar to $\alpha_4\beta_1$ integrins, might also mediate

adhesion to endothelium via VCAM-1, thus $\alpha_4\beta_7$ could participate in homing of progenitors to the thymus rudiment.

The adhesion receptor CD44 is expressed by progenitors and is transiently downregulated early in differentiation (Res & Spits, 1999). CD44 mediates adhesion to the glycosaminoglycan HA and might promote rolling on HA-coated surfaces (Dunon et al., 1996). CD44 expression is downregulated as progenitors differentiate and lose their adhesion dependence on mesenchymal tissue (Anderson et al., 1996). β_6 integrins mediate adhesion of pro-thymocytes to endothelial cells (Dunon & Imhof, 1993) suggesting CD44 and β_6 integrins might mediate adhesion of circulating progenitor cells to the mesenchyme and vascular endothelial cells, respectively, that are proximal to the primordial thymus. However, it can only be speculated that these receptor interactions function in homing of progenitors to the thymic rudiment. The low frequency of thymocyte progenitors makes it difficult to directly assess the potential involvement of molecules in homing, especially in fetal models.

A more definitive approach to assess receptors involved in homing of progenitors to the thymus is to use murine models in which receptor expression has been eliminated. β_1 and α_4 integrin knockout mice fail to seed the thymus with bone marrow-derived cells (Hirsch et al., 1996; Arroyo et al., 1996). This implicates $\alpha_4\beta_1$ integrin in homing of thymocyte progenitors to the thymus. $\alpha_4\beta_1$ integrins mediate adhesion of peripheral leukocytes to VCAM-1 expressed on endothelial cells of blood vessels (Dunon et al., 1996). This interaction can facilitate rolling and adhesion to blood vessel walls (Reinhardt et al., 1997b) prior to leukocyte extravasation. The inability of bone marrow-derived progenitors to roll and adhere to blood vessels and initiate extravasation could

abrogate colonization of the thymic rudiment. $\alpha_4\beta_1$ integrins also mediate cell migration through basement membranes and tissue spaces by binding to the ECM component Fn. Early in thymic ontogeny Fn is detectable throughout the thymic epithelium, in basement membranes and perivascular spaces (Haynes, 1984; Lannes-Vieira et al., 1991). This suggests $\alpha_4\beta_1$ integrin could mediate migration of progenitors into the developing thymus.

Immature thymocytes are more abundant than thymocyte progenitors, so more data is available regarding the role of adhesion receptors in fetal and neonatal models when the thymus is developed. Interactions between stromal cells and developing thymocytes are required for positive and negative selection and for exchange of soluble factors like cytokines and thymic hormones (Ritter & Boyd, 1993; Mello-Coeho et al., 1998). There are several molecules expressed by immature thymocytes and thymic stromal cells that mediate intercellular interactions. The homotypic adhesion molecule, E-cadherin, is expressed by day 16 fetal mouse thymocytes and thymic epithelial cells suggesting E-cadherins mediate interactions between these two cell types early in ontogeny and perhaps direct homing of progenitors to the thymus rudiment (Lee et al., 1994). $\alpha_E\beta_7$ integrin has been reported to bind E-cadherin (Cepek et al., 1994) and is expressed by day 14 fetal thymocyte precursors (Anderson et al., 1996). CD2 is expressed at low levels by human thymocyte progenitors and expression is increased on pro-thymocytes (Haynes, 1986). LFA-3, the ligand of CD2, is expressed by all intra-thymic epithelial cells. All thymocyte subsets adhere to LFA-3^{+} TEC cultures via CD2 and this interaction stimulates thymocytes to proliferate and upregulate IL2-R expression. This indicates CD2 acts as a co-stimulatory molecule for differentiating thymocytes.

However, CD2 does not likely mediate entry of progenitors into the developing thymus, since there is no expression of LFA-3 on subcapsular epithelium (Watt et al., 1992).

LFA-1 is highly expressed by murine and human thymocytes (Sawada et al., 1992; Crisa et al., 1996). MAbs to common domains of CD45 stimulate homotypic aggregation of thymocytes that is at least partially mediated by LFA-1/ICAM-3 interactions (Bernard et al., 1994). Thymocyte LFA-1 molecules also interact with ICAM-1 on thymic epithelial cells and these interactions are required for the maturation of DN thymocytes to the DP stage (Fine & Kruisbeek, 1991). LFA-1 interactions with ICAM-1 on dendritic cells also seem to be required for negative selection to be initiated (Carlow et al., 1992). These receptors might stabilize inter-cellular interactions while signaling between TCR and MHC molecules occurs. These data suggest LFA-1 mediates intercellular adhesion throughout thymocyte differentiation. Although LFA-1 mediates extravasation of monocytes through endothelial cell monolayers (Weber & Springer, 1998), subcapsular cortical epithelium does not express ICAM-1 in the neonatal thymus (Watt et al., 1992) suggesting extravasation of progenitors is mediated by different receptor interactions prior to the vascularization of the thymus. However, this observation does not rule out that ICAM-1 is expressed by primordial capsular tissue early in ontogeny or that ICAM-2 or ICAM-3 might be involved, especially since ICAM-2 can act as a homing ligand in non-inflamed tissue (Springer, 1994).

The distribution patterns of ECM components alter during thymic ontogeny and thymocyte differentiation, thus several groups have examined thymocyte ECM-binding integrins to determine if a correlation exists between thymocyte development and integrin expression and function. Immunohistochemical staining of the human thymus as well as

staining of thymocyte suspensions and thymic epithelial cultures indicate a number of integrins are expressed on both cell types. Both fetal and post-natal epithelial cultures express α_3, α_6, and β_1 integrin subunits and weakly express α_2 integrin (Watt et al., 1992). All thymocyte subsets express variable levels of α_4, α_5, α_6 and β_1 integrins while α_2 and α_3 integrins are very weakly expressed (Watt et al., 1992; Salomon et al., 1994). α_4 integrin expression is higher on immature thymocytes compared with mature SP thymocytes while the reverse is true for α_6 integrin expression. Immunohistochemical staining of thymus sections indicates α_6 integrin is highly expressed by thymocytes at the subcapsular cortex and medulla, but is restricted to perivascular areas in the cortex. α_4 integrin expression is higher on cortical thymocytes than on medullary thymocytes. These observations suggest integrins might function on thymocytes during different stages of thymocyte differentiation (Fig. 1.1). $\alpha_6\beta_4$ integrin binds laminin and is predominantly expressed by DN murine thymocytes (Wadsworth et al., 1992). Laminin (or perhaps merosin) is distributed at the thymic capsule early in ontogeny and might guide pro-thymocytes into the developing organ early in ontogeny. The merosin binding integrin $\alpha_6\beta_1$ is also expressed by immature murine thymocytes (Chang et al., 1993).

Fn is abundantly expressed throughout the developing thymus and is also expressed in the medulla, the subcapsular region and at low levels in the cortex once the thymus is compartmentalized (Berrih et al., 1985; Watt et al., 1992; Crisa et al., 1996). This has led to a close examination of the expression patterns of the Fn-binding integrins $\alpha_4\beta_1$ and $\alpha_5\beta_1$ on thymocyte subsets. The majority of murine DN thymocytes

Thymocyte Subset	Integrins Mediating Adhesion to Fn	Integrins Mediating Motility to Fn
CD3⁻4⁻8⁻ (MN)	$\alpha_4\beta_1$ +/- $\alpha_5\beta_1$ integrins	$\alpha_4\beta_1$ integrins
CD4⁺8⁺ (DP)	$\alpha_4\beta_1$ integrins	Poorly motile on Fn
CD4⁺8⁻ & CD4⁻8⁺ (SP)	Poorly adhesive to Fn	$\alpha_4\beta_1$ and $\alpha_5\beta_1$ integrins

Figure 1.1 As human thymocytes differentiate, both cell behavior and usage of Fn-binding receptors alters.

The flow chart summarizes work from different reports. The boxes indicate the major thymocyte subsets based on their expression of CD4 and CD8 and the arrows indicate the sequence of differentiation. Adjacent to each subset the predominent type of behavior on Fn is indicated as are the integrins mediating the behavior.

spontaneously adhere to Fn-coated plates and to stromal cell monolayers utilizing α_4 predominantly and α_5 integrin to a lesser extent (Utsumi et al., 1991; Sawada et al., 1992). Fn is indicated as are the integrins mediating the behavior. Neither unfractionated nor DN thymocytes adhere to collagen-, laminin- nor vitronectin-coated surfaces. As murine thymocytes mature to the DP and SP stage they express lower levels of α_4 integrin and the adhesive function of α_4 is downregulated while expression of LFA-1 is concomitantly increased (Sawada et al., 1992). *In vitro* culture of DN thymocytes on stromal cells promotes differentiation of a fraction of this subset to the DP stage and anti-Fn antibodies alone or in combination with $\alpha_4\beta_1$ or $\alpha_5\beta_1$ integrin-specific Fn peptides abrogate differentiation (Utsumi et al., 1991). CD3-dependent proliferation of DN thymocytes is co-stimulated by Fn or immobilized mAbs to α_4 or α_5 integrin subunits (Halvorson et al., 1998) suggesting thymocyte interactions between integrins, Fn and stromal cells stimulate thymocyte maturation. Detectable proliferation of thymocytes occurs in the subcapsular cortex (Haynes, 1984) and Fn is also detectable in this region (Watt et al., 1992). However, thymocyte proliferation is also CD3-dependent suggesting intercellular interactions are required. This suggests that for $\alpha_4\beta_1$ integrin to be co-stimulatory, it might require interactions with VCAM-1 expressed on thymic epithelial cells.

MN human thymocytes contain Fn-adherent cells and mAbs to α_4, α_5 and β_1 integrin subunits inhibit adhesion to Fn, suggesting $\alpha_4\beta_1$ and $\alpha_5\beta_1$ integrins also mediate interactions of immature human thymocytes with thymic stroma or ECM components (Gares et al., 1998). Although human thymocytes maintain expression levels of $\alpha_4\beta_1$

integrins as they mature to the DP stage while murine DP thymocytes downregulate α_4 integrin expression, the adherent fraction of DP thymocytes in mice and humans is equivalent (Sawada et al., 1992; Salomon et al., 1994). Fn-adherent human thymocytes have a phenotype consistent with DP cells that have not yet received a positive selection signal ($CD4^{hi}8^{hi}3^{med}69^{lo}$) while non-adherent thymocytes contain DP thymocytes with a "post-selection" phenotype ($CD4^{med}8^{med}3^{hi}69^{hi}$) indicating the non-adherent DP cells are more mature cells (Salomon et al., 1994). However, α_4 integrin expression on non-adherent cells is equivalent to that of less mature DP thymocytes, suggesting the lack of adhesive behavior results from the downregulation of α_4 integrin function. The correlation between adhesive behavior and subsequent maturation of DP thymocytes suggests $\alpha_4\beta_1$ integrins might facilitate strong adhesion between thymocytes and cortical epithelial cells during positive selection. Primary TEC cultures express VCAM-1 and α^4 integrins mediate interactions between thymocytes and cultured TECs (Salomon et al., 1997). Immunohistochemical analysis indicates VCAM-1 expression is restricted to TECs in the cortex and corticomedullary junction. This suggests strong adhesive interactions between thymocytes and stromal cells likely occur in these two thymic regions. There is considerable evidence that positive selection occurs in the cortex, followed by migration to the cortico-medullary junction and the medulla.

Since one of the consequences of positive selection appears to be an alteration of $\alpha_4\beta_1$ integrin to a conformation promoting de-adhesion, the motility of thymocyte subsets has been assessed to determine if decreased adhesion correlates with motile behavior. Although MN thymocytes express both α_4 and α_5 integrins, only mAbs to α_4 or β_1 inhibit motility suggesting $\alpha_4\beta_1$ integrin mediates motility for MN thymocytes (Gares & Pilarski,

1999). DP and SP thymocytes use a combination of $\alpha_4\beta_1$, $\alpha_5\beta_1$ and RHAMM to mediate motility on Fn-coated surfaces or through Fn-coated transwells (Crisa et al., 1996; Gares et al., 1998). Phenotypic analysis of migratory thymocytes indicates the majority of this fraction contains SP thymocytes and $CD3^{hi}4^{med}8^{med}69^{hi}$ thymocytes, the latter postulated to be migratory cells that have undergone positive selection (Crisa et al., 1996). Purification of thymocyte subsets prior to assessing their motility indicates approximately 40% of MN thymocytes are motile along with a fraction of the DP subset and $CD4^+$ SP thymocytes (Gares et al., 1998; Gares & Pilarski, 1999). The expression and function of $\alpha_4\beta_1$ and $\alpha_5\beta_1$ integrins on thymocytes that have presumably undergone positive selection and the prevalent distribution of Fn in the cortico-medullary junction and the medulla suggest these integrins function to guide positively selected thymocytes from the cortex into the medulla.

Laminin (or merosin) and collagen are also distributed to the cortico-medullary junction and in the medulla, but integrins that interact with these components are poorly expressed by thymocytes and *in vitro* assays show poor adhesion and poor migration of thymocytes on surfaces coated with these components (Utsumi et al., 1991; Crisa et al., 1996). Although a contribution by these components to thymocyte migration cannot be ruled out, it might be more subtle and difficult to quantitate. $\alpha_E\beta_7$ integrin is expressed by a subset of SP thymocytes and $\alpha_4\beta_7$ integrin is expressed by a subset of SP $CD4^+$ thymocytes (Andrew et al., 1996), but anti-$\alpha_4\beta_7$ mAbs do not abrogate Fn-mediated migration (Crisa et al., 1996). Since these integrins are involved with trafficking of peripheral lymphocytes to secondary lymphoid organs, the expression of β_7 integrins on

mature thymocytes might identify mature thymocytes that have survived selection and are ready to emigrate the thymus.

These experiments using thymocyte differentiation as a model to study integrin function suggest integrins and the ECM play an important role in guiding thymocytes as they migrate through the thymus. Integrin-mediated signaling also co-stimulates thymocyte proliferation. This might be required because the co-stimulatory receptors normally used by mature T cells are uncoupled in immature thymocytes (Amsen & Kruisbeek, 1998). Integrins also function in the peripheral lymphoid system to promote adhesion and motility. Receptor occupancy of LFA-1 on T lymphoblasts downregulates adhesion of $\alpha_4\beta_1$ to VCAM-1 and Fn and promotes α_5 integrin-mediated migration (Porter and Hogg, 1997). Chemokines stimulate a sequential activation of $\alpha_4\beta_1$ then $\alpha_5\beta_1$ integrins on monocytes that promote motility (Weber et al., 1996). In the thymus, the high binding avidity of $\alpha_4\beta_1$ integrins on immature DP thymocytes supports interactions with cortical and cortico-medullary TECs that are presumably required during positive selection. In addition, the low distribution level of Fn in the cortex suggests interactions between thymocytes and cortical ECM are likely to be low avidity interactions that might promote motility while $\alpha_4\beta_1$ integrins are still in a high affinity binding conformation. As positively selected DP thymocytes migrate toward the cortico-medullary junction and the medulla, Fn concentrations increase, but $\alpha_4\beta_1$ integrin expression is decreased and low avidity interactions might support migration on higher concentrations of Fn.

1.3 The HA binding Protein RHAMM Mediates Cell Motility

RHAMM is an HA-binding protein that was originally isolated from locomotory embryonic chick heart fibroblasts (Turley, 1989) and subsequent molecular cloning indicated the nucleotide sequence was distinct from the HA binding protein, CD44 (Hardwick et al., 1992). Examination of developing tissues in which cells are required to be migratory indicates RHAMM is expressed and functions as a motility receptor (Turley at al., 1990; Boudreau et al., 1991; Pilarski et al., 1993; Nagy et al., 1995; Kornovski et al., 1994; Gares et al., 1998; Pilarski et al., 1999). RHAMM is also overexpressed by B cells isolated from patients with B cell malignancies and by human breast cell tumors implicating RHAMM in the malignant process (Crainie et al., 1999; Wang et al., 1998).

1.3.1   Cell surface RHAMM expression and HA binding are associated with motility

HA is a ubiquitously expressed glycosaminoglycan of the ECM and is a large polysaccharide consisting of repeating dimers of glucuronate and N-acetylglucosamine. HA plays a structural role in ECM providing turgor pressure in tissue spaces and acts as a cushion in joints, but smaller fragments of HA have been shown to mediate a number of cellular effects upon interaction with HA binding proteins or hyaladherins (Knudson & Knudson, 1993; Sherman et al., 1994; Entwistle et al., 1996; Fraser et al., 1997; Toole, 1997; Borland et al., 1998). These investigations have indicated that HA mediates motility, endocytosis, signal transduction and cytokine secretion upon interaction with the hyaladherins RHAMM or CD44.

HA is a poorly adhesive substrate, so early models suggested HA was involved in the detachment process of locomotion. Using an embryonic chick heart fibroblast model

system, it was shown that addition of HA promoted membrane ruffling and random locomotion of cells (Turley & Torrance, 1985). HA also generates the production of second messengers indicating an HA binding receptor (s) is involved (Turley, 1989). Isolation of an HA binding protein (HABP) from fibroblast cell lines and primary chick heart fibroblasts led to the generation of immune sera and subsequent characterization of this protein. Using anti-HABP antibodies and labeled HA indicated HA and the HABP (RHAMM) co-localize and distribute to the leading and trailing edges of locomoting chick heart fibroblasts (Turley & Torrance, 1985).

Transmission electron microscopy and scanning electron microscopy of embryonic chick heart fibroblasts stained with anti-RHAMM sera and gold particles clearly demonstrate surface expression of RHAMM predominently on cell protrusions (Turley et al., 1990). However, when cells are cultured longer than 12 H, surface expression is downregulated and RHAMM is found distributed intracellularly in a perinuclear and intranuclear pattern (Turly & Torrance, 1985). Other types of motile cells express cell surface RHAMM as indicated by flow cytometric analysis and fluorescence microscopy. Cell surface RHAMM is detectable on cells undergoing developmental processes or differentiation such as thymocytes, neurons, sperm cells and stem cells (Pilarski et al., 1993; Kornovski et al., 1994; Nagy et al., 1995; Pilarski et al., 1999). Malignant and transformed cells also express cell surface RHAMM (Turley & Auersperg; 1989; Turley et al., 1993; Masellis-Smith et al., 1996; Crainie et al., 1999). Since cells from developing tissues are often migratory and highly malignant cells are often metastatic, cell surface expression of RHAMM correlates with locomotory behavior. This suggests RHAMM is involved with the motile process. Several different murine and

human carcinoma cell lines have been examined for RHAMM expression and only intracellular RHAMM is detected in cell lines (Assmann et al., 1998; Hofmann et al., 1998; Assmann et al., 1999). This suggests RHAMM might be expressed as an intracellular protein by most adherent cells, but under conditions stimulating cell motility RHAMM is also expressed at the cell surface.

Other model systems indicate RHAMM-mediated motility can be stimulated within 1 to 6 H following wounding of smooth muscle cell monolayers or subculture of fibroblast cell lines (Turley, 1992; Savani et al., 1995). Fibroblasts transfected with an inducible *ras* gene or treated with TGFβ express cell surface RHAMM and become highly motile, with peak surface expression of RHAMM correlating with peak motility (Turley et al., 1991; Samuel et al., 1993). Smooth muscle monolayers begin to express cell surface RHAMM at wound edges coincident with the onset of migration by cells at the wound edge (Savani et al., 1995). The addition of HA also rapidly upregulates cell motility which can be blocked by RHAMM-specific antibodies. This rapid adaptation of cells to a change in their microenvironment suggests HA might modulate RHAMM expression and cell behavior.

1.3.2 Molecular and biochemical characterization of RHAMM

The RHAMM DNA sequence was initially isolated from a λgt11 cDNA expression library prepared from 3T3 fibroblasts (Hardwick et al., 1992). Antiserum and mAbs generated against the original HABP isolate were used to identify clones that expressed HABP. Subsequent cloning and DNA sequencing indicated the RHAMM sequence encodes a 476 amino acid (aa) protein with a sequence distinct from CD44. Antiserum generated against a peptide sequence of the deduced amino acid sequence of

the cloned RHAMM sequence was used to stain TGFβ-stimulated fibroblasts and to inhibit cell motility. The anti-RHAMM peptide serum stains cells and decreases motility similarly compared with mAbs and antiserum generated against the original HABP. Thus, it was concluded the isolated DNA sequence encoded a protein identical to the original HABP isolate.

RHAMM was originally isolated and purified using sepharose-HA affinity columns and the purified fraction actually contained three proteins with apparent molecular weights of 70, 66 and 56 Kd. These three proteins were assumed to exist on the cell surface as a complex of proteins called the HA receptor complex (HARC) (Turley et al., 1987). A protein band of 58 Kd is detected in lysates of TGFβ-stimulated cells immunoblotted with anti-RHAMM peptide serum, suggesting RHAMM is the 56 Kd component of HARC (Hardwick et al., 1992). However, biochemical analysis of murine fibroblast, *ras*-transformed fibroblast, lung carcinoma and melanoma cell lines using a different anti-RHAMM serum detects a much larger 95 Kd protein (Hofmann et al., 1998). Sequence analysis of genomic murine RHAMM indicates the RHAMM gene is comprised of 18 exons predicted to be translated into a 95 Kd protein (Fieber et al., 1999), verifying the biochemical data. Comparison of the original RHAMM sequence indicates the clone used to sequence RHAMM begins in approximately the middle of the actual RHAMM sequence and includes the carboxy terminus (Hardwick et al., 1992).

Human RHAMM DNA was sequenced using a λgt11 cDNA expression library prepared from human breast cells in combination with mRNA isolated from a human breast epithelial cell line (Wang et al., 1996). The DNA sequence indicates human RHAMM encodes a 725 aa protein with a predicted molecular weight of 84 Kd, although

immunoblots of breast epithelial cell lysates detect RHAMM protein bands of 84, 70 and 60 Kd. Comparison of the human sequence with the complete murine RHAMM sequence indicates the deduced aa sequences are approximately 85% homologous (Hoffmann et al., 1998).

Immunoblots of lysates prepared from various cell types consistently detect RHAMM protein bands of two to three different apparent molecular weights (Turley et al., 1987; Kornovski et al., 1994; Nagy et al., 1995; Wang et al., 1996; Hofmann et al., 1998) suggesting multiple isoforms of RHAMM are expressed. Analysis of RHAMM mRNA from different cell types has identified four RHAMM variants. Three different RHAMM transcripts have been isolated from *ex vivo* B and plasma cells from multiple myeloma patients (Crainie et al., 1999). One form is a full length transcript containing all encoding exons (RHAMM^{FL}), a second species contains a 48 bp deletion (RHAMM^{-48}) that corresponds to excision of exon 4 and the third species contains a 147 bp deletion (RHAMM^{-147}) that corresponds to excision of exon 13 (Fig. 1.2). RHAMM^{FL} and RHAMM^{-48} mRNA are highly expressed by B or plasma cells isolated from myeloma, lymphoma and leukemia patients, but not from B cells isolated from Crohn's patients or normal individuals. RHAMM^{-147} mRNA is less frequently expressed in B or plasma cells from myeloma patients and is undetectable in other types of malignant or normal B cells. Human breast carcinoma cell lines express RHAMM mRNA that corresponds to RHAMM^{FL} and RHAMM^{-48} except one GAA codon is absent such that only 45 bp are contained in exon 4 (Assmann et al., 1998). Human cervical cancer cell lines also express transcripts corresponding to RHAMM^{-147} and an additional type of RHAMM
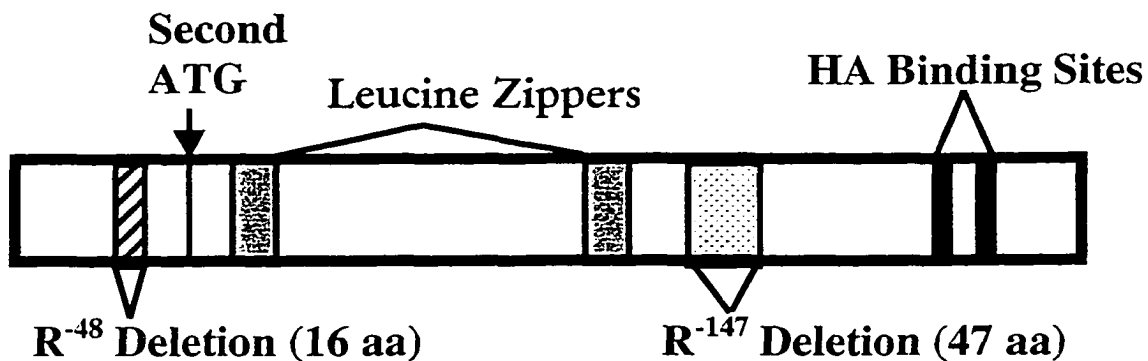
Figure 1.2 Characterized domains of RHAMM

The full length RHAMM molecule (RHAMM^{FL}) is depicted and the approximate locations of characterized domains are indicated. The approximate location of exon 4 (R^{-48} deletion) and exon 13 (R^{-147} deletion) are indicated and excision of these two exons from the coding sequence produces RHAMM^{-48} or RHAMM^{-147}, respectively. The two leucine zipper motifs are predicted from the amino acid sequence. The two HA binding domains are encoded by exons 16 and 17.

transcript in which both exon 4 and exon 13 have been spliced out (Assmann et al., 1999). Each of these molecularly characterized RHAMM isoforms is translated into a protein with a molecular weight consistent with that predicted from the deduced amino acid sequence (Assmann et al., 1999).

RHAMM also contains two translation start codons (Fig. 1.2). Translation of human RHAMM mRNA from the +1 position would give rise to a 725 aa protein, whereas translation from the second start codon would yield a protein of 610 aa (Crainie et al., 1999). Variant usage of these start codons is currently being investigated and could provide another explanation for the size variation of RHAMM proteins. RHAMM might also be subject to partial degradation and this could account for the low molecular weight bands detected in immunoblots. Whether RHAMM is subject to post-translational modification such as glycosylation or phosphorylation is not known, but protein domain prediction programs indicate there are four N-glycosylation sites and several potential phosphorylation sites. There are also three potential N-myristylation sites and two leucine zipper motifs.

1.3.3   Functional domains of RHAMM

RHAMM was originally isolated by its ability to bind to a HA-sepharose affinity column indicating RHAMM should contain HA binding domains. Motility assays indicate exogenous HA stimulates RHAMM-dependent locomotion and TGFβ-stimulation or *ras*-transfection stimulates endogenous production of HA (Turley et al., 1991; Samual et al., 1993). Bovine smooth muscle monolayers also secrete HA after wounding and HA is distributed exclusively to the wounded edge along with RHAMM (Savani et al., 1995). The HA binding domain was identified using truncated RHAMM

fusion proteins and a transblot assay and is localized to two regions near the carboxy terminus (Yang et al., 1993). The HA binding motif was characterized using mutational analysis and consists of two basic amino acids with an intervening span of seven non-acidic amino acids (BX_7B) (Yang et al., 1994). HA binding is optimal if at least one of the intervening residues is also basic. The two HA binding motifs near the carboxy end of RHAMM are encoded by exons 16 and 17 (Fig. 1.2). HA binding to both domains appears to be additive, indicating the two HA binding domains function independent of one another. Peptides to the HA binding domains decrease locomotion indicating HA binding to RHAMM is required to mediate motility for TGFβ-stimulated fibroblasts (Samual, et al., 1993).

This HA binding motif has also been localized to characterized HA binding regions in the hyaladherins CD44 and link protein (Yang et al., 1994), thus may be a universally used HA binding motif. One of the HA binding motifs identified in the CD44 sequence corresponds precisely to a recently identified ERM protein binding region (Legg & Isacke, 1998). The ERM protein ezrin binds to CD44 between aa 292 – 300, an intracellular membrane proximal region of CD44. This region is not a characterized HA binding region of CD44, but ERM proteins in general bind to protein sequences with a motif that is virtually identical to the characterized HA binding motif (Bretscher, 1999). Interactions of HA and hyaladherins during embryonic chick joint development demonstrates the ERM protein moesin redistributes with actin to sites of joint cavity formation where cell surface CD44 binds HA (Dowthwaite et al., 1998). Moesin-mediated interactions between CD44 and the actin cytoskeleton might stimulate HA binding by activating CD44. Endocytosed HA might bind to the intracellular HA binding

domain of CD44 and interrupt the interaction of moesin and CD44. Alternatively, moesin might protect this site from interaction with endocytosed HA. The effect of these associations is unknown, but CD44 is redistributed to the uropod of migrating T cells where it is associated with ERM proteins in a process that is likely de-adhesive. RHAMM is also expressed in developing joint tissue, so it would be of interest to determine if RHAMM distribution is regulated by interaction with ERM proteins.

Confocal analysis indicates intracellular RHAMM co-localizes with α-tubulin to the MT cytoskeleton and the mitotic spindle in HeLa cells (Assmann et al., 1999). In a human mammary carcinoma cell line, RHAMM distributes to focal adhesions and demonstrates a minor co-localization with actin stress fibers. HeLa cells transfected with GFP tagged to the RHAMM sequence or to RHAMM lacking exon 13 co-localize with the MT cytoskeleton. GFP-RHAMM fusion proteins lacking the exon 4 encoding sequence localize predominantly to the nucleus, do not interact with MTs in cells nor with polymerized tubulin in an *in vitro* tubulin-binding assay. This suggests the MT binding sequence is at least partially encoded by exon 4. However, sequence analysis indicates RHAMM does not share obvious homology with other MT binding proteins. Sequence analysis also predicts the central domain of RHAMM, which contains two leucine zippers (Fig. 1.2), likely forms a coiled-coil domain. This suggests RHAMM could form homodimers or heterodimers.

1.3.4 RHAMM is associated with signal transduction activity

Although RHAMM is expressed at the cell surface, sequence analysis does not indicate a distinct transmembrane domain, so RHAMM might use a docking protein to maintain surface expression (Entwistle et al., 1996). Despite the lack of an obvious

transmembrane domain, HA binding to RHAMM is associated with activation of signal transduction components. HA stimulation of *ras*-transfected fibroblasts might enhance locomotion by causing turnover of FAs. Addition of HA or certain anti-RHAMM antibodies to fibroblasts correlates with the rapid phosphorylation of FAK and several other proteins and the increased deposition of vinculin in FAs (Hall et al., 1994). These events occur rapidly following the addition of HA, but are turned over within 15 min. Using murine fibroblasts expressing a dominant negative mutant of $pp60^{src}$ inhibits RHAMM-dependent locomotion, while a cell line expressing a constitutively active v-*src* gene demonstrates enhanced motility that is independent of RHAMM (Hall et al., 1996). This suggests src is a downstream factor of the signal transduction path stimulated by HA binding to RHAMM.

Examination of metastatic cells isolated from breast cancer patients indicates that RHAMM is overexpressed compared with cells from the primary tumor and RHAMM overexpression correlates with overexpression of *ras* and ERK (Wang et al., 1998). Anti-RHAMM antibodies decrease the PDGF-stimulated activation of ERK in murine fibroblasts, suggesting RHAMM acts as a co-stimulator of the ERK signal transduction cascade (Zhang et al., 1998). Transfection of fibroblasts with antisense sequences corresponding to a murine RHAMM isoform, RHAMMv4, or transfection of cells using RHAMM dominant negative genes inhibits *ras*-mediated activation of ERK and subsequent nuclear localization. Conversely, overexpression of RHAMM correlates with constitutive activity of ERK. Anti-RHAMM antibodies co-immunoprecipitate ERK1 and MEK1 suggesting intracellular RHAMM associates with ERK1 and MEK1. The reciprocal experiment indicates that anti-ERK1 antibodies co-immunoprecipitate

RHAMM. These observations suggest HA interactions with cell surface RHAMM are associated with signal transduction events that turn over FAs and stimulate cell locomotion. This suggests HA interactions with RHAMM mediate de-adhesive events for locomotory cells by decreasing adhesive contacts. Intracellular RHAMM is associated with the activation of signal transduction factors involved in proliferation, integrin-mediated adhesion and motility, thus intracellular RHAMM might have an indirect role in promoting or inhibiting cell locomotion.

1.4 Thesis Objectives

Background:

As thymocytes differentiate they migrate through the thymic microenvironment. Integrins are expressed by thymocytes and promote adhesive or motile behavior, thus are intimately associated with thymocyte development. Cell surface RHAMM is also expressed by thymocytes and mediates motility for thymocytes on Fn-coated surfaces (Pilarski et al., 1993). This suggests RHAMM interactions with HA might be associated with decreases of integrin affinity or avidity that promote locomotion. Three isoforms of RHAMM have been characterized (Crainie et al., 1999), thus regulation of RHAMM isoform expression might contribute to modulation of thymocyte behavior.

Overall Objective:

To examine how interactions between Fn and β_1 integrins and HA interactions with RHAMM stimulate adhesion or motility for *ex vivo* human thymocytes.

Working Hypothesis:

That the patterns of expression and function of β_1 integrins and RHAMM on *ex vivo* thymocytes will reflect the requirements of *in vivo* thymocytes to remain anchored or to migrate as they differentiate in the thymus. That modulation of the expression and function of Fn-binding β_1 integrins and of the HA binding receptor RHAMM will determine or contribute to anchored or migratory behavior of human thymocytes.

Specific Objectives:

1   To examine the relationship between β_1 integrins and RHAMM to determine how integrin-based adhesion to Fn and HA-stimulated, RHAMM-mediated motility are balanced to promote either cell adhesion or cell motility for differentiating thymocytes. These experiments will be done using timelapse microscopy to directly record and analyze cell behavior

2   To examine the expression of RHAMM by thymocytes to determine if multiple isoforms of RHAMM are expressed and to determine how HA interactions with RHAMM stimulate motility. A combination of immmunofluorescent, molecular and biochemical techniques will be used.

3   To examine the cellular distribution of three different RHAMM isoforms using COS cells transfected with GFP-RHAMM expression plasmids. These experiments will be done using confocal microscopy.

2 MATERIALS AND METHODS

2.1 Antibodies

2.1.1 Monoclonal antibodies (mAbs)

Anti-integrin mAbs included JB1A (anti-β_1 subunit), and JBS5 (anti-α_5 subunit, both from Dr John Wilkins, Univ. of Manitoba, Winnipeg, MB), 163H.1 (anti-α_4 subunit, from Dr Mike Longenecker, Biomira Inc., Edmonton, AB), QE.2E5 (forces β_1 integrins into a high affinity binding conformation, from Dr Randall Faull, Royal Adelaide Hospital, Adelaide, Australia), anti-RHAMM mAbs 3T3-5 and 3T3-9 were from Dr Eva Turley (Univ. of Toronto, Toronto, ON), anti-CD44 mAb 50B4 was from Dr Michele Letarte (Univ. of Toronto, Toronto, ON), OKT3 (anti-CD3, hybridoma was from ATCC), anti-CD45RO mAb UCHL-1 was from Dr P. Beverley (London, UK). All of these mAbs were used as ascites or were purified before use as described in section 2.1.3. Anti-CD3 conjugated to fluoroscein isothiocyanate (FITC, Leu 4-FITC), anti-CD4-FITC (Leu 3a-FITC), anti-CD8-FITC (Leu 2a-FITC), anti-CD8-phycoerythrin (PE, Leu2a-PE) and anti-CD19-FITC (Leu 12-FITC) were purchased from Becton Dickinson (Mississauga, ON). Anti-CD4-quantum red (QR), pan-specific anti-CD45-QR and isotype-matched control mAbs conjugated to QR were purchased from Sigma-Aldrich, (Oakville, ON). Isotype-matched control mAbs either unconjugated or conjugated to either FITC or PE were from Southern Biotechnology Inc. (Birmingham, AL) or Becton Dickinson.

2.1.2 Polyclonal antibodies and miscellaneous

Polyclonal rabbit anti-RHAMM serum AP-HV4-1.2 raised to the peptide sequence VSIEKEKIDEKS was from E. Turley and rabbit anti-GFP serum was purchased from Invitrogen (Carlsbad, CA). Affinity purified rabbit anti-mouse IgG, goat

anti-mouse IgG conjugated to PE, TRITC, or horseradish peroxidase (HRP), goat anti-rabbit IgG-HRP, avidin-HRP and avidin-FITC were from Southern Biotechnology Inc. Goat anti-mouse IgG conjugated to Alexa$_{488}$ was from Molecular Probes (Eugene, OR). Biotinylated goat anti-rabbit IgG was purchased from Biogenex (San Ramon, CA) and streptavidin-QR was from Sigma-Aldrich. Purified mouse IgG was purchased from Jackson Immunoresearch Laboratories Inc. (Mississauga, ON) and goat anti-mouse IgG conjugated to alkaline phosphatase was from Sigma-Aldrich.

2.1.3   MAb purification

The hybridomas secreting anti-RHAMM mAbs 3T3-5 and 3T3-9 were recloned prior to their use. Wells containing single macroscopic colonies were selected and an ELISA was used to detect mAb-secreting clones by screening tissue culture supernatants for mouse IgG (section 2.3.1). MAb-secreting clones were expanded and injected into mice to generate ascites fluid. An ELISA with a GST-RHAMM fusion protein adsorbed to the solid phase was used to test ascites fluid to ensure mAbs from recloned hybridomas recognized RHAMM epitopes. Subsequent experiments were done using ascites or mAbs were first enriched using ammonium sulfate precipitation (Harlow and Lane, 1988). A volume of ascites was added to a flask and an equivalent volume of 4.1 M ammonium SO$_4$ was added dropwise at room temperature while the solution was stirred. The solution was left stirring at 4°C for 6 H then precipitated proteins were pelleted by microcentrifugation for 30 min and solubilized in phosphate buffered saline (PBS) followed by dialysis against three changes of PBS. At the end of dialysis, insoluble material was pelleted and the solubilized precipitates were further enriched using protein G affinity columns according to the manufacturer's instructions (Pharmacia, Uppsala,

Sweden). All other mAbs were used as ascites or were enriched by ammonium sulphate precipitation.

2.2 Tissue and Cell Lines

2.2.1 Thymocytes

Thymus organs were obtained, with permission of the ethics approval committee, from children undergoing cardiac surgery at University of Alberta Hospital, Edmonton, AB. The age of the donors was usually less than 3 years. Each thymus was cut into pieces then fragments were gently pushed through mesh screens into 4°C RPMI (Gibco BRL, Burlington, ON) containing approximately 1 mg DNAse I (Sigma-Aldrich) per 30 mL RPMI to suspend thymus cells. Thymocytes were washed by pelleting the cells by centrifugation at 800 g for 8 min at 4°C then suspending the pellet in 4°C RPMI. The suspended cells were layered over Ficoll-paque (Pharmacia) and thymocytes were separated from red blood cells and dead cells by centrifugation at 1000 g for 25 min at room temperature. Cells collected from the interface were washed twice with 4°C RPMI then suspended in 4°C RPMI containing 10% (v/v) FBS (Gibco BRL; R10). Alternatively, freshly suspended thymocytes were pelleted and the cell pellet suspended in ? M ammonium chloride lysis buffer for 5 min at room temperature to lyse red blood cells. After incubation, R10 was added to the suspension and cells were pelleted then washed once more. After suspending thymocytes in R10, cells were counted using a hemacytometer and the cell concentration was adjusted to 5×10^7 cells/mL.

2.2.2 Isolation of multinegative (MN) thymocytes

Thymocytes were partially depleted of $CD3^+$ cells using OKT3 bound Dynabeads® M-450 (Dynal Inc., Lake Success, NY). To prepare the OKT3 bound beads, Dynabeads® coated with sheep anti-mouse IgG were washed in sterile PBS containing 1% (v/v) FBS (PBS/FBS) by pelleting the beads by centrifugation at 800 g for 10 min then suspending the pellet in 10 mL of PBS/FBS. Purified OKT3 antibodies were added at 1 mg antibody/mg of beads. The bead/antibody mixture was incubated at 4°C for 2 H on a rotator. At the end of incubation, beads were washed four times with PBS/FBS using a magnet to separate beads from the supernatant. After the final wash, beads were suspended in RPMI with 1% (v/v) FBS (R1). Freshly prepared thymocytes were pelleted then suspended in R1 at 2.5×10^7 cells/mL. Beads were added at a 4:1 bead to cell ratio and incubated 1 H at 4°C on a rotator. $CD3^+$ cells bound to beads were removed using a magnet. This step was repeated three times then cells remaining in the collected supernatant were pelleted, suspended in R1, and subjected to a second round of bead depletion. Thymocytes remaining after the second round of depletion were washed twice then suspended in R1. An aliquot of cells was used for IF staining to determine the efficiency of the depletion. The remaining cells were stained overnight at 4°C on a rotator with a mixture of anti-CD3-FITC, anti-CD4-FITC, anti-CD8-FITC and anti-CD19-FITC or with isotype-matched IgG-FITC controls (Becton Dickinson). Next day, thymocytes were washed twice with a large volume of 4°C RPMI then suspended in RPMI and kept in aliquots on ice to be sorted. Cells were sorted using an ELITE cell sorter (Coulter, Hialiah, FL) by gating on cells that exhibited the same relative intensity of staining as the isotype control cells (ie: $CD3^-4^-8^-19^-$ or MN), then back gated on size.

MN cells from several different donors always exhibited side and forward scatter characteristics of slightly larger resting lymphocytes compared with unfractionated thymocytes. Sorted cells were collected directly into microfuge tubes containing 50 µL of FBS at 2 x 10^5 cells/tube. Purity of the sorted cells was between 96 to 99%. MN cells were often less than 1% of the thymocyte population and the bead depletion increased the MN cells to 3 - 4% of the population.

2.2.3   Isolation of CD3^{hi} thymocytes

Freshly prepared thymocytes were pelleted then suspended in 4°C R1 and 2 µl/5 x 10^6 thymocytes of Leu4-FITC (anti-CD3-FITC) or IgG-FITC isotype control mAbs (Becton Dickinson) were added. Tubes were wrapped in foil then incubated at 4°C on a rotator for a minimum of 2 H or overnight. After incubation, stained thymocytes were washed twice using a large volume of 4°C RPMI for each suspension. After the second wash, cell pellets were suspended in 4°C R1 at 5 x 10^7 cells/mL and aliquoted to tubes kept on ice for sorting. Separate samples were stained with a combination of anti-CD3-FITC, anti-CD4-QR and anti-CD8- PE or IgG-matched isotype control mAbs conjugated to one of the three fluorophores. These samples were prepared for flow cytometric analysis as described in section 2.3.2. To sort CD3^{hi} thymocytes that were SP with respect to the expression of CD4 or CD8, the separately stained samples were analyzed by flow cytometry by setting a gate on thymocytes that expressed the highest density of CD3. Expression of CD4 and CD8 by cells within this gated population was examined to ensure the majority of thymocytes in the gated region were either CD4$^+$8$^-$ or CD4$^-$8$^+$ SP thymocytes. The sorting gate was set on the proportion of the anti-CD3-FITC stained cell population with a similar density of CD3 expression. CD3^{hi} sorted cells were collected

into microfuge tubes containing 50 μl of FBS. After collection, the sorted cells were pelleted by microcentrifugation at top speed for 1 min then suspended in R10. Suspended cells were added to 6 well tissue culture dishes (Corning Inc., Corning, NY) containing approximately 4 mL of R10 and 50 U/mL of IL2 (R & D Systems, Minneapolis, MN) and thymocytes were incubated overnight at 37°C in a humidified environment with 5% CO_2 to 95% air atmosphere. Next day, cells were collected from the petri dishes by pipetting the solution into a centrifugation tube, pelleting the cells and suspending cells in 4°C R10. The sorted cells were counted by hemacytometer then used to assess adhesion and motility as described in section 2.4.1.

2.2.4   Culture of MN Thymocytes

The wells of Lab-Tek® 8 well chamber slides (Nalge-Nunc, Naperville, IL) were pre-coated with Fn (Sigma-Aldrich) by adding 200 μL/well of 10 μg/mL of Fn in PBS to each well then incubating the slides for 2 H at 37°C. The Fn solution was aspirated just before the cell solution was added. After sorting, MN thymocytes were pelleted by microcentrifugation at top speed for 1 min then approximately 2 x 10^6 cells were suspended in 500 μL of R10 containing 50 U/mL IL2 and added to Fn-coated wells at 250 μL/well. The chamber slides were incubated for 2 days at 37°C in a humidified environment containing 5% CO_2 to 95% air atmosphere. After 2 days, cells were collected from the wells into microfuge tubes, pelleted by microcentrifugation for 1 min and suspended in 300 μL/tube assay medium as described in section 2.4.1.

2.2.5   Maintenance and transfection of COS cells

COS 7 cells (ATCC) were grown in T75 tissue culture flasks (Corning Glass, Corning, NY) in R10 to ~80% confluence then monolayers were washed with room

temperature PBS and detached with 1X trypsin-EDTA (Gibco BRL) for 5 min at room temperature. Detached cells were collected and added to centrifuge tubes containing approximately 10 mL/tube of 4°C R10. The tubes were filled with additional R10 then pelleted by centrifugation at 800 g for 6 min. Pelleted cells were suspended in R10, counted by hemacytometer then added to fresh flasks at 0.5 – 1 x 10^6 cells/flask.

To transfect COS cells, detached cells were washed three times with 4°C OPTI-MEM (Gibco BRL), counted by hemacytometer and the final suspension adjusted to 1 x 10^7 cells/mL. Cells were added to cuvettes (Invitrogen) at 4 x 10^6 cells/cuvette and 1 μg/cuvette of purified GFP or GRP-RHAMM plasmid DNA was added (described in section 2.5). Cuvettes were incubated on ice for 10 min, gently suspended and pulsed using a Gene Pulser™ set at 250V, 960 μF (Bio-Rad Laboratories, Mississauga, ON). After electroporation, cells were incubated at room temperature for 10 min then added to tissue culture-treated 100 x 20 mm petri dishes (Corning Glass) containing R10 and 10 μg/mL gentamicin (Gibco BRL). For confocal analysis (section 2.3.3), 5 x 10^4 cells/well were added to wells of an Lab-Tek® 8 well chamber slide (Nalge-Nunc) left untreated or coated with 10 μg/mL of Fn in PBS as described in section 2.1.4 and containing freshly added R10, 10 μg/mL gentamicin and 20 μg/mL HA. Transfected cells were incubated for 6, 24 or 48 H at 37°C in a humidified incubator with 5% CO_2 atmosphere then prepared for confocal analysis.

To assess transfection efficiency or to stain membranes with PKH26 (section 2.3.3), transfected cell monolayers were washed with PBS and detached from petri dishes using 4 mM EDTA in PBS, pH 7.4 for 5 min at room temperature. Detached cells were washed three times with PBS then samples were fixed in 1% formalin and GFP

fluorescence was assessed by flow cytometry. The remainders of harvested cells were used for lysis (section 2.6.1) or were stained with PKH26 to delineate the cell membrane.

2.3 Immunoassays

2.3.1 Enzyme linked immunosorbent assay (ELISA)

An ELISA with purified rabbit anti-mouse IgG (Southern Biotechnology) adsorbed to the solid phase was used to screen supernatants from recloned hybridomas and to quantitate mAb concentrations in ascites. Anti-RHAMM ascites were also tested for specificity using a glutathione-S-transferase (GST)-RHAMM (amino acids 319 - 795) fusion protein (from E. Turley) prepared as described (Yang et al., 1994). GST-RHAMM fusion protein or purified rabbit anti-mouse IgG was diluted in PBS at 2 µg/ml, added to wells of 96 well, flat-bottomed Titertek® polyvinyl chloride microtitre plates (Flow Laboratories, McLean, VA) at 50 µl/well and allowed to adsorb overnight at 4°C. Next day, fluid was flicked out of the wells and 100 µl/well of PBS containing 20% FBS was added to block uncoated surfaces. Incubation was for 30 min at 37°C then wells were washed by submerging the plates into PBS containing 0.05% (v/v) Tween 20 four times, shaking out fluid between each submersion. Serial dilutions of the ascites or purified mouse IgG (Jackson Immunoresearch Laboratories Inc.) were prepared in assay diluent [PBS containing 2% (w/v) bovine serum albumen (BSA), 0.05% (v/v) Tween 20 and 0.02% (w/v) Na azide] and added to wells at 50 µl/well followed by incubation at 37°C for 30 min. After incubation, wells were washed as described above then goat anti-mouse IgG conjugated to alkaline phosphatase diluted 1:5000 with assay diluent was added to washed wells at 50 µl/well and incubated for 30 min at 37°C. After incubation, plates

were again washed and 100 µl/well of enzyme substrate solution (1 mg/ml *p*-nitrophenyl phosphate (Sigma-Aldrich) dissolved in 0.1 M glycine buffer containing 1 mM $MgCl_2$ and 1mM $ZnCl_2$, pH 10.4) was added and color was allowed to develop at room temperature for 30 - 60 min. Optical density was quantitated at 405 nm using a plate reader interfaced with SOFTmax® software (Molecular Devices Corp., Menlo Park, CA). Concentrations of the ascites were calculated by interpolating values against the standard curve generated from the mouse IgG standards.

2.3.2 Immunofluorescent (IF) staining and cytometric analysis

For single color staining, thymocytes were stained using an indirect IF method. One x 10^6 thymocytes/well were distributed to Linbro® 96 well, v-bottomed microtitre plates (ICN Biomedicals Inc., Aurora, OH). Thymocytes were pelleted by centrifugation at 2000 rpm for 2 min at 4°C and suspended in 40 – 50 µL/well of PBS containing 1% (v/v) FBS +/- 0.02% (v/v) Na azide (assay diluent). After adding an appropriate volume of antibody to each well, plates were incubated at 4°C for 30 min. Each incubation step was at 4°C for 30 min followed by two washes with assay diluent unless otherwise indicated. Appropriate isotype matched controls were always used to stain separate samples to determine background fluorescence. Goat anti-mouse IgG-PE or goat anti-mouse-Alexa$_{488}$ was used in the second step. After the last wash, cells were suspended in PBS containing 1% (v/v) formalin (Fisher Scientific, Nepean, ON) and analyzed on a FACSsort (Becton Dickinson, Mississauga, ON). Files of 10,000 – 100,000 cells were collected for each sample. Analysis was done using Cellquest™ software (Becton Dickinson).

For two color IF experiments, HA (Pharmacia) diluted to 1 mg/ml in PBS was conjugated to FITC using FITC-Celite (Calbiochem-Novabiochem Corp., San Diego, CA) using a method described for the conjugation of FITC to mAbs (Salomon, 1991). 1 mg/mL of HA was combined with 1 mg of FITC-Celite, covered with foil and incubated at room temperature for 4 H on a rotator. After incubation, FITC conjugated to HA (HA-FITC) was separated from unbound FITC using a Sephadex G-25 column (PD-10 column, Pharmacia). Optimal volumes for IF staining were determined by titration using thymocytes. HA-FITC was added to cells after the second step then cells were incubated and washed. For experiments involving pre-treatments, 50 μg/ml HA, HA-FITC or 0.05 U/ml phosphatidylinositol-specific phospholipase C (PLC, Sigma-Aldrich or Boehringer-Mannheim, Laval, PQ) was added to thymocytes, incubated at room temperature or 37°C for 60 min, washed and the remainder of the IF was done as described above. To permeabilize thymocytes, cells were pre-treated with IF diluent containing 0.03% (w/v) saponin (Acros Organics, New Jersey, CO) for 30 min on ice, then antibodies were added and the IF done as usual except IF buffer containing 0.03% saponin was used throughout the assay.

For three color IF experiments, unconjugated mAbs were added, followed by goat anti-mouse IgG-PE. After the last wash, 10 μg/well of purified mouse IgG was added and cells were incubated for 10 min at room temperature then an appropriate volume of assay diluent was added to each well followed by anti-CD4-QR and anti-CD8-FITC. Isotype-matched IgG-FITC and IgG-QR were added to control wells. Separate samples were stained with OKT3 then goat anti-mouse IgG-PE, or anti-CD4-QR or anti-CD8-FITC and one sample was stained with all three of these reagents. These samples were

used to set gains and compensations to minimize cross talk between the three fluorophores. The remainder of the assay was done as described for single color IF.

2.3.3 Confocal microscopy

Thymocytes were stained using the two-color IF assay described above except goat anti-mouse IgG-TRITC or goat anti-mouse IgG-Alexa$_{488}$ was used in the second step. After the second step, cells were washed and incubated with HA-FITC or were treated with 1 μg/well of purified mouse IgG then anti-CD45-QR was added and cells were incubated at 4°C for 30 min. After the final wash, cells were suspended in 4°C PBS, a drop placed onto a glass slide and mixed with an equal volume of Fluoromount G (Southern Biotechnology). A coverslip was placed over the suspension and the slides were allowed to set at 4°C in the dark. Images were acquired using a Leica confocal laser scanning microscope (LSM) and processed on a silicon graphics workstation. Alternatively, images were acquired using a Zeiss confocal LSM 510 and processed with Photoshop 5.02 software (Adobe Systems Inc., San Jose, CA). Samples stained with only one of the two fluorophores were always included so filters and voltages could be set to exclude cross talk between the two fluorophores.

Transiently transfected COS cells were grown in Lab-Tek® 8 well chamber slides as described in section 2.2.5 and culture medium was aspirated after 6, 24 or 48 H of culture. Monolayers were washed three times with room temperature PBS then cells were fixed and permeabilized with Intraprep (Immunotech, Marseille, France). Reagent 1 (fixative) was added to monolayers at 100 μL/well and cells were incubated in the dark at room temperature for 15 min. The solution was then aspirated and the monolayers were washed with room temperature PBS three times. After the final wash, PBS was aspirated

and 100 µL/well of reagent 2 (permeabilizing solution) were added and chambers were incubated at room temperature in the dark for 15 min. The monolayers were washed three times then antibodies diluted in PBS were added at 200 µL/well. All subsequent incubation steps were for 1 H in the dark at room temperature and were followed by three washes with PBS. Cell monolayers were stained with non-immune rabbit serum or rabbit antiserum to RHAMM or GFP. In the second step, goat anti-rabbit conjugated to biotin diluted with PBS was added to washed monolayers and in the third step streptavidin-QR diluted in PBS was added to washed monolayers. After the final wash, chambers were removed from the glass slide and a drop of Fluoromount G was added to each area containing cells and a coverslip placed over the slide. Alternatively, transfected COS cells were harvested from petri dishes (section 2.3.3) except the final wash was done using room temperature RPMI and membranes were labeled using the PKH-26GL fluorescent cell linker kit following the manufacturer's directions (Sigma-Aldrich). Approximately $4 - 5 \times 10^6$ cells/mL were pelleted by centrifugation, the pellet was tapped loose and combined with the manufacturer's assay buffer. Immediately PKH26 dye was added to a final concentration of 2×10^{-6} M and cells were immediately mixed and incubated at room temperature for 2 to 5 min. After incubation, FBS was added to neutralize the reaction and cells were washed 3 times with R10. After labeling, washed cells were placed onto slides as described for thymocytes.

2.4 Analysis of Cell Behavior

2.4.1 Adhesion and motility assay

96 well flat-bottom Linbro® plates (ICN Biomedicals Inc.) or 8 well chamber slides were coated with 10 µg/ml of fibronectin (Fn) +/- 20 µg/ml HA in PBS at 200 µl/well. Plates were incubated at 37°C for a minimum of 2 H or overnight and the solution aspirated just before cells were added. Two x 10^5 thymocytes were pre-treated with 1 µg/ml of antibody in R10 containing 15 U/ml recombinant human IL2 (Chiron, Seattle, WA or R & D Systems), +/- 20 µg/ml HA (assay medium) for 30 min on ice or with 0.05 U/ml of PLC in PBS at room temperature or 37°C then washed once with 4°C R10 medium and suspended in 300 µl of 37°C assay medium. Suspended cells were added to a coated well of the microtitre plate or chamber slide and gently settled by centrifugation at 500 rpm for 2 min at room temperature followed by incubation at 37°C for 30 min in a 5% CO_2 : 95% air atmosphere. Following incubation, the plate or chamber was placed onto a 37°C heated microscope stage of an inverted microscope (Olympus IX70, Carsen Group Inc., Markham, ON) and atmosphere was maintained by flowing a 5% CO_2 : 95% air mixture over the plate or chamber. A field was selected and videotaped for 30 min at 72 H speed. Cell behavior was analyzed using Videoblaster™ software (Creative Labs, Inc., Milpitas, CA). Alternatively, a camera port attached to the microscope was interfaced with a computer and images were saved every 15 sec for a total of 80 images (~30 min) using Northern Eclipse image analysis software (Northern Eclipse, Mississauga, ON). Both methods yielded comparable results. At least 75 - 100 cells were analyzed for each treatment and adhesive cells were defined as cells that remained attached to the substrate over the entire period of the recording. The majority of

adherent thymocytes extended small protrusions and demonstrated shape changes (deformed), but did not migrate, while an extremely minor fraction remained completely round for the entire filming period. Motile cells were defined as cells that were both deforming and randomly migrating. To be considered motile, a cell had to migrate more than one cell diameter over the filming period. The majority of migratory cells migrated several cell diameters or completely out of the field of view before the final frame was recorded. Statistical significance was determined by Student's t test using Sigma Stat software (SSPS Inc., San Rafael, CA).

2.4.2   Adhesion assay with washing

At the end of filming, non-adherent and weakly adherent cells were removed by gentle pipetting followed by removal of 250 μL of total volume. An equivalent volume of fresh 37°C assay medium was added to the well, cells were pelleted as described above and again allowed to equilibrate at 37°C for 30 min. At the end of incubation, cells were filmed as described above.

2.5 Molecular Techniques

2.5.1   Reverse transcriptase polymerase chain reaction

Five x 10^6 freshly isolated thymocytes were pelleted by microcentrifugation, suspended in 1 ml of Trizol (Gibco BRL) and stored at -80°C. RNA was extracted according to the manufacturer's directions, suspended in diethyl pyrocarbonate-treated water and stored at -80°C. RNA (0.5 - 1.0 μg) was denatured at 70°C for 10 min, annealed to 0.5 μM oligo dT_{15} (Gibco BRL) and reverse transcribed using a solution containing 0.5 mM dNTPs (Boehringer-Mannheim), 0.01 M DTT, 200 U superscript™

reverse transcriptase and 1X RT buffer (Gibco BRL) in a volume of 20 μl, then incubated at 42°C for 60 min and heat-inactivated at 99°C for 3 min using a GeneAmp PCR machine (Perkin-Elmer, Mississauga, ON). A separate aliquot of thymocyte RNA was incubated without superscript™ to discriminate between amplification from cDNA template, synthesized by reverse transcription and potential amplification from genomic DNA. The cDNA was amplified in a 50 μl PCR reaction mix (Gibco BRL) containing 1X PCR buffer, 0.2 mM dNTPs, 0.4 μM each of upstream and downstream primers, 1 U Taq DNA polymerase and 10μL of cDNA template. The PCR cycling parameters were denaturation for 5 min at 94°C, followed by 35 cycles of denaturation for 1 min at 94°C, annealing for 30 sec and extension at 72°C for 2 min, with a final extension period of 7 min at 72°C. Primer annealing temperature (T_A) was calculated as: $T_A = 4(G + C) + 2(A + T) - 5$. To detect expression of RHAMM^{FL} and RHAMM^{-48}, 10 μl of cDNA was amplified with RHAMM primer pair:

5' GGCCGTCAACATGTCCTTTCCTA; 3' TTGGGCTATTTTCCCTTGAGACTC.

To detect expression of RHAMM^{FL} and RHAMM^{-147}, 10 μL of cDNA was amplified with RHAMM primer pair:

5' TTAAAGCAAACACTGGATGAGCTTG; 3' CTTCTTTTAATGGGGTCTTCAGGG.

The amplified products were analyzed on 1% agarose gels containing ethidium bromide, 50 mM Tris, 45 mM Boric acid and 0.5 mM EDTA, pH 8.3.

2.5.2   Preparation of RHAMM plasmids

Complete RHAMM^{FL}, RHAMM^{-48} and RHAMM^{-147} sequences were amplified in 1X PCR buffer containing 2 mM MgCl$_2$, 0.2 mM dNTPs, 0.4 μM RHAMM primers and 0.5 U Platinum Hi FI Taq (Gibco/BRL). RHAMM primers were:

5'GGCCGTCAA**CATG**TCCTTTCCTA; & 3'**GTTA**CTTCCATGATTCTTGACACTC.

RHAMM start and stop codons are in bold. The PCR cycling parameters were denaturation for 5 min at 94°C, followed by 35 cycles of denaturation for 45 sec at 94°C, annealing for 30 sec at 65°C and extension at 72°C for 2 min followed by a final extension period of 15 min at 72°C. cDNA of each RHAMM isoform was inserted into the pcDNA3.1/V5/His-TOPO cloning vector then used to transform TOP10F' competent cells according to the manufacturer's instructions (Invitrogen). Bacterial colonies that contained RHAMM/pcDNA3.1 plasmid were identified using PCR. Individual bacterial colonies were introduced into a PCR reaction mix containing 1X PCR buffer, 2 mM MgCl$_2$, 0.2 mM dNTPs, 0.5 U Taq DNA Polymerase (Gibco/BRL) and 0.4 µM T7 forward and pcDNA3.1/BGH reverse primers (Invitrogen):

5' TAATACGACTCACTATAGGG and 3' TAGAAGGCACAGTCGAGG

The PCR cycling parameters were bacterial lysis for 10 min at 94°C, followed by 25 cycles of denaturation for 1 min at 94°C, annealing at 52°C for 30 sec and extension at 72°C for 2 min followed by a final extension period of 7 min at 72°C. Amplified products were separated by electrophoresis through 2% (w/v) agarose gels and RHAMM/pcDNA3.1 transformed bacteria were identified based on amplification of a PCR product of the correct size. Positive colonies were selected and grown in LB broth (Gibco BRL) containing 10 µg/mL ampicillin for 18 – 20 H at 30°C with aeration. Bacteria were pelleted by centrifugation and plasmids were prepared for subsequent sequencing and transfection using a plasmid mini kit (Qiagen Inc., Mississauga, ON). Each RHAMM/pcDNA3.1 expression construct was sequenced to verify the RHAMM

gene was inserted into the plasmid in the correct orientation using RHAMM antisense primer:

ACTGGTCCTTTCAATACTTCTAAAGT.

RHAMM^{-48}/pcDNA3.1 and RHAMM^{-147}/pcDNA3.1 plasmids were also sequenced using RHAMM primers:

GGCGCCCTTGAAACGCAA   and   TCCTAGAAGAAAAGCTGAAAGGGAA, respectively, to confirm the 48 bp deletion or the 147 bp deletion that characterizes each isoform was present.   Sequencing was done using the ABI PRISM dRhodamine Terminator Cycle Sequencing Ready Reaction DNA Sequencing Kit on a Perkin Elmer 310 DNA Sequencer (Perkin Elmer Applied Biosystems).

2.5.3   Preparation of GFP-RHAMM plasmids

RHAMM^{FL}, RHAMM^{-48} and RHAMM^{-147} sequences were amplified in 1X PCR buffer containing 2 mM MgSO$_4$, 0.2 mM dNTPs, 0.4 µM RHAMM primers 0.5 U Platinum Hi FI Taq. RHAMM primers were:

5' CGCTCGAGATATGTCCTTTCCTAAG, which contains a Xho 1 restriction site and 3' CCGGTACCCTTCCATGATTCTTG, which contains a Kpn 1 restriction site.   Both restriction sites are underlined and the RHAMM start (ATG) codon is in bold type.   The PCR cycling parameters were denaturation for 5 min at 94°C, followed by 10 cycles of denaturation for 45 sec at 94°C, annealing for 30 sec at 42°C, and extension at 72°C for 2 min, followed by 35 cycles of denaturation for 45 sec at 94°C, annealing for 30 sec at 70°C and extension at 72°C for 2 min, with a final extension period of 15 min at 72°C. Each isoform was inserted into the pCR TOPO cloning vector (Invitrogen) then used to transform TOP10F' competent cells according to the manufacturer's directions

(Invitrogen). Bacterial colonies containing RHAMM/pCR TOPO plasmid were identified by PCR screening of individual colonies using RHAMM primers:

5' GGCGCCCTTGAAACGCAA and 3' CGAGACTCCTTTGGGTGACCTG, as described in section 2.5.3. Positive colonies were identified and grown in LB broth containing 50 μg/mL of kanamicin then plasmids were isolated using a plasmid mini kit (Qiagen Inc.). To subclone into the E-GFP C1 vector (Clontech Laboratories Inc., Palo Alto, CA), each RHAMM/pCR TOPO construct was digested with Kpn I for 2 H in 1X OPA buffer (Pharmacia) followed by digestion with Xho I for 2 H in 2X OPA buffer. The digested RHAMM inserts were separated by electrophoresis through agarose gels and purified on Ultrafree-DA filters (Millipore Corp. Bedford, MA). Each RHAMM isoform was ligated to Xho 1/Kpn 1 digested E-GFP C1 vector and used to transform TOP10F' competent cells. Bacterial colonies containing RHAMM/GFP-C1 plasmid were identified by PCR screening of colonies using E-GFP sequencing primer (Clontech) and RHAMM primer:

5' CATGGTCCTGCTGGAGTTCGTG and 3' TTGGGCTATTTTCCCTTGAGACTC, respectively, as described above. Each RHAMM/GFP-C1 construct was sequenced with the E-GFP sequencing primer to verify the RHAMM sequence was in frame with GFP. This strategy also confirmed that the 48 bp deletion and the 147 bp deletion were present in GFP-RHAMM^{-48} and GFP-RHAMM^{-147} constructs, respectively.

2.6 Biochemical Techniques

Transfected COS cells were harvested 48 H after transfection by washing the monolayer with PBS then adding 4 mM EDTA in PBS, pH 7.2 for 5 min at room

temperature to detach cells. Detached cells were washed three times with 4°C PBS then lysed by suspending the washed cell pellet at 5×10^6 cells/mL in lysis buffer [50 mM Tris-Cl-buffered 137 mM saline, pH 7.4 containing 1mM EGTA, 1% (w/v) CHAPS, 10 µg/mL leupeptin, 10 µg/mL antipain and 1 mM phenylmethylsulfonyl fluoride (all from Sigma-Aldrich)]. Thymocytes were washed three times using 4°C PBS then suspended in lysis buffer at 5×10^7 to 5×10^8 cells/mL. All other steps were the same for COS cell lysates and thymocyte lysates. Incubation was for 30 – 45 min on ice with occasional mixing. After lysis, nuclei were pelleted by centrifugation at ~1100 g for 10 min at 4°C. The supernatant (lysate) was collected and clarified by microcentrifugation at top speed for 30 min at 4°C. Lysates were pre-adsorbed with washed protein A-conjugated sepharose beads (Pharmacia) for 1.5 – 2 H at 4°C mixing end over end. Beads were pelleted by microcentrifugation and the pre-adsorbed lysate was collected and stored at –80°C. RHAMM or RHAMM-GFP fusion proteins were precipitated from 0.5 mL of COS cell lysate (equivalent to ~2.5×10^6 COS cells) or 1 mL of thymocyte lysate using polyclonal anti-GFP or anti-RHAMM antibodies. The mixture was incubated at 4°C for 2 H or overnight on a rotator. Protein A-sepharose beads (Pharmacia) were washed three times with lysis buffer, suspended in a 1:1 slurry in lysis buffer and added at 50 µL/tube then incubated for 2 H at 4°C on a rotator. After incubation, beads were pelleted by microcentrifugation and washed twice with lysis buffer, once with 50 mM Tris-buffered saline, pH 7.4 and once with 50 mM Tris-Cl, pH 6.8. Washed beads were boiled for 5 min with 2X sample buffer (125 mM Tris containing 4% (w/v) SDS, 20% glycerol and 0.02% (w/v) bromphenol blue) then pelleted by microcentrifugation. The supernatants were collected and 2-

mercaptoethanol was added to a final concentration of 5%. The supernatants were incubated for 1 H at 37°C then cooled on ice and loaded onto a 5% polyacrylamide stacking gel and separated through a 7 or 7.5% polyacrylamide gel using 25 mM Tris containing 192 mM glycine and 0.1% (w/v) SDS, pH 8.3 using a minigel apparatus (Bio-Rad Laboratories). Biotinylated molecular weight markers (broad range) were from Bio-Rad Laboratories.

2.6.2   Immunoblotting

Gels were blotted onto Immobilon P nitrocellulose membranes (Millipore Corp.) using a Bio-Rad blotting assembly. After proteins were separated, the gel apparatus was disassembled and gels were allowed to equilibrate in 25 mM Tris containing 192 mM glycine and 20% (v/v) methanol, pH 8.3 (transfer buffer) for 30 min on a rocker at room temperature. Nitrocellulose membranes were wetted by soaking for 15 sec in methanol followed by submersion in distilled deionized water for 2 min then membranes were equilibrated in transfer buffer along with blotting paper. Blots were assembled and the transfer was done at 100 V for 1 H or at 30 V overnight at 4°C in transfer buffer. After transfer, membranes were dried at 37°C for 1 H then blocked for 1 H at room temperature on a rocker by immersing the membrane in 3% (w/v) BSA in PBS. Membranes were incubated on a rocker with primary antibody diluted in PBS containing 1% (w/v) BSA and 0.05% (v/v) Tween 20 (assay diluent) for 2 H at room temperature or overnight at 4°C. After incubation, membranes were washed twice for 30 sec, once for 15 min and once for 5 min at room temperature with PBS containing 0.005% (v/v) Tween 20. Washed membranes were incubated with secondary HRP-conjugated antibodies diluted in assay diluent for 1 H at room temperature on a rocker. Secondary antibodies consisted of

a combination of goat anti-rabbit-HRP and avidin-HRP. After incubation, membranes were washed as described above and treated with ECL chemiluminescence reagent (Amersham) by flooding the membrane with the chemiluminescence reagent and incubating for 1 min at room temperature. Excess reagent was poured off and membranes were immediately exposed to Hyperfilm (Amersham) and the film processed.

CHAPTER 3. β_1 Integrins and RHAMM Promote Adhesion or Motility for Thymocytes

Both murine and human thymocytes adhere to and locomote on Fn-coated surfaces, but bind poorly to other ECM components such as laminin, vitronectin or collagen. Thymocytes also express the Fn-binding integrin receptors $\alpha_4\beta_1$ and $\alpha_5\beta_1$ (Utsumi et al., 1991; Sawada et al., 1992; Pilarski, 1993b; Salomon et al., 1994; Crisa et al., 1996; Gares et al., 1998). This suggests these β_1 integrins facilitate adhesion of thymocytes to ECM or stromal cells as well as mediating motility through the thymic microenvironment as thymocytes differentiate.

Specific Objective 1

To examine the relationship between β_1 integrins and RHAMM to determine how integrin-based adhesion to Fn and HA-stimulated, RHAMM-mediated motility are balanced to promote either cell adhesion or cell motility for differentiating thymocytes. These experiments will be done using timelapse microscopy to directly record and analyze cell behavior

3.1 All Human Thymocyte Subsets Express Fn-binding Integrins

$\alpha_4\beta_1$ and $\alpha_5\beta_1$ integrins are the predominant Fn-binding integrins expressed by human thymocytes (Pilarski, 1993b; Salomon et al., 1994; Mojcik et al., 1995). We used anti-integrin mAbs for phenotypic and functional analyses to determine if these mAbs produced similar results compared with the previous reports. Integrin expression on the four major thymocyte subsets, as defined by CD4 and CD8 expression, was analyzed using flow cytometry. Cells were stained sequentially with anti-integrin mAbs followed by anti-CD4-QR and anti-CD8-FITC then fluorescently stained cells were acquired using a FACSort. DN ($CD4^-8^-$), DP ($CD4^+8^+$) and the two SP subsets ($CD4^+8^-$ and $CD4^-8^+$) were gated based on their expression of CD4 and/or CD8 followed by analysis of integrin expression on each subset (Fig. 3.1). Expression of α_4 integrin subunits was relatively high on most immature DN cells and all DP thymocytes as indicated by the intensity of mAb staining (Fig. 3.1c & d). α_5 integrin expression was relatively high on a subset of DN thymocytes, decreased to relatively low expression levels on DP thymocytes and was increased slightly on both SP subsets in comparison with DP thymocytes (Fig. 3.1g – j). The staining intensity of α_4 integrin was decreased on the majority of SP cells compared with DP thymocytes (Fig. 3.1d – f). Expression of the $\beta1$ subunit was also high on the DN and DP thymocyte subsets (Fig. 3.1k & l). $\beta1$ expression was slightly decreased on the $CD8^+$ SP subset (Fig. 3.1n), but a bimodal distribution pattern of β_1 integrin expression was observed on $CD4^+$ SP thymocytes (Fig. 3.1m). The expression patterns of β_1 integrin subunits on thymocyte subsets are consistent with previous reports indicating our mAbs are comparable for phenotypic analysis (Pilarski, 1993b; Salomon et al., 1994;
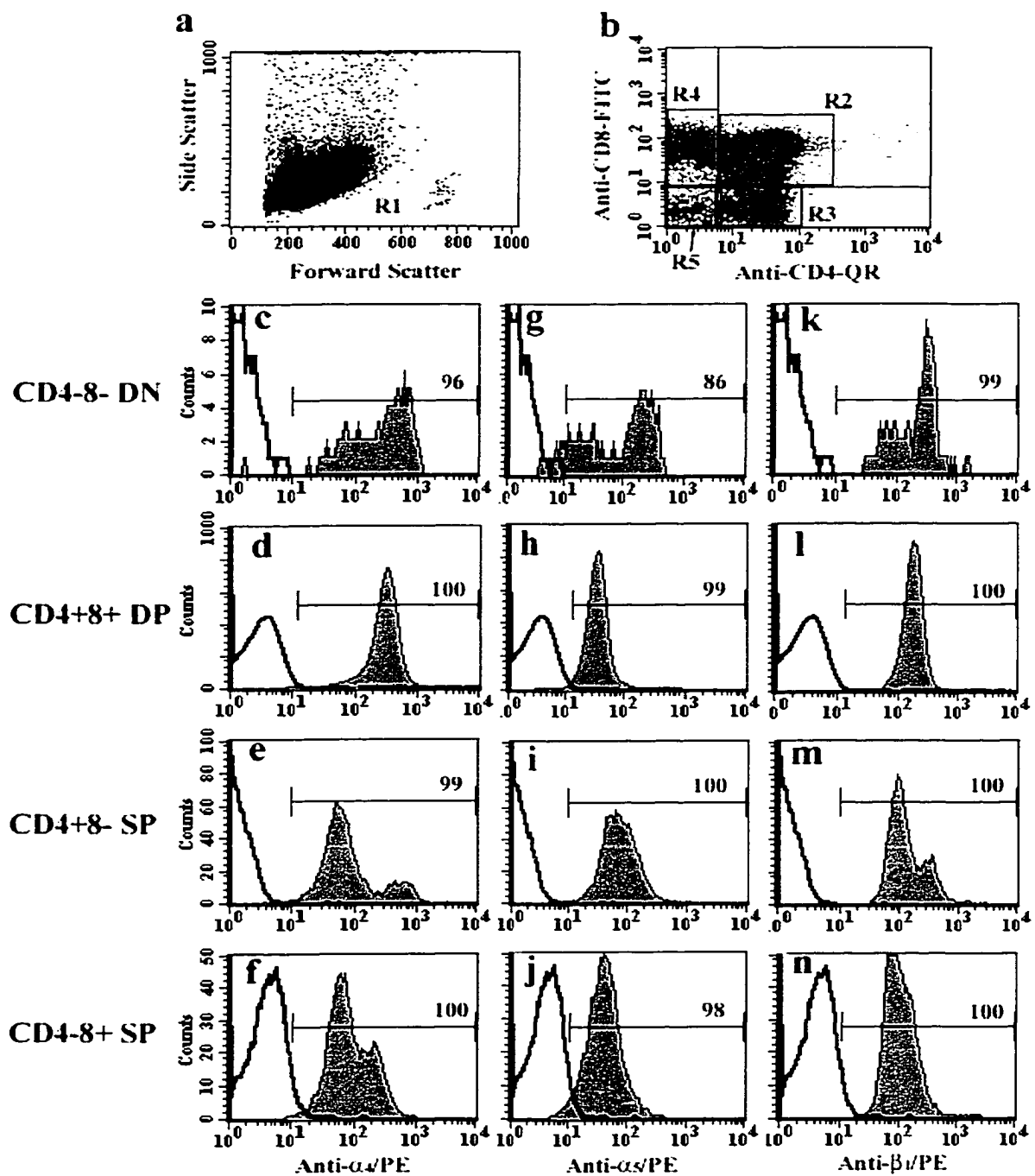
Figure 3.1 Human thymocytes express α_4, α_5 and β_1 integrin chains.

Legend is on the following page.

Figure 3.1 Human thymocytes express α_4, α_5 and β_1 integrin chains.

Thymocytes were sequentially stained with mAbs to α_4 (c – f), α_5 (g – j), β_1 (k – n) integrin chains or isotype-matched control mAbs in the first step, goat anti-mouse-PE in the second step and anti-CD4-QR and anti-CD8-FITC in the third step. 100,000 cells were acquired from each sample using a FACSort. Samples were analyzed by first drawing a gate around lymphoid cells (a, gate R1) then subsets were gated again based on CD4 and CD8 expression (b). Vertical and horizontal bars were set to indicate the intensity of background fluorescence of 98% of cells from samples stained with isotype-matched control IgG-QR and IgG-FITC, respectively. Gate R2 includes CD4$^+$8$^+$ DP cells (d, h, l), gate R3 includes CD4$^+$8$^-$ SP cells (e, i, m), gate R4 includes CD4$^-$8$^+$ SP cells (f, j, n) and gate R5 includes CD4$^-$8$^-$ DN cells (c, g, k). Filled curves in each histogram indicate the staining intensity of anti-integrin mAbs and unfilled curves indicate the background fluorescence of identically gated cells stained with an isotype-matched control mAb. The bars indicate the percentage of cells in each filled histogram with staining intensity greater than 95 – 98% of control mAb stained cells. The staining profiles are of thymocytes from one thymus preparation, but profiles were similar for thymocytes from a total of three separate thymus preparations.

Mojcik et al., 1995). These data suggested virtually all human thymocytes expressed $\alpha_4\beta_1$ and $\alpha_5\beta_1$ integrins, but that expression levels were modified as cells differentiated.

3.2 β_1 Integrins Mediate Both Adhesion and Motility for Thymocytes

In murine systems, both $\alpha_4\beta_1$ and $\alpha_5\beta_1$ integrins mediate adhesion to Fn and stromal cell monolayers for DN thymocytes (Utsumi et al., 1991). However, $\alpha_4\beta_1$ integrin alone facilitates adhesion of more mature murine and human thymocytes to Fn or to VCAM-1 expressed on thymic epithelial cells (Sawada et al., 1992; Salomon et al., 1994; 1997). To determine if the anti-integrin mAbs we obtained produced similar results, unfractionated thymocytes were pre-treated with mAbs to α_4, α_5 or β_1 integrin subunits, singly or in combination then the proportion of adherent cells was assessed on Fn-coated surfaces using timelapse microscopy to record cell behavior. Adhesive cells were identified as those cells that remained attached to Fn over the entire period of filming. Sixty-three per cent of unfractionated thymocytes adhered to Fn and the number of adherent thymocytes was not decreased by mAbs to α_5 or β_1 integrin subunits compared with cells pre-treated with isotype-matched control mAbs (Fig 3.2a). Anti-α_4 integrin mAbs significantly decreased the number of Fn-adherent cells to 33%. However, cell adhesion to Fn was almost completely abrogated when thymocytes were pre-treated with a combination of anti-α_4 and anti-α_5 mAbs. Only 6.6% of thymocytes adhered to Fn when both α_4 and α_5 integrin chains were simultaneously bound by mAbs, a highly significant decrease in the number of Fn-adherent cells. This indicated both α_4 and α_5 integrins mediated adhesive interactions with Fn for human thymocytes. The anti-β_1
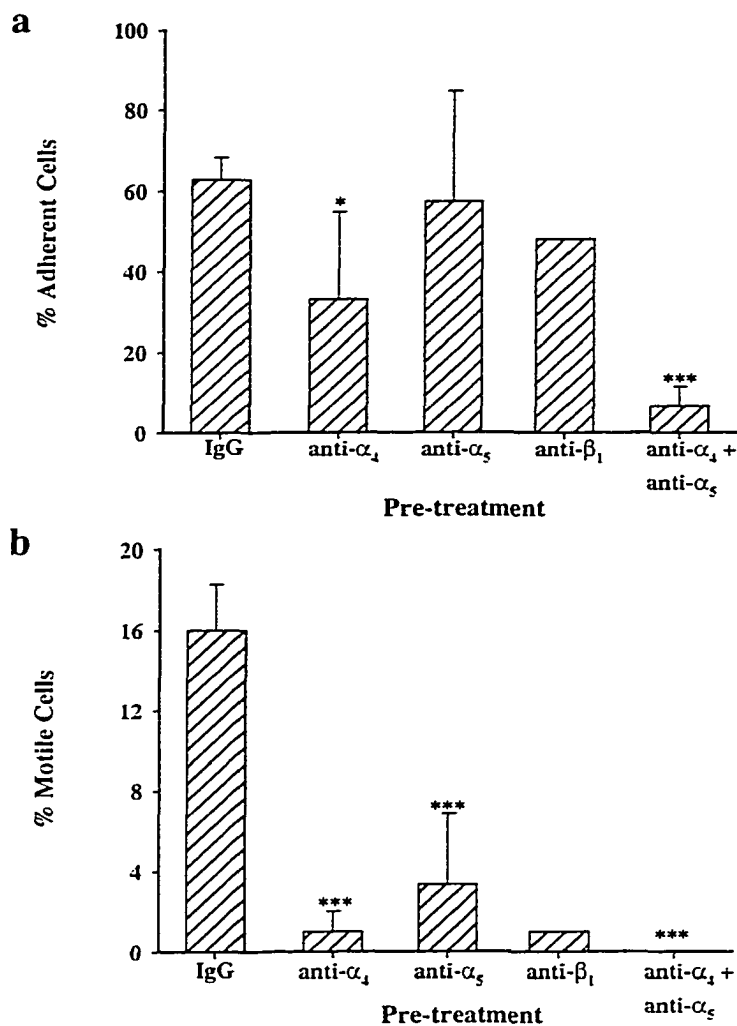
Figure 3.2 β_1 **integrins mediate adhesion and motility for thymocytes.**

Thymocytes were pre-treated with the indicated mAbs + IL2 + HA then washed and added to Fn-coated wells. Cell behavior was recorded for ~30 min using timelapse microscopy then the recorded images were analyzed to quantitate the percentage of adherent, non-motile cells (a) or motile cells (b) in each sample. Each value except anti-β_1 is the mean +/- SD using thymocytes from 3 − 6 different thymus preparations. Statistical comparisons were between the IgG-treated samples (isotype-matched control) and anti-integrin mAb-treated samples. * = $p < 0.05$, ** = $p < 0.01$, *** = p < 0.005

integrin mAb used here did not decrease adhesion of thymocytes to Fn; however, other anti-β_1 mAbs did significantly decrease adhesion to Fn (data not shown), suggesting a combination of $\alpha_4\beta_1$ and $\alpha_5\beta_1$ integrins facilitated adhesion of thymocytes to Fn.

By recording cell behavior, both the number of Fn-adherent cells and the number of motile cells could be assessed using the same recordings. Fn-adherent thymocytes were defined as cells that remained attached to Fn throughout the period of recording. These cells included deforming, non-motile cells and a minority of non-deforming, non-motile cells. Motile thymocytes were defined as cells that deformed and clearly locomoted across the substrate during the period of recording. Of all unfractionated thymocytes, 16% of cells displayed random motility on Fn (Fig. 3.2b). Pre-treating thymocytes with mAbs to α_4, α_5, or β_1 integrin chains significantly decreased the number of locomoting cells suggesting $\alpha_4\beta_1$ and $\alpha_5\beta_1$ integrins facilitated motile behavior. When thymocytes were treated with a combination of mAbs to both α_4 and α_5 integrin subunits, no motile cells were observed suggesting α_4 and α_5 integrins were the dominant integrins that facilitated locomotion for human thymocytes. These data are consistent with previous reports in which a different method of analysis was used (Salomon et al., 1994; Crisa et al., 1996).

3.3 Thymocyte Subsets Express the Motility Receptor RHAMM

RHAMM is expressed by thymocytes and mediates thymocyte locomotion on Fn (Pilarski et al., 1993). To assess RHAMM expression on thymocyte subsets defined by expression of CD4 and CD8, thymocytes were sequentially stained using one of two different anti-RHAMM mAbs followed by anti-CD4-QR and anti-CD8-FITC. Analysis

of each thymocyte subset indicated anti-RHAMM mAb 3T3-5 bound to cell surfaces very weakly and a range of 13 – 35% of thymocytes of all four subsets exhibited weak staining above background levels (Fig. 3.3c – f). The peak staining intensity of IgG control stained thymocytes was in channel 1 (peak channel) whereas the peak staining intensity of thymocytes stained with mAb 3T3-5 ranged from channel 5 to 13 among the four subsets. Anti-RHAMM mAb 3T3-9 demonstrated a slightly stronger staining intensity on thymocytes (Fig. 3.3g - j). DN thymocytes stained with mAb 3T3-9 had peak staining intensity in channel 47 compared with a peak channel of 13 for mAb 3T3-5 stained DN thymocytes (compare Fig. 3.3c & g). Thirty-eight per cent of DP thymocytes were stained weakly with mAb 3T3-9 (peak channel 13), but above background levels (Fig. 3.3h) and the CD4$^+$ and CD8$^+$ SP subsets contained a proportion of thymocytes with a peak of staining in channel 31 and 33, respectively (Fig. 3.3i & j). Overall, 62% of CD4$^+$ SP and 75% of CD8$^+$ SP cells were RHAMM$^+$ as indicated by staining with mAb 3T3-9. The weak staining intensity suggested RHAMM was expressed at the cell surface at a relatively low density.

CD3 expression levels were also assessed for each thymocyte subset. CD3 is expressed along with TCR heterodimers, thus CD3 expression is a phenotypic marker for thymocytes that have successfully rearranged at least one TCR gene. Therefore, CD3 expressed, even at low density, indicates thymocytes have begun to differentiate. The DN subset contained thymocytes with weak CD3 expression as well as cells with high CD3 expression (Fig. 3.3k, peak channels 12 and 2813, respectively). This indicated the DN
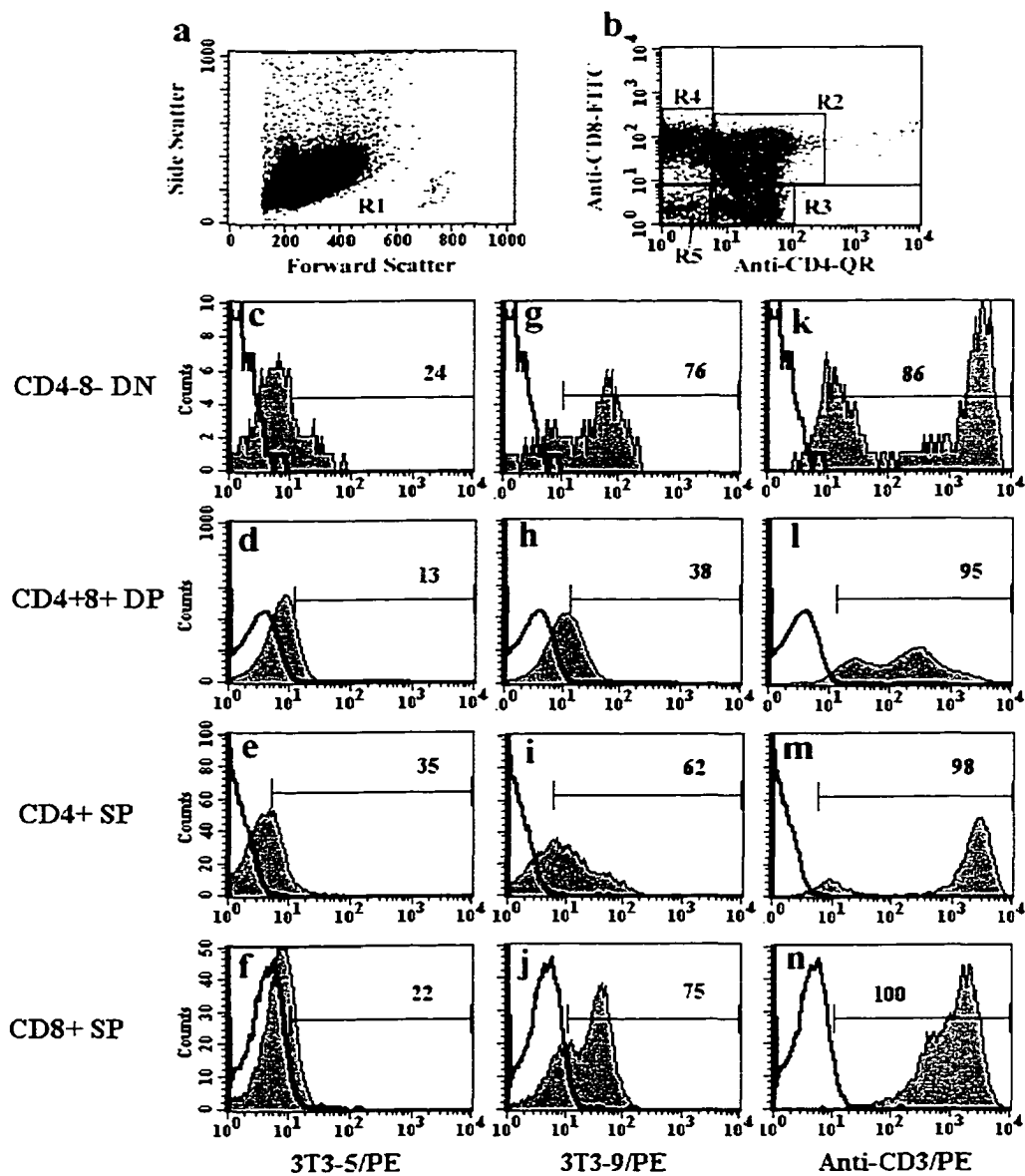
Figure 3.3 Thymocyte subsets express the motility receptor RHAMM.

Thymocytes were sequentially stained with anti-RHAMM mAb 3T3-5 (c – f), 3T3-9

(g – j), or anti-CD3 (k – n) followed by goat anti-mouse-PE then anti-CD4-QR and

anti-CD8-FITC. Gates were set and cells analyzed as described in the legend to Fig.

3.1. The data represent staining profiles of thymocytes from one thymus preparation,

but thymocytes from two other thymus preparations produced similar results.

subset was a mixture of relatively immature CD3^{lo} cells and mature CD3^{hi} cells, the latter likely comprised of TCR$_{\gamma\delta}^{+}$ thymocytes as data from murine models indicates (Sawada et al., 1992; Halvorson et al., 1998). Only 14% of DN thymocytes could be considered CD3^{-} thymocytes. CD3 expression levels on the DP and SP subsets were intermediate (peak channel 330) and high (peak channel ranged from 1274 to 2713), respectively, consistent with an upregulation of CD3 expression as thymocytes mature (Fig. 3.3l – n).

3.4 RHAMM Mediates Motility for the Majority of Motile Thymocytes on Fn and HA

To determine if the two anti-RHAMM mAbs used to assess RHAMM expression affected thymocyte adhesion to or motility on Fn, thymocytes were pre-treated with anti-RHAMM mAbs 3T3-5 or 3T3-9 then cell behavior was recorded and assessed. These adhesion/motility assays were done in the presence of HA, the ligand of RHAMM. CD44 is another HA receptor expressed by thymocytes. To determine if HA-stimulated adhesion or motility was mediated by CD44, anti-CD44 mAbs were used to pre-treat separate aliquots of thymocytes. The proportion of Fn-adhesive thymocytes pre-incubated with anti-RHAMM mAb 3T3-9 or anti-CD44 mAbs was comparable with the adhesive fraction of cells pre-treated with control mAbs (Fig. 3.4a). Pre-treating thymocytes with anti-RHAMM mAb 3T3-5 slightly, but significantly, increased the number of Fn-adherent cells from 63% to 77%. When motility was assessed, 16% of thymocytes were motile on Fn and anti-CD44 mAbs did not significantly affect the
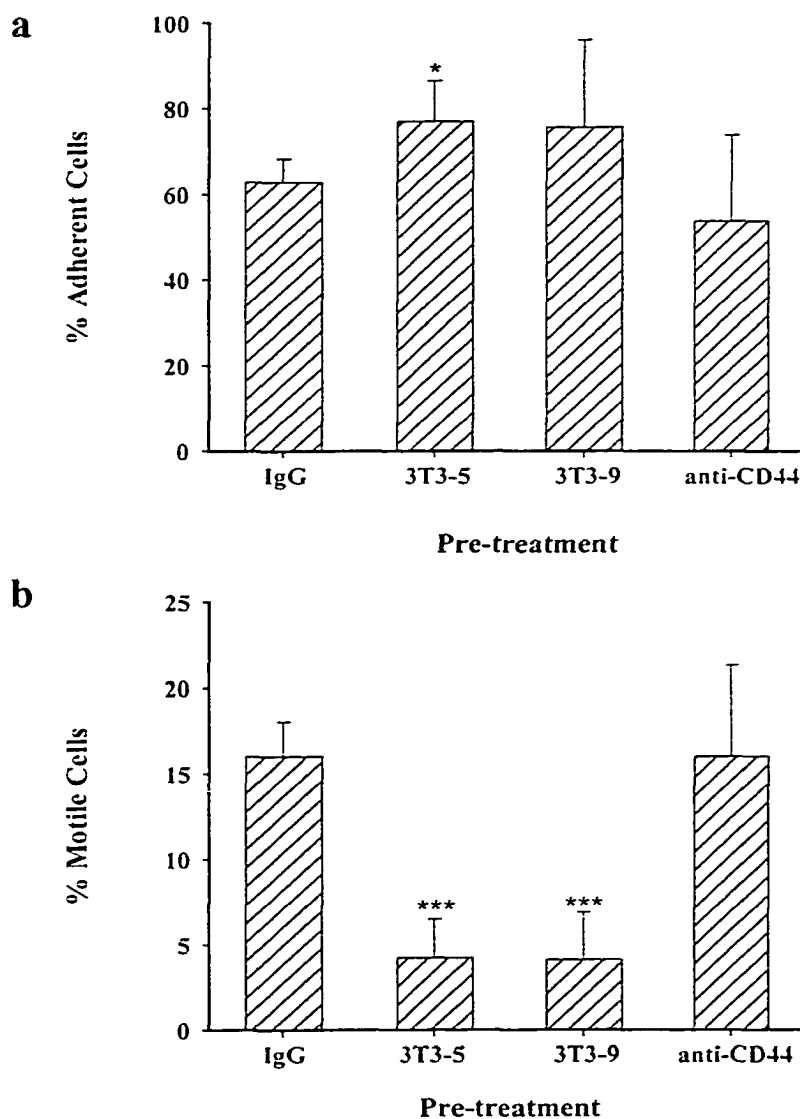
Figure 3.4 RHAMM mediates motility for the majority of motile thymocytes.

Thymocytes were pre-treated with the indicated mAbs then washed and added to Fn-coated wells for analysis as described in the legend to Fig. 3.2. The number of adherent (a) or motile (b) cells is shown as the mean +/- SD of each treatment using thymocytes from 3 – 6 different thymus preparations. Each treatment was compared with the IgG-treated group for statistical analysis.

number of thymocytes that locomoted on Fn (Fig. 3.4b). This suggested CD44 did not mediate adhesion or motility on Fn even in the presence of HA. This suggests human thymocytes do not express CD44 in an activated form able to interact with HA. However, anti-RHAMM mAbs significantly decreased the number of motile cells suggesting RHAMM participated in the motile process. Interestingly, although anti-RHAMM mAb 3T3-5 bound only weakly to cell surface RHAMM, these mAbs significantly inhibited cell motility.

3.5 $\alpha_4\beta_1$ Integrins, but not RHAMM Facilitate Adhesion and Motility for MN Thymocytes

Expression levels of α_4, α_5 and β_1 integrin subunits were high on the DN subset of human thymocytes suggesting this subset might demonstrate high avidity binding to Fn. To examine this possibility, MN thymocytes were prepared using magnetic beads to partially deplete CD3$^+$ thymocytes followed by cell sorting to remove CD3$^+$4$^+$8$^+$19$^+$ thymocytes. Using this approach, MN thymocytes constitute <1 – 3% of the thymocyte population. To assess Fn-mediated adhesion and motility, MN thymocytes were added to Fn-coated wells and cell behavior was recorded. Thirty-one per cent of MN thymocytes adhered to Fn-coated wells (Fig. 3.5a). Pre-treating MN thymocytes with mAbs to α_4 or β_1 integrin subunits significantly decreased the number of Fn-adhesive cells to 11% or 17%, respectively. However, neither anti-α_5 integrin mAbs, nor anti-RHAMM mAbs significantly decreased the number of Fn-adherent cells. Thus, assessment of cell
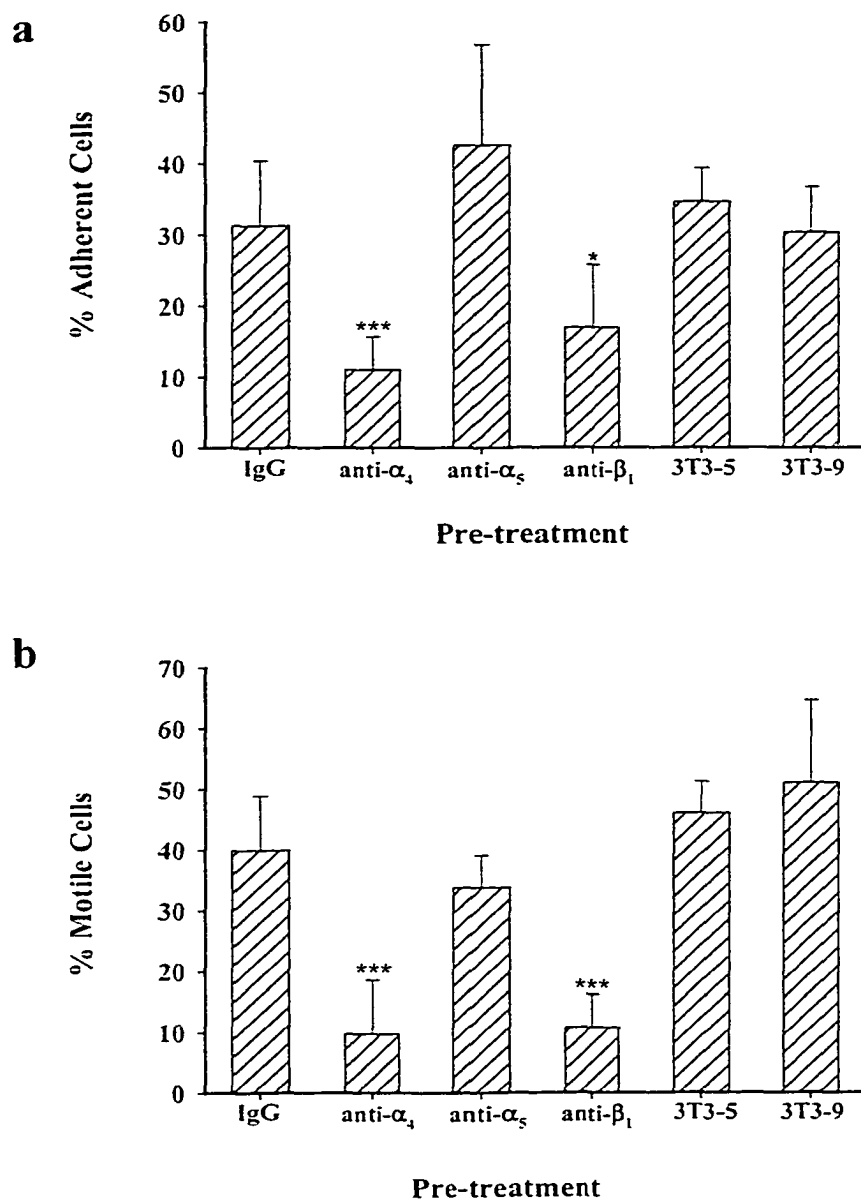
Figure 3.5 $\alpha_4\beta_1$ **integrins mediate adhesion and motility for MN thymocytes.**

MN thymocytes were pre-treated with the indicated mAbs then washed and added to Fn-coated wells for analysis as described in the legend to Fig. 3.2. The number of adherent (a) or motile (b) cells is shown as the mean +/- SD using purified MN thymocytes from 3 − 8 different thymus preparations. Each treatment was compared with the IgG-treated group for statistical analysis.

behavior using timelapse microscopy indicated $\alpha_4\beta_1$ integrins were the dominant integrins mediating adhesive interactions with Fn for MN thymocytes.

The number of motile MN thymocytes was also quantitated from the recorded images. Forty per cent of MN thymocytes were locomotory on Fn-coated surfaces (Fig. 3.5b). MAbs to α_4 or β_1 integrin subunits significantly decreased the number of motile cells indicating $\alpha_4\beta_1$ heterodimers mediated motility for MN thymocytes. MAbs to α_5 integrin did not significantly alter the proportion of motile cells. In contrast to unfractionated thymocytes, RHAMM-specific mAbs did not inhibit motility of the MN thymocytes. Although RHAMM was expressed on DN thymocytes, staining profiles of MN thymocytes indicated this very immature, CD3$^-$ subset was RHAMM$^-$ (Gares & Pilarski, 1999). These data suggested $\alpha_4\beta_1$ integrins mediated adhesive interactions with Fn for one portion of MN thymocytes and mediated motility for a different portion of MN thymocytes. In contrast to unfractionated thymocytes, neither α_5 integrins nor RHAMM mediated motility for MN thymocytes.

3.6 β_1 Integrins and RHAMM Mediate Motility for Maturing Thymocytes

The DP thymocyte subset consisted of approximately 85% of all thymocytes, thus the majority of thymocytes were immature, CD3^{med} cells. Thymocytes that expressed the highest levels of CD3 corresponded predominantly to the SP subsets (Fig. 3.3m & n). These two subsets had a different pattern of α_4 and α_5 expression than DN or DP thymocytes. CD3^{hi} thymocytes were purified by cell sorting to determine if different patterns of β_1 integrin expression resulted in modification of adhesion to or motility on

Fn. After culturing the sorted cells overnight, adhesion and motility on Fn-coated wells were assessed. Thirty-eight per cent of CD3^{hi} thymocytes pre-treated with control mAbs adhered to Fn (Fig. 3.6a) and this proportion was similar to the number of Fn-adherent cells in the MN subset (Fig. 3.5a). MAbs to α_4 subunits, α_5 subunits, RHAMM or CD44 did not significantly decrease adhesion to Fn. A combination of anti-α_4 and anti-α_5 integrin mAbs decreased the proportion of Fn-adhesive CD3$^+$ cells to 14%, but this decrease was insignificant.

Approximately 16% of CD3$^+$ thymocytes were motile on Fn (Fig. 3.6b) and this proportion was substantially less than the motile fraction of MN thymocytes (Fig. 3.5b). MAbs to α_4, α_5 and RHAMM significantly decreased the number of motile CD3$^+$ thymoyctes, whereas anti-CD44 mAbs had no effect (Fig. 3.6b). Although a smaller proportion of CD3$^+$ thymocytes were motile compared with the MN subset, α_5 integrin and RHAMM along with α_4 integrins were required for locomotion of cells in this subset. As thymocytes differentiated from CD3$^-$ to CD3^{hi} cells, the binding avidity of β_1 integrins to Fn might be decreased as suggested by the decreased expression of α_4 integrin. The expression and participation of RHAMM in locomotory behavior of CD3$^+$ thymocytes also suggested RHAMM expression and function was upregulated as thymocytes differentiated.

3.7 High Affinity Binding Conformations of β_1 Integrins Promote Adhesion to Fn and Decrease Motility

Anti-α_4 and anti-α_5 integrin mAbs moderately decreased or did not decrease adhesion of unfractionated and CD3^{hi} thymocytes to Fn, but each mAb significantly
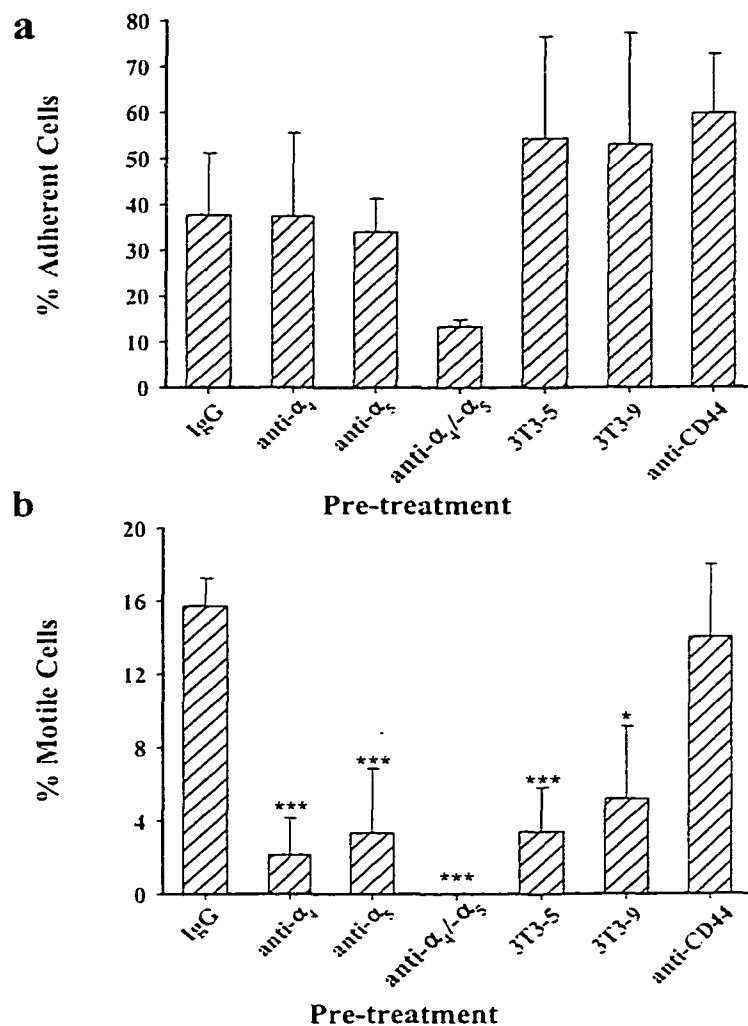
Figure 3.6 β_1 **integrins and RHAMM mediate adhesion and/or motility for CD3^{hi} thymocytes.**

Sorted CD3^{hi} thymocytes were pre-treated with the indicated mAbs then washed and added to Fn-coated wells for analysis as described in the legend to Fig. 3.2. The number of adherent (a) or motile (b) cells is shown as the mean +/- SD for each treatment using CD3^{hi} thymocytes purified from 3 different thymus preparations. Each treatment was compared with the IgG-treated group for statistical analysis.

decreased motility (Fig. 3.2). This suggested the majority of motile thymocytes expressed β_1 integrins in low affinity binding conformations that promoted locomotion. To test this hypothesis, thymocytes were pre-treated with a β_1 integrin activating mAb, QE2E5, that forces β_1 integrins into a high affinity binding conformation. When cell behavior was assessed, QE2E5-treated cells were significantly less motile on Fn compared with control mAb-treated cells (Fig. 3.7). Approximately 16% of IgG-treated thymocytes were motile on Fn and the proportion decreased significantly to 6.5% when cells were pre-incubated with β_1 integrin activating mAbs. The proportion of Fn-adhesive cells was concomitantly increased from approximately 60% for IgG-treated thymocytes to 81% for QE2E5-treated thymocytes. Increasing the shear force by washing Fn-bound cells before quantitating the number of adherent cells indicated the adhesiveness of QE2E5-treated thymocytes was significantly enhanced compared with IgG control-treated thymocytes. Approximately 13% of IgG-treated, washed thymocytes adhered to Fn and this proportion increased to 45% when thymocytes were pre-treated with QE2E5 mAbs. These data suggested that assessing the number of adherent cells using timelapse microscopy included cells that adhered to Fn via both low affinity/avidity and high affinity/avidity interactions. The increased adhesion and decreased motility associated with QE2E5 treatment indicated a significant number of *ex vivo* thymocytes expressed β_1 integrins in low affinity binding conformations.
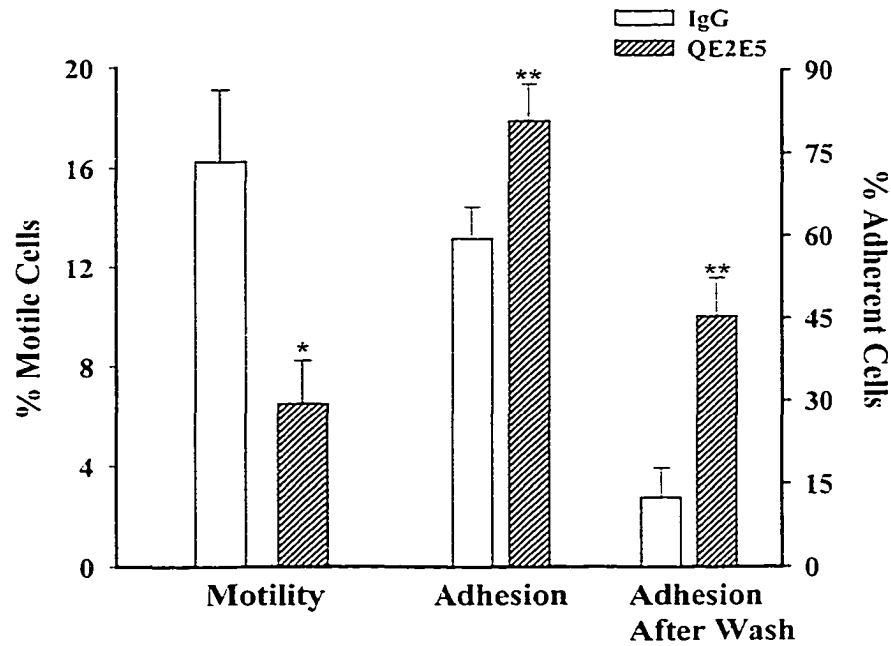
Figure 3.7 High affinity binding conformations of β_1 integrins promote adhesion to Fn and decrease motility.

Thymocytes were pre-treated with control mAbs (IgG) or anti-β_1 integrin mAb QE2E5 then washed and added to Fn-coated wells for analysis as described in the legend to Fig. 3.2. Alternatively, thymocytes were pre-treated with mAbs and allowed to adhere to Fn-coated wells then washed and the remaining cells were filmed (adhesion after wash group). Each value is the mean +/- SD of thymocytes from 3 – 4 different thymus preparations. Statistical comparisons were made with the similarly treated IgG control.

3.8 RHAMM-dependent Motility is Stimulated by Culture of MN Thymocytes on Fn

RHAMM is not detectable at the cell surface of MN thymocytes, but expression is apparent on a subset of $CD3^{lo}$ DN thymocytes (Pilarski et al., 1993 & Fig. 3.3). This suggested RHAMM expression occurs early in thymocyte development. RHAMM surface expression is spontaneously upregulated by culturing MN thymocytes on Fn-coated wells (Pilarski et al., 1993). To determine if RHAMM surface expression was affected by receptor occupancy of Fn-binding integrin receptors, MN thymocytes were cultured in the presence or absence of Fn and immobilized mAbs to $\beta1$, $\alpha4$, $\alpha5$ integrin chains or RHAMM for 2 – 7 days. RHAMM expression was transiently upregulated by day 2 in the absence of Fn, but dependent on the presence of Fn for *in vitro* expression after longer culture periods (Gares & Pilarski, 1999). Anti-RHAMM mAbs did not affect the upregulation of RHAMM expression. However, immobilized function-blocking mAbs to α_4, α_5 or β_1 integrin subunits significantly inhibited RHAMM expression in the presence or absence of Fn. These data suggested high avidity interactions of β_1 integrins with specific mAbs modulated RHAMM expression.

To determine if the onset of RHAMM expression correlated with increased motility, MN thymocytes were purified then cultured on Fn-coated wells. After two days of culture, thymocytes were harvested and pre-treated with control or anti-RHAMM mAbs then adhesion and motility were assessed. Culture of MN thymocytes on Fn decreased the number of Fn-adherent thymocytes. Approximately 14% of cultured thymocytes adhered to Fn compared with 63 - 67% of *ex vivo* MN thymocytes (Fig. 3.8,
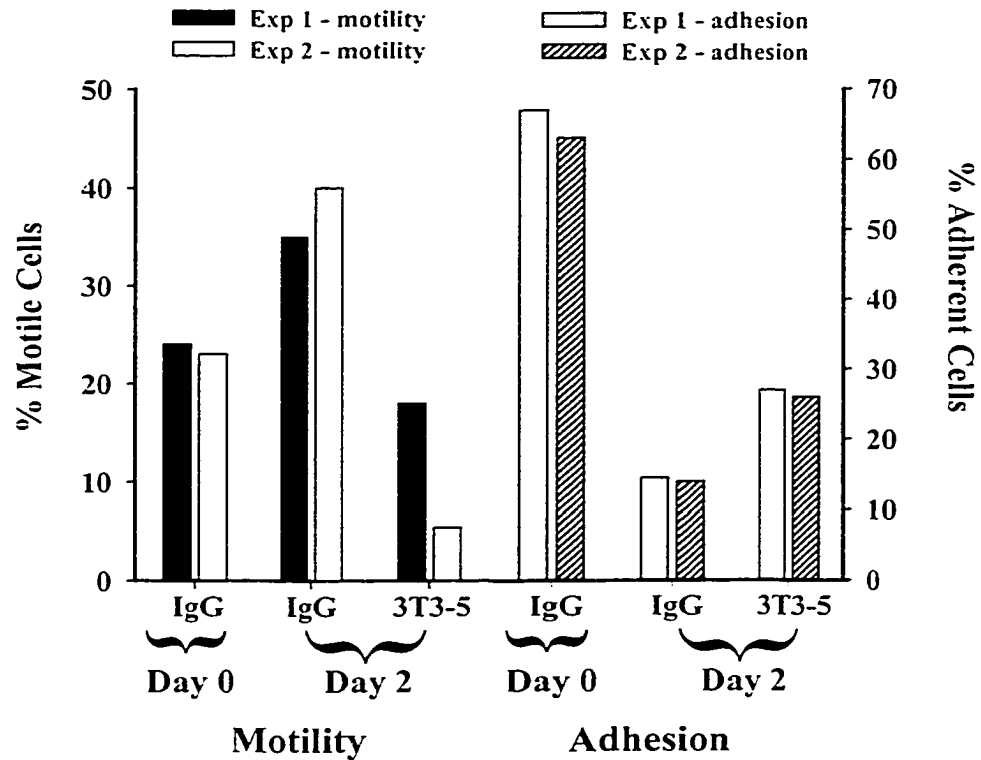
Figure 3.8 Culture of MN thymocytes on Fn stimulates RHAMM-dependent motility.

MN thymocytes were pre-treated with IgG control mAbs then washed and added to Fn-coated wells for analysis as described in the legend to Fig. 3.2 (Day 0). Separate MN cells were cultured for two days on Fn-coated wells then harvested, pre-treated with the indicated mAbs then washed and added to Fn-coated wells for analysis (Day 2). Thymocytes from 2 separate thymus preparations were used as indicated (exp 1 and exp 2).

compare adhesion Day 0 and Day 2). In contrast, the number of motile cells increased. Before culture, approximately 24% of *ex vivo* MN thymocytes were locomotory and after two days of culture, 35 – 40% of thymocytes were motile. RHAMM also began to participate in locomotion, since pre-treating cultured thymocytes with anti-RHAMM mAbs decreased the number of motile cells (compare Fig. 3.5b with Fig. 3.8). Anti-RHAMM mAbs also enhanced adhesion to Fn, since 26% of anti-RHAMM mAb-treated thymocytes adhered to Fn compared with 14% of IgG-treated thymocytes.

3.9 Summary: Low Avidity Interactions Between Fn and β_1 Integrins Promote RHAMM-mediated Motility

The Fn-binding integrins $\alpha_4\beta_1$ and $\alpha_5\beta_1$ were expressed by all thymocyte subsets defined by the expression of CD4 and CD8, although the density of α_4 and α_5 subunits varied between thymocyte subsets. The patterns of β_1 integrin expression were consistent with phenotypic analyses done by other groups (Salomon et al., 1994; Mojcik et al., 1995). Consistent with the high expression levels of Fn-binding integrin receptors, 62% of unfractionated thymocytes adhered to Fn. However, only function-blocking mAbs to α_4 integrins significantly decreased the number of cells adhering to Fn. In contrast, by blocking interactions of both α_4 and α_5 chains with Fn, cell adhesion to Fn was very strongly inhibited. Although Fn-binding β_1 integrins were the predominant integrins expressed by thymocytes, mAbs to the β_1 subunit did not decrease adhesion. Other anti-β_1 integrins mAbs did decrease adhesion of thymocytes to Fn (McNeil & Pilarski, unpublished observations), suggesting both $\alpha_4\beta_1$ and $\alpha_5\beta_1$ integrins facilitated adhesion

of thymocytes to Fn. Unfractionated thymocytes were also locomotory on Fn and motility was mediated by both α_4 and α_5 integrins. Approximately 16% of thymocytes were motile and specific mAbs to α_4 and α_5 integrin subunits significantly decreased the number of motile cells. The anti-β_1 mAb JB1A also decreased the number of motile cells. This indicated the majority of motile thymocytes utilized a combination of $\alpha_4\beta_1$ and $\alpha_5\beta_1$ integrins to mediate motility.

RHAMM is expressed by and promotes motility for many differentiating types of cells including thymocytes (Pilarski et al., 1993). RHAMM expression on the four thymocyte subsets was analyzed using two different anti-RHAMM mAbs. MAb 3T3-5 stained a fraction of thymocytes within each subset, but the staining intensity was barely above background. However, a second anti-RHAMM mAb, 3T3-9, stained a larger proportion of thymocytes within each subset with low intensity. This suggested RHAMM was expressed at low density by cells within each thymocyte subset. DN and CD8$^+$ SP thymocytes in particular contained a substantial proportion of RHAMM$^+$ cells. Consistent with the function of RHAMM as a mediator of motility, both anti-RHAMM mAbs significantly inhibited motility. MAb 3T3-5 also significantly increased adhesion to Fn. These data indicated $\alpha_4\beta_1$ integrins, $\alpha_5\beta_1$ integrins and RHAMM participated in cell locomotion.

Analysis of integrin expression on different thymocyte subsets indicated downregulation of $\alpha 4$ expression correlated with increasingly differentiated cells while $\alpha 5$ expression was decreased on DP thymocytes then slightly upregulated on the most mature SP thymocytes. The highest expression levels of α_4, α_5 and β_1 chains were observed on the least mature DN subset suggesting cells with this phenotype might

demonstrate high avidity interactions with Fn. To assess the adhesion and motility of the most immature subset, thymocytes were purified to remove $CD3^+4^+8^+19^+$ cells. These cells were referred to as MN thymocytes to distinguish them from DN thymocytes. MN thymocytes are $RHAMM^-$ and do not contain $CD3^{lo}TCR^+$ cells that are present in the DN subset (Pilarski et al., 1993), thus representing a more homogeneous immature population than the immature subset defined only by CD4 and CD8 expression.

Timelapse microscopic analysis indicated MN thymocytes actually contained a smaller proportion of Fn-adhesive cells than unfractionated thymocytes and an increased proportion of motile cells. Only 31% of MN thymocytes adhered to Fn compared with 62% among unfractionated thymocytes while 40% of MN thymocytes were motile compared with 16% among the unfractionated population. Although α_5 integrins were expressed at a relatively high density on DN thymocytes, only α_4 and β_1 integrin chains were involved in mediating adhesion and motility for MN thymocytes on Fn. Consistent with the lack of cell surface RHAMM expression on MN thymocytes, mAbs to RHAMM did not inhibit motility.

Adhesion of MN thymocytes to Fn has also been assessed using a conventional adhesion assay that includes a washing step to dislodge poorly adhesive cells from the substrate prior to fluorometric analysis. This method indicated 71% of MN thymocytes adhered to Fn and adhesion was strongly decreased by anti-α_5 mAbs and only moderately decreased by anti-α_4 mAbs or the α_5-specific Fn peptide RGDS (Gares et al., 1998). The conventional adhesion assay is expected to measure the proportion of cells that have high avidity interactions with the substrate, yet a larger proportion of MN thymocytes were Fn-adherent compared with the proportion of thymocytes that were Fn-adherent using

timelapse microscopy. The different results observed using these two methods might reflect the lack of homogeneity of the MN population used in the conventional adhesion assay. Purifying the MN subset using a combination of bead depletion and cell sorting indicated MN thymocytes usually constituted less that 1% of the population. In comparison, using only magnetic beads to deplete $CD3^+4^+8^+19^+$ thymocytes indicated 8% of the population was constituted by MN thymocytes. This suggested a combination of magnetic bead depletion and cell sorting was a more rigorous method to isolate MN thymocytes. It is likely that thymocytes expressing low levels of CD3, CD4 and CD8 will not be depleted as efficiently using bead depletion as will thymocytes expressing high levels of these receptors, thus the high proportion of adhesive cells observed using the conventional adhesion assay might include $CD3^{lo}$ thymocytes.

As thymocytes undergo differentiation and selection, the expression and function of α_4 and α_5 integrins alters. Immature DP thymocytes have been reported to be adhesive and poorly motile, whereas more mature (post-positive selection) DP and SP thymocytes are less adhesive and more motile (Sawada et al., 1992; Crisa et al., 1996). However, these analyses were done using indirect methods to assess adhesion and motility. We directly assessed the adhesion and motility of the most mature subsets using timelapse microscopy. Thymocytes were purified based on CD3 expression. Approximately 38% of $CD3^{hi}$ thymocytes adhered to Fn and only a combination of anti-α_4 and anti-α_5 integrin mAbs decreased the number of Fn-adherent thymocytes. The proportion of Fn-adherent $CD3^{hi}$ thymocytes was similar to the proportion of Fn-adherent MN thymocytes, but less than the adhesive fraction of unfractionated thymocytes that are predominantly DP thymocytes. Therefore, this data was consistent with previous reports indicating the

adhesive functions of integrins on SP thymocytes are decreased compared with DP thymocytes.

α_4 integrins along with α_5 integrins and RHAMM mediated motility for CD3^{hi} thymocytes. However, the number of motile cells was equivalent to that of unfractionated thymocytes and less than the number of motile MN thymocytes. This suggested decreased adhesion was not necessarily correlated with increased motility among the SP subsets. Alternatively, experimental manipulations including staining, cell sorting and culture might adversely affect the locomotory activities of CD3^{hi} thymocytes. To determine if integrin affinity was related to adhesion and motility, unfractionated thymocytes were treated with an activating anti-β_1 mAb that forced β_1 integrins into a high affinity binding conformation. Activating anti-β_1 mAbs enhance the strength of interactions between β_1 integrins and their ligand, thus increase adhesion. In contrast, function-blocking anti-β_1 integrin mAbs decrease or inhibit the interaction of integrins with ligand and decrease adhesion. Pre-treatment of thymocytes with activating mAb QE2E5 significantly increased adhesion to Fn and concomitantly decreased motility. This correlation suggested β_1 integrins in high affinity binding conformations promoted adhesion or anchored behavior for unfractionated thymocytes while lower affinity interactions between integrins and Fn were required to promote cell locomotion. The ability of the activating mAbs to significantly increase adhesion to Fn suggested β_1 integrins on a large proportion of *ex-vivo* thymocytes are in a low affinity binding conformation.

Low affinity and low avidity interactions of β_1 integrins with Fn might provide traction for locomotory thymocytes. It has been suggested that HA, a ligand for

RHAMM, promotes de-adhesion for locomotory cells (Turley & Torrance, 1985). Direct analysis of cell behavior using timelapse microscopy supported this possibility. Thymocytes pre-treated with anti-RHAMM mAbs generally displayed decreased motility and a concomitant increase in adhesion. Increased adhesion was significant among unfractionated thymocytes pre-treated with anti-RHAMM mAb 3T3-5. The corollary is that blocking integrin receptors that provide traction for cells should decrease motility *and* adhesion. Our observations for unfractionated thymocytes and MN thymocytes were consistent with this hypothesis. Anti-α_4 integrin mAbs significantly decreased the number of adherent and motile cells among unfractionated thymocytes and MN thymocytes. However, exogenous HA did not enhance thymocyte motility and did not decrease the adhesion of thymocytes to Fn. However, endogenous synthesis of HA by thymocytes might support de-adhesive activities of *ex vivo* migratory thymocytes. Thymocytes pre-treated with hyaluronidase become non-locomotory on Fn unless exogenous HA is added to the motility assay (Gares et al., 1998). This suggests that HA is required to mediate thymocyte motility and interactions between RHAMM and HA could facilitate cell de-adhesion.

Consistent with the high density of β_1 integrins expressed by immature thymocytes, this subset included Fn-adhesive cells, but also contained a similar proportion of motile cells. Comparison of individual experiments indicated the proportion of adhesive and motile cells correlated. If a thymocyte preparation contained fewer adhesive cells, there was an increased proportion of motile cells and vice versa. Motility of MN thymocytes was RHAMM-independent, consistent with the lack of RHAMM expressed on this immature subset. Culture of MN thymocytes on Fn is

associated with upregulation of RHAMM expression (Pilarski et al., 1993; Gares & Pilarski, 1999) suggesting integrin-mediated signaling might promote RHAMM expression. While undergoing sessile phases of differentiation thymocytes would not require RHAMM, thus our working hypothesis was that high avidity interactions of integrins might inhibit RHAMM expression. Consistent with this hypothesis, immobilized mAbs to α_4, α_5, and β_1 integrins, that emulate high avidity interactions between β_1 integrins and ligand, inhibited RHAMM expression (Gares & Pilarski, 1999). As MN thymocytes continue to differentiate, they become migratory cells. Integrin avidity is decreased, RHAMM expression is upregulated and cells can become motile. *In vitro* culture of MN thymocytes indicated that after two days of culture on Fn, the number of Fn-adherent cells decreased while the number of motile cells concomitantly increased. In addition, motility was RHAMM-dependent, since anti-RHAMM mAbs decreased the number of motile cells. This data suggested RHAMM expression correlated with early differentiation of thymocytes and presumably with the onset of migration of thymocytes through the thymus.

CHAPTER 4. Thymocytes Express Two RHAMM Isoforms

RHAMM is detected on the surface of cells in tissues undergoing development and reorganization. RHAMM's ligand HA is detected at the wounded edge of tissues and HA distribution co-localizes with the upregulation of cell surface RHAMM on cells at the wounded edge (Savani et al., 1995). This suggests HA might stimulate the expression of RHAMM. HA is distributed in the fetal and neonatal thymus and the distribution pattern is similar to that of Fn (Patel et al., 1995). The distribution of integrin ligands in the thymus as well as the regulation of expression and function of β_1 and β_2 integrins on thymocytes might guide thymocytes through the thymus as they differentiate and undergo selection. RHAMM and HA might function in a similar capacity for migratory thymocytes.

Specific Objective 2

To examine the expression of RHAMM by thymocytes to determine if multiple isoforms of RHAMM are expressed and to determine how HA interactions with RHAMM stimulate motility. A combination of immmunofluorescence, molecular and biochemical techniques will be used.

4.1 Thymocytes Express Two HA Binding Receptors

Thymocyte subsets expressed a low density of cell surface RHAMM detected by

the anti-RHAMM mAb 3T3-9, but a second anti-RHAMM mAb, 3T3-5, had even weaker

binding to cell surface RHAMM (Fig. 3.3). The staining pattern of these two mAbs was

consistent for thymocytes isolated from dozens of different thymi. For comparison, the

histograms of unfractionated thymocytes stained with anti-RHAMM mAb 3T3-9 or 3T3-

5 are presented. The peak staining intensity for thymocytes stained with MAb 3T3-9 was

channel 6 and generally 30% to greater than 60% of thymocytes from different donors

were stained above background levels by this mAb (Fig. 4.1a). MAb 3T3-5 also stained

thymocyte cell surfaces very weakly (peak channel 4) and approximately 15 - 20% of

thymocytes from different donors exhibited weak staining above background levels (Fig

4.1b). In contrast, the HA-binding receptor CD44 was expressed at medium to high

density (peak channel 1433) on virtually all thymocytes (Fig. 4.1c). Separate samples

were stained with HA-FITC to test the ability of thymocytes to bind HA. Although

thymocytes expressed an abundance of HA receptors, the staining intensity of HA-FITC

stained thymocytes was moderate (peak channel 31) (Fig. 4.1d). For comparison with

HA-FITC stained cells, separate samples were stained with avidin-FITC (Fig. 4.1d,

unfilled curve) or with IgG-FITC. Thymocytes stained with either avidin-FITC or control

IgG-FITC had staining profiles substantially less intense than HA-FITC stained

thymocytes (peak channel 1).
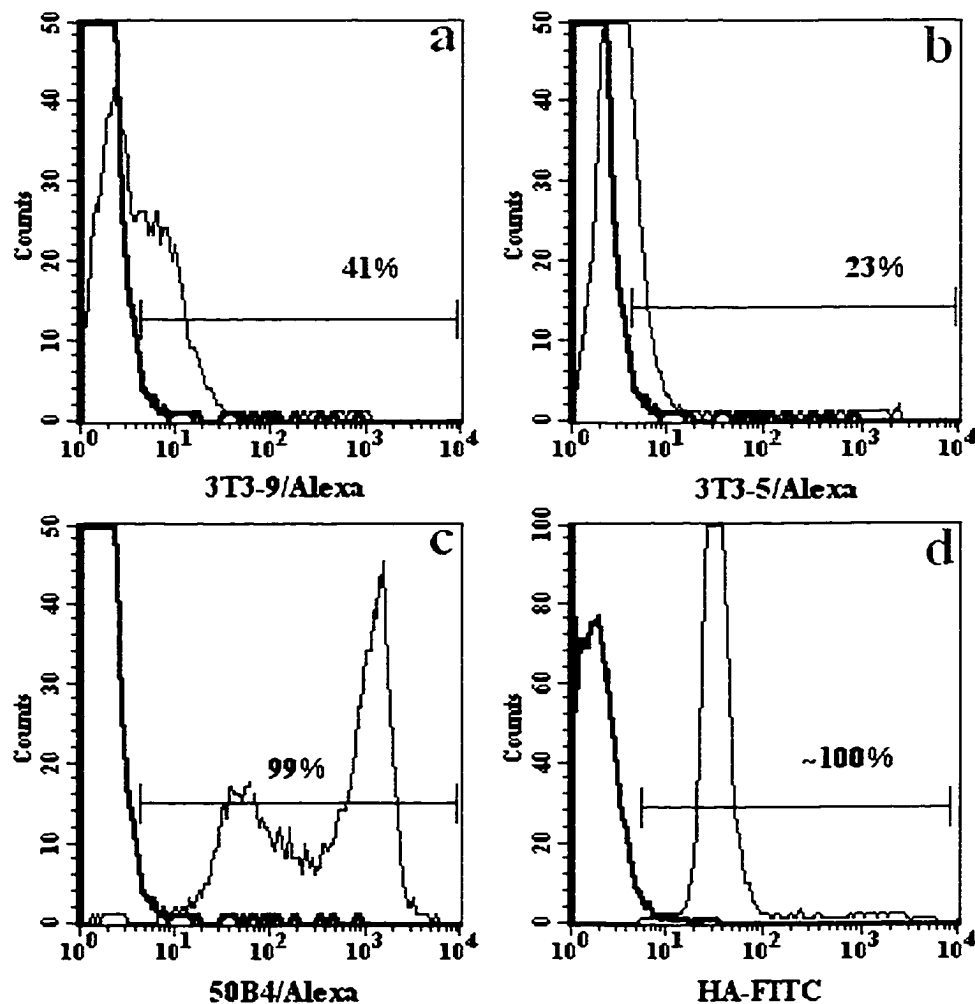
Figure 4.1 Thymocytes express two HA binding receptors, RHAMM and CD44

Human thymocytes were stained by indirect IF with anti-RHAMM mAbs 3T3-9 (a), 3T3-5 (b) or anti-CD44 mAb 50B4 (c) followed by goat anti-mouse IgG-Alexa$_{488}$ or were stained with HA-FITC (d) and analyzed by flow cytometry (filled curves). Unfilled curves represent staining by an isotype matched control mAb (a — c) or avidin-FITC (d). Bars and percentages are defined in the legend to Fig. 3.1. The histograms shown are from one donor, but represent typical staining patterns observed for several different donors.

4.2 Both Anti-RHAMM MAbs Bind to a RHAMM Fusion Protein

To compare the binding of the two anti-RHAMM mAbs to their ligand, an ELISA was done using assay plates coated with either rabbit anti-mouse capture antibodies or a GST-RHAMM fusion protein. Serial dilutions of each antibody solution were made in order to titrate each mAb solution and to assess ligand binding. The titration curves of mAbs 3T3-5 and 3T3-9 generated using rabbit anti-mouse IgG-coated plates were similar indicating similar concentrations of antibody were contained in each preparation (Fig. 4.2a). Titration of each anti-RHAMM mAb solution against the RHAMM fusion protein also indicated similar binding of each mAb to its ligand, whereas anti-CD45 mAb UCHL-1 or purified mouse IgG did not bind to the RHAMM fusion protein (Fig. 4.2b). The anti-RHAMM mAbs interacted with the RHAMM fusion protein, thus each mAb binds to a RHAMM epitope. However, mAb binding to the fusion protein appeared to be relatively low affinity or avidity compared with mAb binding to rabbit anti-mouse IgG.

4.3 Cell Surface RHAMM Expression Co-localizes with HA Binding Sites

Two color confocal analysis of thymocytes stained with anti-RHAMM mAb 3T3-9 and HA-FITC was done to determine if sites of HA-FITC binding at the cell surface coincided with sites of RHAMM expression as indicated by mAb staining. HA-FITC staining was clearly observed in discrete areas on the cell surface (Fig. 4.3a). Anti-RHAMM staining was localized to the same regions of the cell stained by HA-FITC (Fig. 4.3b). This suggested HA was binding to RHAMM expressed at these sites. Consecutive optical sections of stained cells indicated that staining by HA-FITC and mAb 3T3-9 were
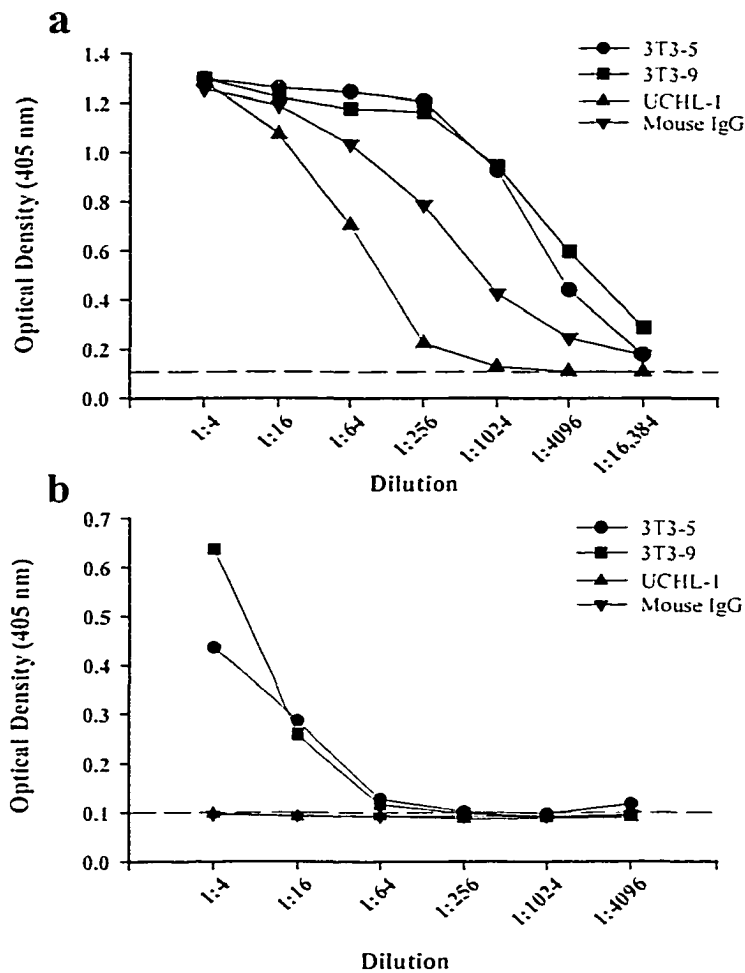
Figure 4.2. Both anti-RHAMM mAbs bind to a RHAMM fusion protein.

Purified rabbit anti-mouse IgG (a) or GST-RHAMM fusion protein (b) was adsorbed to 96 well microtitre plates and serial dilutions of anti-RHAMM mAb 3T3-5 (●), 3T3-9 (■), anti-CD45 mAb UCHL-1 (▲) or mouse IgG (▼) were added followed by goat anti-mouse-alkaline phosphatase, then enzyme substrate solution. Optical density was quantitated at a wavelength of 405 nm. Plotted values are the means of triplicate wells. The dotted lines represent optical density values for the conjugate blanks for each assay.
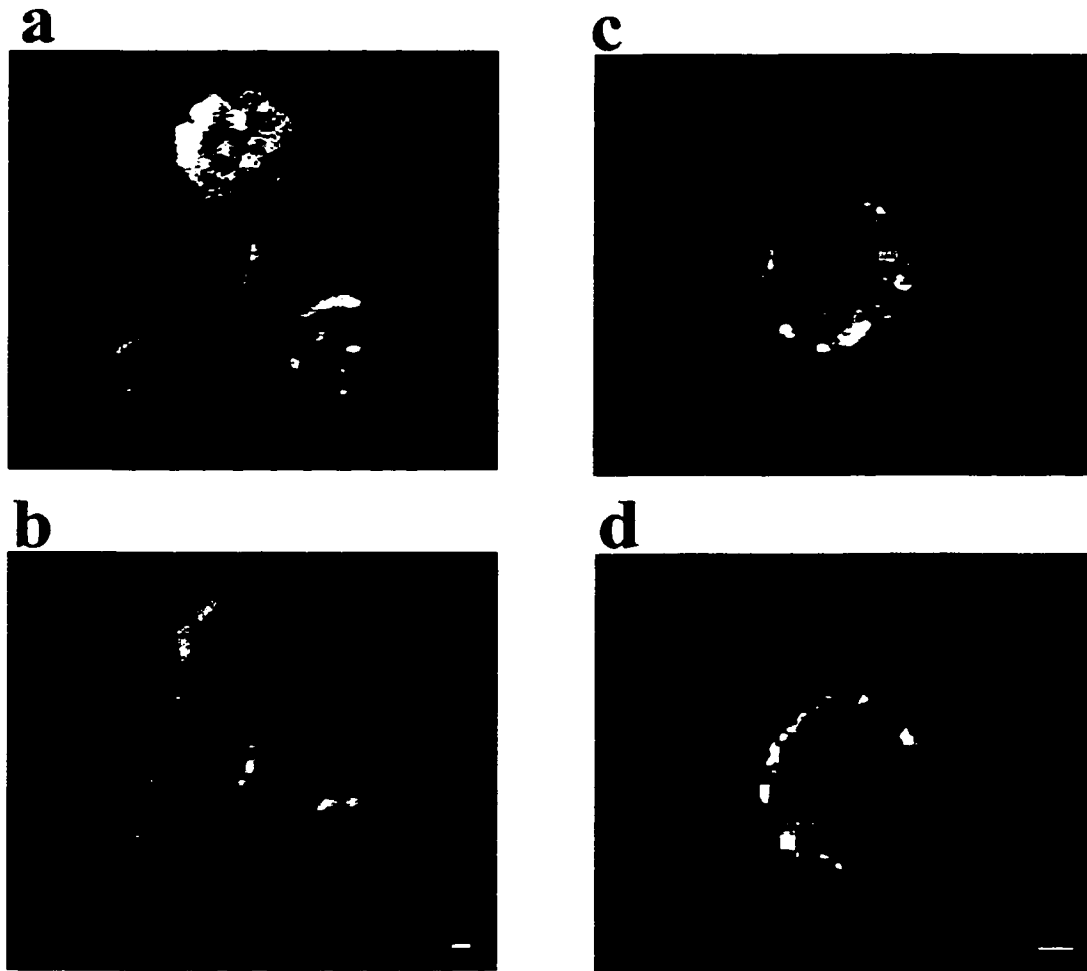
Figure 4.3 Cell surface RHAMM expression co-localizes with HA binding sites.

Thymocytes were stained sequentially using anti-RHAMM mAb 3T3-9 (a) or anti-CD44 mAbs (c) in the first step, goat anti-mouse-TRITC in the second step and HA-FITC in the third step (b & d). The stained cells were analyzed using a Leica confocal LSM. Images of the two fluorophores (a & b or c & d) were acquired by scanning the same field in PMT2 then PMT1 channels, respectively. The bar represents 1 μm.

restricted to the cell surface. Thymocytes stained with mAb 3T3-5 did not demonstrate detectable surface staining. Confocal analysis of thymocytes stained with anti-CD44 and HA-FITC indicated the majority of cell surface sites expressing CD44 (Fig. 4.3d) did not correlate with regions of HA-FITC binding (Fig. 4.3c). Many cell types, including hematopoietic cells express CD44, but are unable to bind HA suggesting activation of CD44 is required to initiate HA binding (Borland et al., 1998). The lack of co-localization of CD44 expression and HA-FITC binding suggested thymocytes did not express CD44 in an active conformation able to bind HA. This suggested that RHAMM mediated HA binding for thymocytes.

4.4 Interaction with HA Increases Cell Surface RHAMM Expression

To determine if ligand binding affected cell surface RHAMM expression, thymocytes were pre-incubated with HA-FITC followed by staining with anti-RHAMM mAbs. Flow cytometric analysis indicated anti-RHAMM mAb 3T3-9 staining was increased by pre-incubation of thymocytes with HA (Fig. 4.4a & b). Pre-treatment with HA also strongly increased surface expression of the epitope detected by anti-RHAMM mAb 3T3-5 which we termed RHAMM-5 (compare Fig. 4.4d and e). Both the number of RHAMM-5$^+$ cells and the expression level of RHAMM-5 increased as indicated by the intensity of staining. When the experiment was done in the presence of the metabolic inhibitor sodium azide, binding by mAb 3T3-5 was decreased (Fig. 4.4f), indicating the HA-dependent increase in surface expression of the RHAMM-5 epitope was energy-dependent. However, azide did not affect the HA-induced increase of mAb 3T3-9
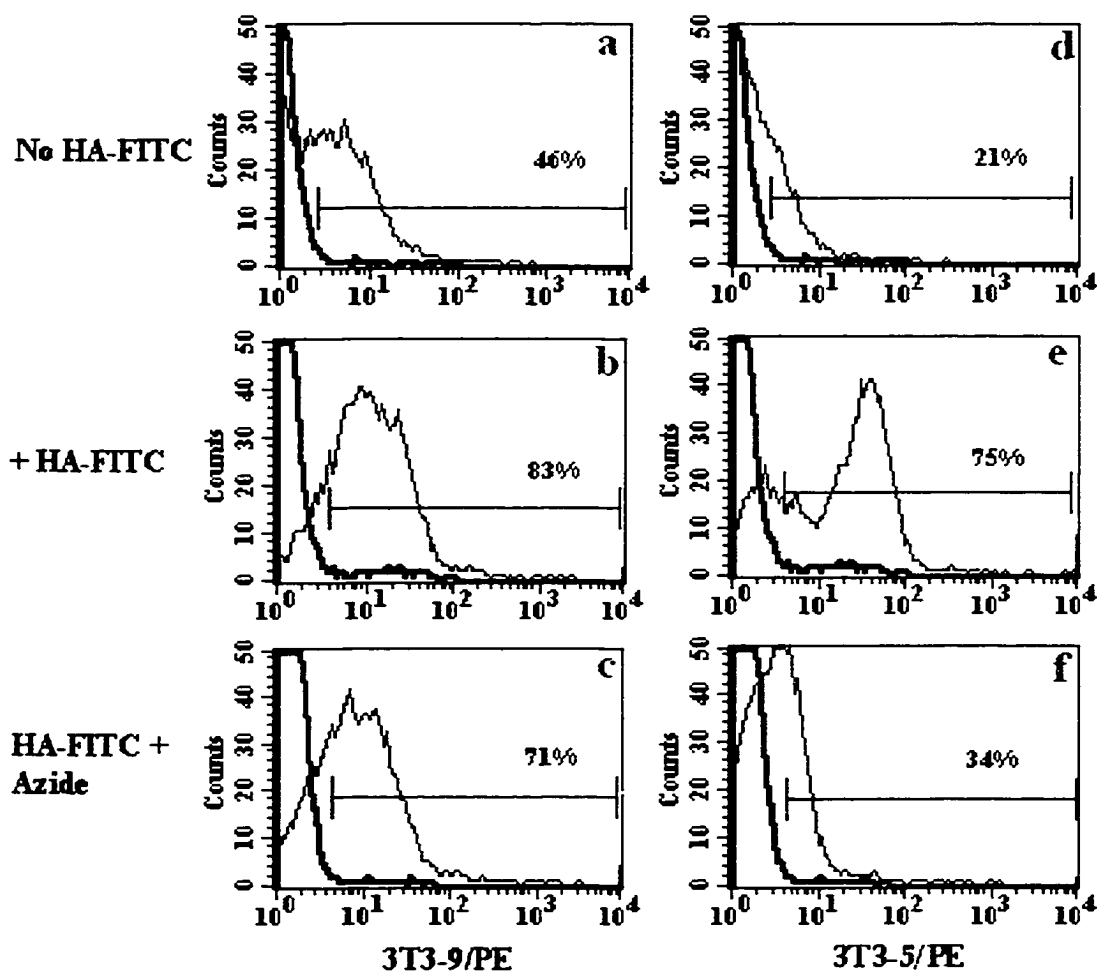
Figure 4.4 Pre-incubation with HA increases cell surface expression of RHAMM.

Thymocytes were stained by indirect IF using anti-RHAMM mAb 3T3-9 (a - c, filled curves) or 3T3-5 (d - f, filled curves) followed by goat anti-mouse-PE (a & d) or were pre-incubated with HA-FITC then stained (b & e) or were pre-incubated with HA-FITC in azide-containing buffer then stained (c & f). The unfilled curves represent staining of like-treated cells using an isotype matched control antibody. Bars and percentages indicated on each histogram are as defined in the legend to Figure 2.1. The histograms represent staining by thymocytes of one donor, but similar staining was observed for cells from three different donors.

staining (Fig. 4.4c). These results suggested that HA might have caused a conformational change in cell surface RHAMM that revealed the RHAMM-5 epitope. HA binding might also initiate clustering of cell surface proteins that are required for the 'expression' of the RHAMM-5 epitope. An alternative possibility is that RHAMM-5 was redistributed to the cell surface from a putative intracellular pool.

4.5 Intracellular RHAMM is Expressed by the Majority of HumanThymocytes

To determine if thymocytes expressed an intracellular form of RHAMM, cells were permeabilized with saponin and subsequently stained by the anti-RHAMM mAbs and analyzed by flow cytometry. For comparison, intact thymocytes were sequentially stained with anti-RHAMM mAbs 3T3-5 or 3T3-9 followed by HA-FITC (Fig. 4.5a & b, respectively). MAb 3T3-5 detected only low levels of surface RHAMM on 18% of untreated thymocytes (Fig. 4.5a), but stained 70% of permeabilized thymocytes (Fig. 4.5c) suggesting the RHAMM-5 epitope was predominantly intracellular. The surface-reactive mAb 3T3-9 stained 28% of intact thymocytes (Fig. 4.5b), but did not stain thymocytes above background (Fig. 4.5d) suggesting saponin treatment caused the loss of this epitope. The intensity of cell staining by HA-FITC increased when thymocytes were permeabilized (compare Fig. 4.5a & b with c & d). This suggested HA was bound by the majority of permeabilized thymocytes through interactions with exposed intracellular RHAMM-5. These data indicated thymocytes expressed a form of RHAMM containing an epitope recognized by mAb 3T3-5 that was predominantly intracellular (RHAMM-5).
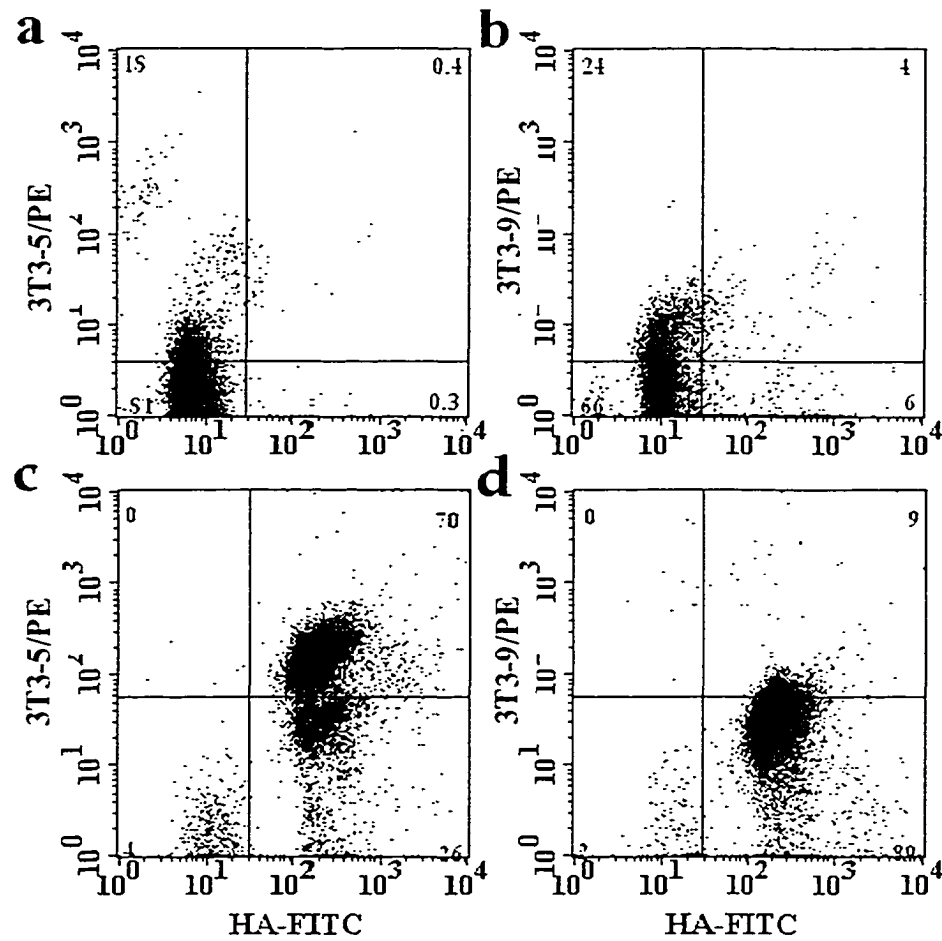
Figure 4.5 The majority of thymocytes express intracellular RHAMM.

Thymocytes were left intact (a & b) or permeabilized by saponin (c & d) then incubated sequentially with anti-RHAMM mAb 3T3-5 (a & c) or 3T3-9 (b &d) in the first step, goat anti-mouse-PE in the second step, then HA-FITC. The horizontal bars were set to indicate the staining intensity of 98% of thymocytes stained with an isotype-matched control mAb. The vertical bar was set to indicate HA-FITC binding by non-permeabilized cells. Numbers in each quadrant indicate the percentage of cells in that quadrant. The dot plots shown are from one thymus donor, but represent typical staining patterns observed for several different donors.

Thymocytes also expressed RHAMM with a second epitope recognized by mAb 3T3-9 that was predominantly expressed at the cell surface (RHAMM-9).

To further examine the intracellular localization of RHAMM-5, permeabilized thymocytes were stained sequentially with mAb 3T3-5 followed by goat anti-mouse-Alexa$_{488}$ then anti-CD45-QR, to stain the cell surface receptor CD45. Stained cells were examined by confocal microscopy. Although thymocytes are relatively small cells with a narrow ring of cytoplasm making specific intracellular localization of staining difficult, RHAMM-5 expression was clearly prevalent within the cell (green fluorophore) and weak on the cell's outer membrane (Fig. 4.6a). However, there were a few areas of overlap between the two fluorophores (yellow-orange) indicating a low density of RHAMM-5 was at the cell surface (Fig 4.6a, arrows), consistent with the flow cytometric profiles (Fig. 4.1b). As a control to confirm the ability to detect co-localized surface staining, thymocytes were stained with a combination of anti-CD3 and anti-CD45 mAbs. Confocal microscopic analysis indicated CD3 expressed on the cell surface co-localized with CD45 to produce yellow-orange staining (Fig. 4.6b, yellow-orange). Developing thymocytes express intracellular CD3 as well as cell surface CD3 and this was indicated by green fluorophore inside the cells.

4.6 Intracellular RHAMM is Recruited to the Cell Surface by HA

The HA-dependent increase in surface expression of RHAMM-5 could reflect ligand-dependent exposure of the epitope through a conformational change of existing
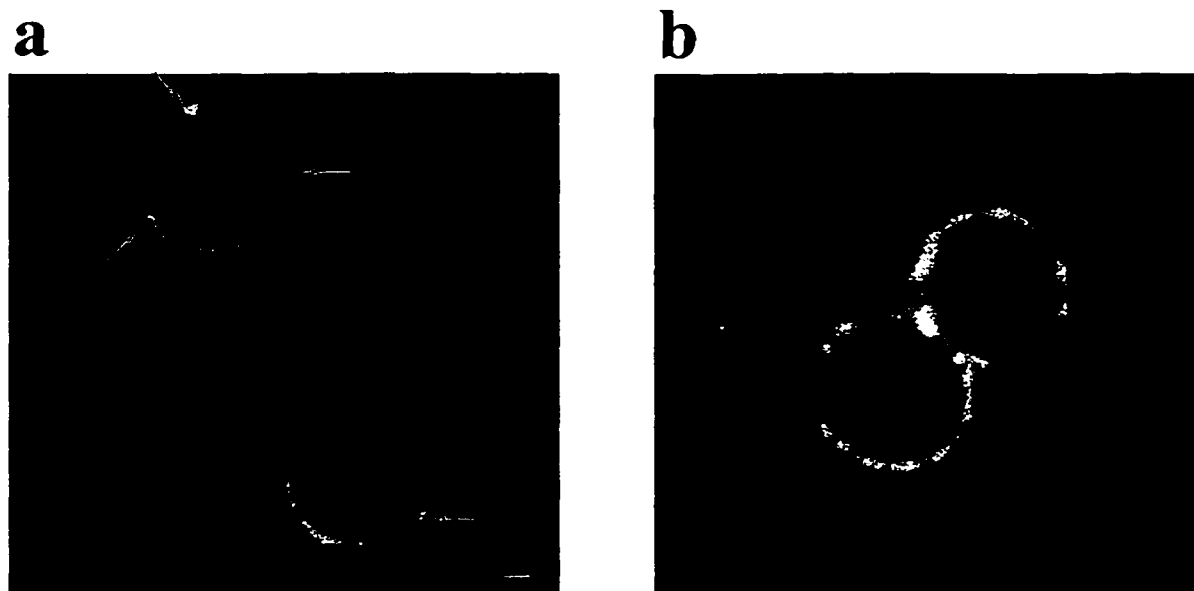
Figure 4.6 Confocal microscopy confirms thymocytes express intracellular RHAMM.

Thymocytes were permeabilized and stained sequentially with anti-RHAMM mAb 3T3-5 or anti-CD3 then goat anti-mouse-$Alexa_{488}$ and anti-CD45-QR in the third step. Confocal images were acquired on a Zeiss confocal LSM. Anti-RHAMM/$Alexa_{488}$ staining (a) and anti-CD3/$Alexa_{488}$ staining (b) is shown as green. Anti-CD45-QR (a & b) staining is shown as red. Areas where both fluorophores overlap appear yellow. Arrows indicate surface co-localization of anti-RHAMM mAbs and anti-CD45-QR staining. The bar represents 1 μm.

cell surface RHAMM-9. Alternatively, intracellular RHAMM-5 could be recruited to the cell surface. To distinguish these possibilities, we attempted to remove cell surface RHAMM by pre-treating thymocytes with PLC. It has been postulated that RHAMM might associate with a gpi-anchored protein at the cell surface (Klewes, 1993). Thymocytes were then treated or not with HA, followed by staining with mAb 3T3-5 or 3T3-9. Cell staining by mAb 3T3-9 generally remained unchanged by PLC pre-treatment (Fig. 4.7a & b). Subsequent addition of HA enhanced the intensity of staining of 3T3-9, consistent with previous observations (compare Fig. 4.7c with 4.4b). The normal weak staining intensity of mAb 3T3-5 was decreased by pre-treatment with PLC (compare Fig. 4.7d & e) suggesting RHAMM-5 was removed from the cell surface by cleaving the putative gpi anchor of RHAMM or an associated protein. However, subsequent exposure of the PLC-treated cells to HA increased the number of RHAMM-5$^+$ cells and the intensity of fluorescence, indicating the density of surface RHAMM-5 was increased by HA even after enzymatic removal of RHAMM-5 from the cell surface (Fig. 4.7f). The density of RHAMM-5 after HA treatment was greater than the density of RHAMM-9 on untreated thymocytes (compare Fig. 4.7a & f), so increased RHAMM-5 expression was not likely the result of an HA-induced conformational change of surface RHAMM. Increased RHAMM-5 expression was more likely the result of HA recruiting intracellular RHAMM-5 to the cell surface.
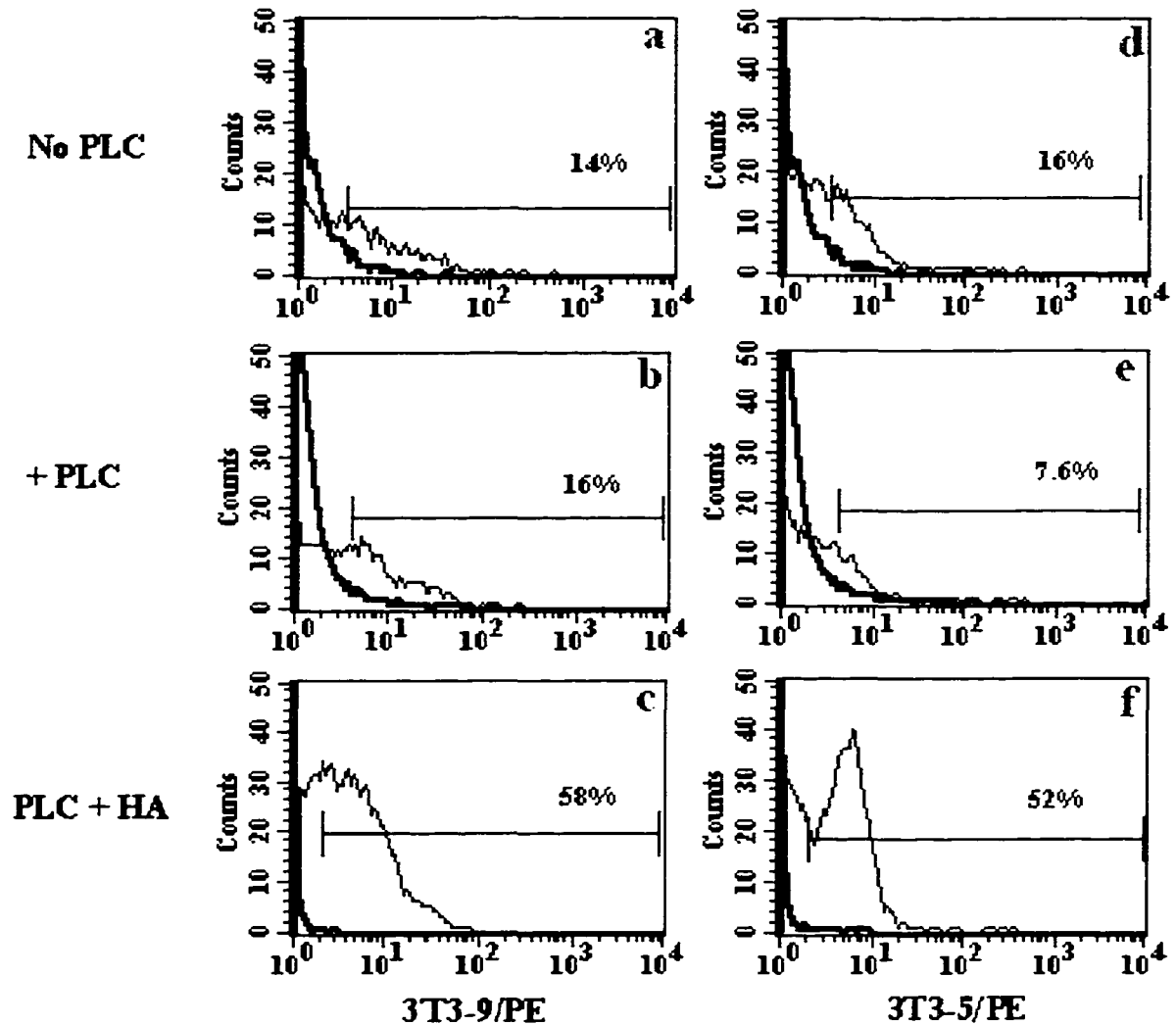
Figure 4.7   HA stimulates redistribution of intracellular RHAMM to the cell surface.

Thymocytes were stained sequentially using anti-RHAMM mAb 3T3-9 (a - c) or 3T3-5 (d - f) then goat anti-mouse-PE (a & d) or were pre-treated with PLC (b & e) or PLC followed by HA (c & f) then stained. Unfilled curves represent staining of like treated cells with an isotype matched control mAb. Bars and percentages are defined in the legend to Figure 2.1. The histograms represent staining by thymocytes of one donor, but similar staining was observed for cells from three different donors.

4.7 RHAMM and HA Function in Thymocyte Motility

RHAMM mediates Fn-dependent motility for thymocytes (Pilarski et al., 1993) and both mAb 3T3-9 and mAb 3T3-5 significantly decreased the number of thymocytes in the presence of HA (Fig. 3.4). To determine if exogenous HA was required for RHAMM to function for locomotion, cells were pre-treated in the presence or absence of HA and Fn-mediated motility was assessed in the presence or absence of exogenous HA. Of total thymocytes, 16% and 15% were motile in the absence or presence of exogenous HA, respectively, (Fig. 4.8, IgG1-treated groups) indicating Fn was the only exogenous ECM component required to support thymocyte motility. In the absence of exogenous HA, pre-treatment of thymocytes with either mAb 3T3-9 or mAb 3T3-5 significantly decreased the number of motile cells. However, inhibition of motility by treatment with mAb 3T3-9 was significantly greater than inhibition caused by mAb 3T3-5 (Fig. 4.8, open bars). This indicated that in the absence of exogenous HA, RHAMM-9 was the predominant mediator of motility as might be expected, since RHAMM-9 was the predominant cell surface form of RHAMM. HA is required by locomoting thymocytes, since hyaluronidase pre-treatment of thymocytes significantly decreases the number of motile thymocytes (Gares et al., 1998). However, endogenous synthesis of HA might support RHAMM-mediated motility as suggested by the expression of hyaluronan synthase genes by thymocytes (Giannakoupolos & Pilarski, unpublished observations).

In the presence of exogenous HA, treatment of cells with either mAb 3T3-9 or mAb 3T3-5 very significantly decreased the number of motile cells. This suggested that
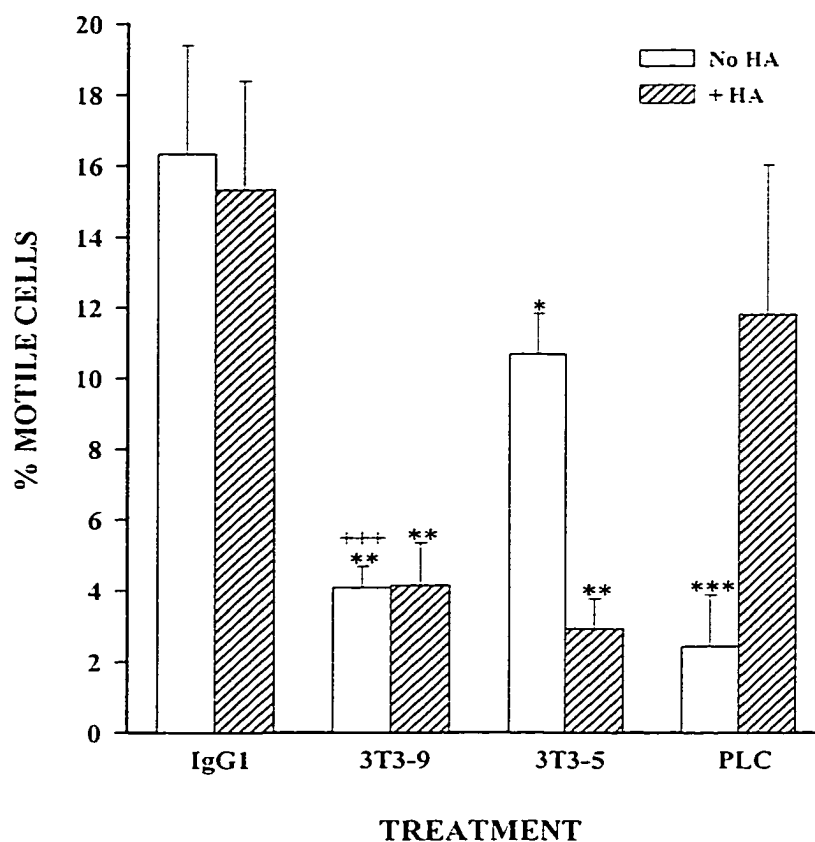
Figure 4.8 Both RHAMM-9 and RHAMM-5 mediate motility.

Thymocytes were pre-treated with the indicated mAbs +/- HA or with PLC then added to Fn-coated wells +/- HA for analysis as described in the legend to Fig. 1.2. Values are the mean +/- SD of three separate experiments using three different thymocyte preparations. Statistical comparisons were made between the IgG1 isotype-matched control group and the corresponding (no HA or + HA) anti-RHAMM mAb- or PLC-treated groups (*) or between mAb 3T3-9 and 3T3-5-treated groups (+). +++ = $p <$ 0.005

HA-dependent redistribution of RHAMM-5 to the cell surface enabled RHAMM-5, along with RHAMM-9 to function for locomotory cells (Fig. 4.8, hatched bars). Pre-treatment of thymocytes with PLC also significantly reduced the number of motile cells, but the presence of exogenous HA following PLC treatment restored motile behavior, aspredicted if HA binding caused rapid surface localization of functionally active RHAMM-5 from intracellular stores.

4.8 Thymocytes Express Distinct Isoforms of RHAMM

The distribution patterns of the RHAMM-9 and RHAMM-5 epitopes in thymocytes suggested these cells might express different isoforms of the RHAMM gene. B cells from multiple myeloma patients express three different isoforms of RHAMM mRNA, two of which are characterized by the absence of 48 bp or 147 bp regions that correlate to the excision of exon 4 or 13, respectively, from the coding sequence (Crainie et al., 1999). RT-PCR was used to amplify RHAMM mRNA isolated from thymocytes to determine if different RHAMM transcripts were expressed. Full length transcripts of RHAMM (RHAMM^{FL}) were expressed by cells isolated from three separate thymocyte preparations as were transcripts containing the 48 bp deletion (RHAMM^{-48}) as indicated by the amplification of PCR products of the appropriate size (Fig. 4.9, lanes 2 - 4). Amplification products of the RHAMM^{FL} isoform are 605 bp and amplification products of RHAMM^{-48} isoforms are 557 bp. A third RHAMM transcript containing the 147 bp deletion (RHAMM^{-147}) was barely detectable in only two of a total of five thymocyte
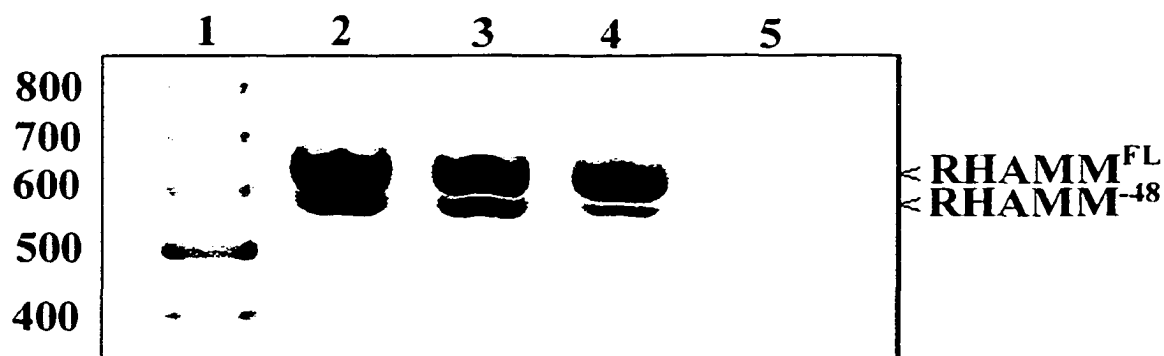
Figure 4.9 Thymocytes express multiple RHAMM mRNA isoforms.

mRNA from three separate thymocyte preparations (lanes 2, 3 and 4) was isolated and amplified by RT-PCR. PCR products were detected by ethidium bromide staining of agarose gels. Molecular weight marker (lane 1) sizes are indicated on the left. PCR products of a size corresponding to RHAMM^{FL} (605 bp) or RHAMM^{-48} (557 bp) are indicated on the right. Lane 5 is a negative control in which superscript™ was omitted from the reverse transcription step. The PCR product shown in lane 2 and the negative control in lane 5 were prepared using the same thymocyte lysate. Negative controls for the other thymocyte preparations were identical to that shown in lane 5.

preparations. This indicated thymocytes predominantly expressed two RHAMM isoforms, RHAMM^{FL} and RHAMM^{-48}.

To determine if RHAMM^{FL} and RHAMM^{-48} mRNA were translated into proteins containing the RHAMM-5 and RHAMM-9 epitopes, thymocyte lysates were prepared from three separate thymus preparations and immunoblotted using anti-RHAMM rabbit serum (Fig. 4.10a). The predicted sizes of RHAMM^{FL} and RHAMM^{-48} are 84.2 and 82.3 Kd. The polyclonal serum detected two bands from each lysate that approximately corresponded with the apparent molecular weight of RHAMM^{FL} and RHAMM^{-48}. Several other bands of unknown identity were also detected by the rabbit antiserum. To reduce the background of proteins on the blots, anti-RHAMM serum, anti-RHAMM mAbs or non-immune serum were used to precipitate RHAMM from thymocyte lysates. Precipitated material was then immunoblotted with the anti-RHAMM serum. One protein band specifically detected by anti-RHAMM serum was approximately 84 Kd (Fig 4.10b, lane 4). Non-immune rabbit serum did not precipitate proteins in this size range (Fig. 4.10b, lane 2) nor did the two anti-RHAMM mAbs (data not shown). The higher molecular weight band (~97 Kd, Fig. 4.10b, lane 4) was frequently detected by both anti-RHAMM and anti-GFP serum (see Fig. 5.1) and does not likely correspond to RHAMM. These data suggested the RHAMM-specific mRNA was translated into two different RHAMM proteins, RHAMM^{FL} and RHAMM^{-48} in thymocytes. Although immunoblots detected two protein bands that correspond to the predicted size of RHAMM^{FL} and RHAMM^{-48}, immunoprecipitation of thymocyte lysates only indicated the presence of one protein band that corresponded to the size of RHAMM^{FL}.
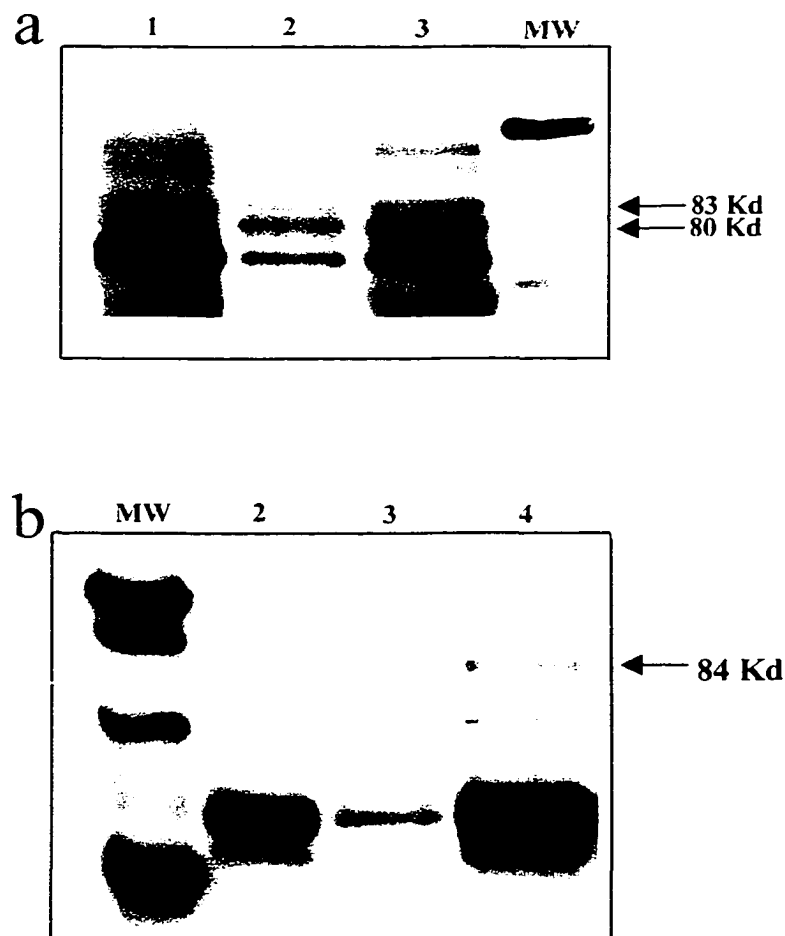
Figure 4.10 Thymocytes express RHAMM^{FL} and RHAMM^{-48} proteins.

Thymocyte lysates prepared from three separate thymus preparations (a, lanes 1 - 3) were separated on 7% gels then immunblotted. Proteins precipitated from a thymocyte lysate using non-immune (b, lane 2) or anti-RHAMM polyclonal serum (b, lane 4) were separated on 7.5% SDS-PAGE gels followed by immunoblotting. Anti-RHAMM serum was added to lane 3 for comparison. Both a & b were blotted using anti-RHAMM rabbit serum. The molecular weight markers shown are, from the top, 116.25, 97.4, 66.2 and 45 (not present in a). Arrows indicate bands with apparent MWs similar to RHAMM.

4.9 Summary: HA Modulates RHAMM Distribution and Thymocytes Express Two RHAMM Isoforms

The ability of integrins to shift between low and high affinity binding conformations enables a cell to rapidly alter cellular behavior. If RHAMM and integrins have a functional relationship, RHAMM might also be expressed in a manner that enables rapid adaptation to microenvironmental cues. To study this we have examined the expression and function of RHAMM in the presence of exogenous HA.

We used two different anti-RHAMM mAbs, 3T3-5 and 3T3-9, to stain thymocytes. The epitope of RHAMM detected by mAb 3T3-9 was expressed at low density on the cell surface of 30 to 60% of thymocytes from different thymus donors. When thymocytes were stained sequentially with mAb 3T3-9 then HA-FITC and examined by confocal microscopy, HA-FITC binding sites co-localized with RHAMM surface expression. CD44 was expressed at relatively high density by thymocytes, but HA binding did not co-localize strongly with sites of CD44 expression. This suggested RHAMM was the predominant cell surface HA binding receptor used by human thymocytes. CD44 receptors expressed by a variety of cell types require activation before HA binding is detectable, including most normal hematopoietic cells (Borland et al., 1997). Certain anti-CD44 mAbs can stimulate HA binding by T cell lines (Lesley et al., 1993) and antigenic stimulation of peripheral T cells also transiently upregulates HA binding (Lesley et al., 1994). Enhanced HA binding by CD44 occurs upon CD44 receptor clustering and is independent of the intracellular domain of CD44 (Perschl et al., 1995; Sleeman et al., 1996). Although CD44 functions in adhesion early in thymocyte ontogeny, expression is transiently downregulated as thymocyte precursors begin to

differentiate (Res & Spits, 1999). Although virtually all unfractionated human thymocytes expressed CD44, the lack of co-localization of CD44 expression and HA binding sites suggested thymocytes expressed CD44 in an unactivated form that does not bind HA.

A second anti-RHAMM mAb, 3T3-5 demonstrated very low to negligible binding to intact thymocytes. However, both anti-RHAMM mAbs could bind to a RHAMM fusion protein as assessed by an ELISA suggesting cell surface RHAMM might lack or conceal the epitope of mAb 3T3-5. Alternatively, these two mAbs might recognize RHAMM epitopes expressed by different isoforms of RHAMM or cross-react with epitopes expressed by cell surface proteins unrelated to RHAMM. Flow cytometric analysis and confocal microscopy indicated mAb 3T3-5 detected an intracellular form of RHAMM, termed RHAMM-5, that is expressed by 70% of thymocytes. MAb 3T3-9 detected cell surface RHAMM (RHAMM-9), but did not stain permeabilized thymocytes suggesting this epitope was destroyed by permeabilization. Analysis of the predicted amino acid sequence of human RHAMM using various motif search programs predict that RHAMM is an intracellular protein. The amino acid sequence contains no obvious signal sequence or transmembrane domain, although there is abundant evidence that RHAMM is expressed at the cell surface of normal and transformed cells (Pilarski et al., 1993; Nagy et al., 1995; Masellis-Smith et al., 1996; Crainie et al., 1999; Pilarski et al., 1999).

To determine if HA binding affected surface expression of RHAMM, intact thymocytes were pre-treated with soluble HA-FITC then stained with mAbs to RHAMM. Surprisingly, HA pre-treatment resulted in detection of cell surface RHAMM by mAb

3T3-5. HA binding increased the number of RHAMM$^+$ cells and increased the density of RHAMM expressed at the cell surface as detected by mAb 3T3-5. Two different models can explain the data. These two mAbs might recognize different, conformation-dependent epitopes on the same RHAMM protein. The RHAMM-9 epitope is always available while the RHAMM-5 epitope is normally hidden. HA binding causes a conformational change of RHAMM revealing the RHAMM-5 epitope while maintaining the RHAMM-9 epitope. Alternatively, the RHAMM-5 epitope might be expressed on intracellular RHAMM. HA-dependent redistribution of intracellular RHAMM-5 to the cell surface makes this epitope available to mAb 3T3-5. The latter possibility suggests intracellular RHAMM is a different isoform than that normally expressed at the cell surface.

These observations suggested thymocytes maintained an intracellular store of RHAMM that mediated motility when redistributed to the cell surface by appropriate microenvironmental cues. RHAMM-5 was required by locomotory thymocytes, as indicated by the significant inhibition of motile cells after treatment with mAb 3T3-5. This observation predicted HA should be required to mediate motility, so intracellular RHAMM-5 can be redistributed to the cell surface. Surprisingly, 16% of thymocytes were motile on Fn-coated wells in the presence or absence of HA suggesting motility was HA-independent. However, pre-treating thymocytes with hyaluronidase significantly decreased Fn-dependent motility (Gares et al., 1998). Addition of exogenous HA to hyaluronidase-treated thymocytes restored motility suggesting RHAMM-mediated locomotion was HA-dependent. This observation also suggested thymocytes synthesize endogenous HA.

To determine if both RHAMM-9 and RHAMM-5 participated in motility, thymocytes pre-treated with anti-RHAMM mAbs in the presence or absence of HA were washed and motility was assessed on Fn-coated wells in the presence or absence of exogenous HA. MAb 3T3-9 significantly inhibited the number of motile cells in the presence or absence of HA indicating RHAMM-9 was a functional mediator of motility. In contrast, mAb 3T3-5 decreased the number of motile cells slightly, but significantly, in the absence of exogenous HA, but inhibited motility much more significantly in the presence of HA. This corresponded to the flow cytometry data indicating redistribution of intracellular RHAMM-5 to the cell surface required an exogenous source of HA. The redistribution of intracellular RHAMM-5 must require high levels of HA and in our experimental system, this can only be achieved when exogenous HA is added.

These experiments indicated both RHAMM-9 and RHAMM-5 mediated motility and both forms of RHAMM were required for motility, since mAbs to either form of RHAMM significantly decreased motility. MAb binding did not block HA binding to RHAMM-9, therefore the inhibition of motility by mAb binding presumably interfered with other functions of RHAMM. The different cellular distribution patterns of RHAMM-5 and RHAMM-9 suggested thymocytes might express two functionally distinct isoforms of RHAMM. PCR analysis indicated thymocytes expressed transcripts for $RHAMM^{FL}$ and $RHAMM^{-48}$. Immunoblots of thymocyte lysates showed two proteins with molecular weights corresponding to $RHAMM^{FL}$ and $RHAMM^{-48}$ were detected using RHAMM-specific antiserum. The same antiserum precipitated only one protein corresponding with the size of $RHAMM^{FL}$. However, numerous attempts to precipitate RHAMM from thymocyte lysates using the two anti-RHAMM mAbs have failed to

precipitate detectable RHAMM protein. These mAbs were also unable to detect RHAMM isoforms in immunoblots. Therefore, this approach was unable to definitively prove the two distribution patterns were related to the expression of two different RHAMM isoforms.

.

CHAPTER 5. Cellular Localization of RHAMM Isoforms

The mAb binding patterns, molecular and biochemical data were consistent with the expression of two different isoforms of RHAMM by thymocytes. However, the mAbs initially used to characterize RHAMM did not detectably precipitate or blot RHAMM in, so a definitive correlation between RHAMM isoforms and cellular distribution patterns could not be made. To try to resolve this issue, a molecular approach was used to characterize the cellular localization of the three different RHAMM isoforms.

Specific Objective 3

To examine the cellular distribution of three different RHAMM isoforms using COS cells transfected with GFP-RHAMM expression plasmids. These experiments will be done using confocal microscopy.

5.1 Transfected COS Cells Express GFP-RHAMM Fusion Proteins

The cDNA sequence of each different RHAMM isoform was inserted into plasmids containing the gene for GFP. RHAMM sequences were inserted downstream of GFP. Purified plasmids were used to transiently transfect COS cells and expression of the fusion proteins was assessed using immunoprecipitation and immunoblotting. COS cells transfected with GFP, GFP-RHAMM^{FL}, GFP-RHAMM^{-147} or GFP-RHAMM^{-48} plasmids were cultured for 48 H following transfection then harvested and lysates prepared. GFP-RHAMM fusion proteins were precipitated from lysates using non-immune serum, anti-GFP or anti-RHAMM polyclonal antibodies and blotted onto nitrocellulose membranes. Fusion proteins were detected by immunoblotting with anti-GFP (Fig. 5.1a) or anti-RHAMM serum (Fig. 5.1b). RHAMM^{FL}, RHAMM^{-147} and RHAMM^{-48} are predicted to be 84.2, 78.4 and 82.3 Kd, respectively, and GFP is 20 Kd. The apparent molecular weight of fusion proteins precipitated from each transfected cell line was 108 Kd for GFP-RHAMM^{FL} (Fig. 5.1a, lane 7 and 5.1b, lanes 6 & 7), 100 Kd for GFP-RHAMM^{-147} (Fig. 5.1a, lane 8 and Fig. 5.1b, lanes 9 & 10) and 104 Kd for GFP-RHAMM^{-48} (Fig. 5.1a, lane 9 and 5.1b, lanes 12 & 13), approximately the expected size of each fusion protein. Each fusion protein was precipitated and blotted with both anti-GFP and anti-RHAMM antiserum indicating these three proteins were translated into proteins containing GFP and RHAMM epitopes, thus are indeed fusion proteins. A strong band of approximately 20 Kd was detectable in lysates prepared from GFP-transfected cells (Fig. 5.1a, lane 6), but bands in the molecular weight range of the fusion
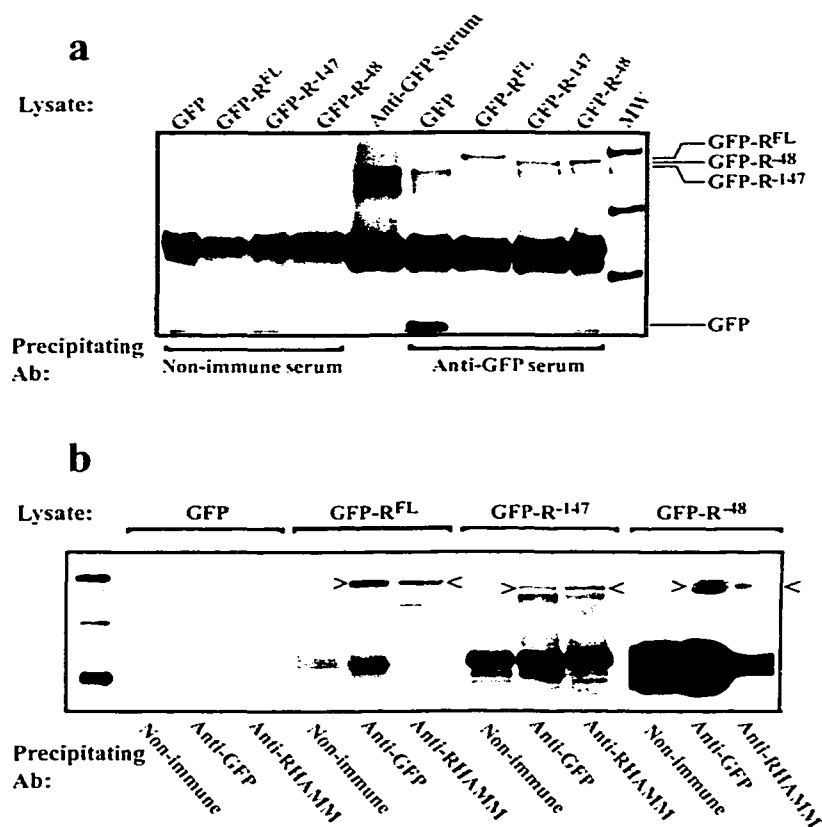
Figure 5.1 Transfected COS Cells Express GFP-RHAMM Fusion Proteins.

Proteins were precipitated from lysates of GFP-, GFP-RHAMM^{FL}-, GFP-RHAMM^{-147}- or GFP-RHAMM^{-48}- transfected cells (lysates are identified at the top of each lane) with non-immune rabbit serum, anti-GFP serum or anti-RHAMM serum (precipitating reagent indicated at the bottom of each lane). Anti-GFP serum was loaded for comparison to lanes loaded with precipitated proteins (a, lane 5). Fusion proteins were visualized by blotting with anti-GFP serum (a) or anti-RHAMM serum AP-HV4-1.2 (b) followed by goat anti-rabbit-HRP and avidin-HRP. Biotinylated MW markers are, from top to bottom, 116.25, 97.4, 66.2 and 45 Kd (a, lane 10 and b, lane1). Unique bands consistent with the expected MW of GFP or GFP-RHAMM fusion proteins are indicated to the right (a) or with open arrowheads (b).

proteins were not precipitated from GFP control lysates (Fig. 5.1a, lane 6 and 5.1b, lanes 3 & 4). Non-immune rabbit serum did not detectably precipitate fusion proteins (Fig. 5.1a, lanes 1 – 4 and 5.1b, lanes 5, 8 & 11) indicating the specificity of anti-GFP and anti-RHAMM sera for their respective epitopes. Anti-RHAMM mAbs 3T3-9 and 3T3-5 were also used to precipitate or to blot the GFP-RHAMM fusion proteins, but proteins of the expected size were not detected (data not shown).

5.2 GFP-RHAMM Isoforms Have Different Distribution Patterns

To determine if the sequences excised from RHAMM^{-48} and RHAMM^{-147} affected cellular localization, COS cells were transiently transfected with the GFP-RHAMM plasmids and cells were examined by confocal microscopy 6, 24 or 48 H after transfection. At each time point, COS cells transfected with GFP plasmids expressed GFP within the nuclear and cytoplasmic regions of the cell (Fig. 5.2a - c) as indicated by intense fluorescence of transfected cells. Aliquots of GFP-transfected cells analyzed by flow cytometry indicated 35 to 60% of cells expressed GFP at each time point. GFP expression was strong 6H following transfection (Fig. 5.2a), peaked 24 H after transfection (Fig. 5.2b), but was still strongly expressed 48 H post-transfection (Fig. 5.2c).

COS cells transfected with GFP-RHAMM^{FL} plasmids were either transfected or expressed the GFP fusion protein with decreased efficiency compared with GFP transfected cells as indicated by a lower number of GFP fluorescing cells when examined by flow cytometry (10 – 15% fluorescing cells). The pattern of fluorescence of GFP-
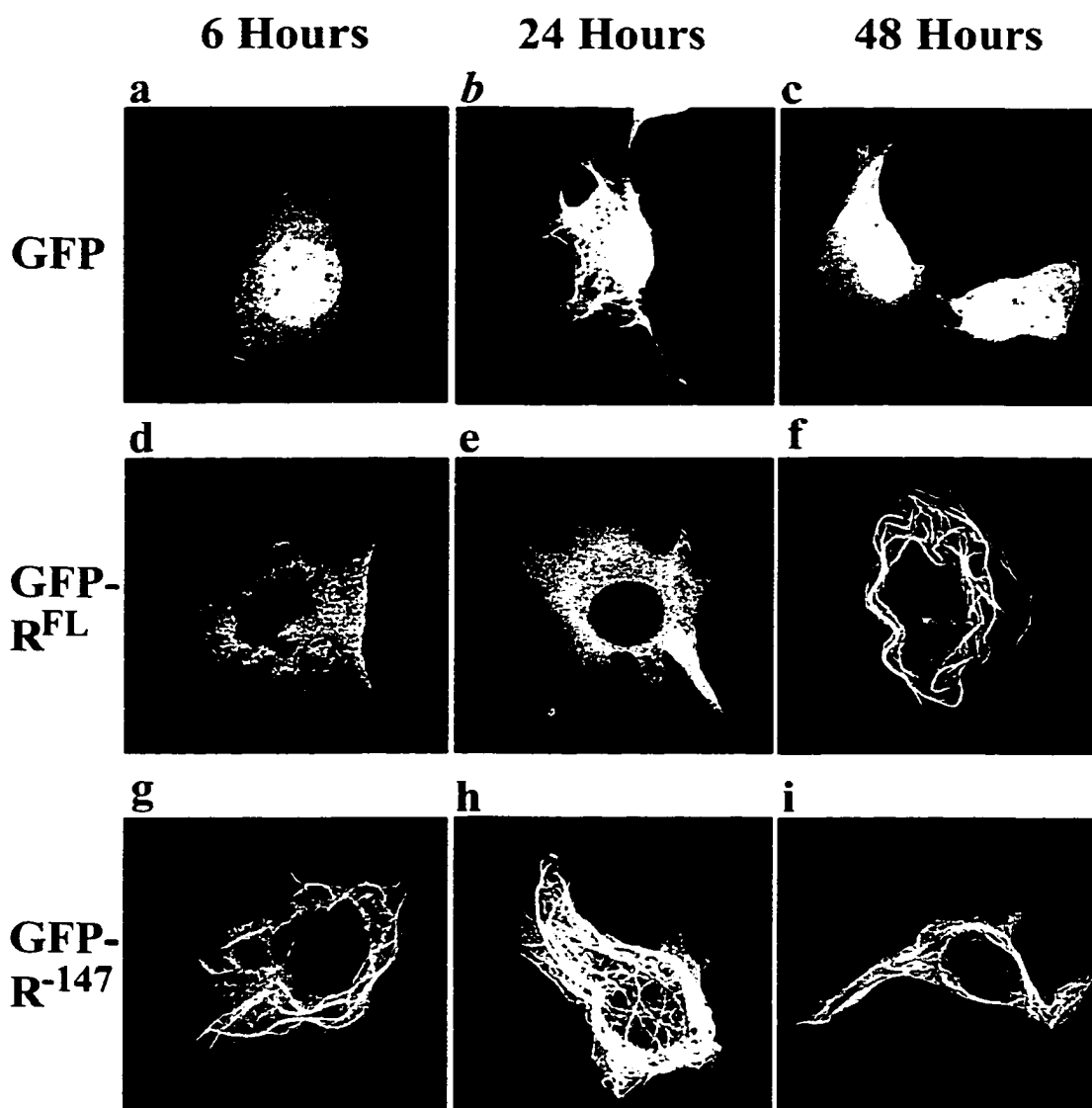
Figure 5.2 GFP-RHAMM isoforms have different cellular distribution patterns.

COS cells were transiently transfected with plasmids containing GFP (a – c), GFP-RHAMM^{FL} (d – f), GFP-RHAMM^{-147} (g – i) or GFP-RHAMM^{-48} (j – m) and cultured for 6 H (a, d, g, j), 24 H (b, e, h, k, m) or 48 H (c, f, i, l) in chamber slides then examined by confocal microscopy. Images (n) and (o) are enlargements of the area indicated in (m) and (k), respectively. Images were acquired on a Zeiss confocal LSM. The bar represents 10 μm.

6 Hours **24 Hours** **48 Hours**

GFP-
R⁻⁴⁸
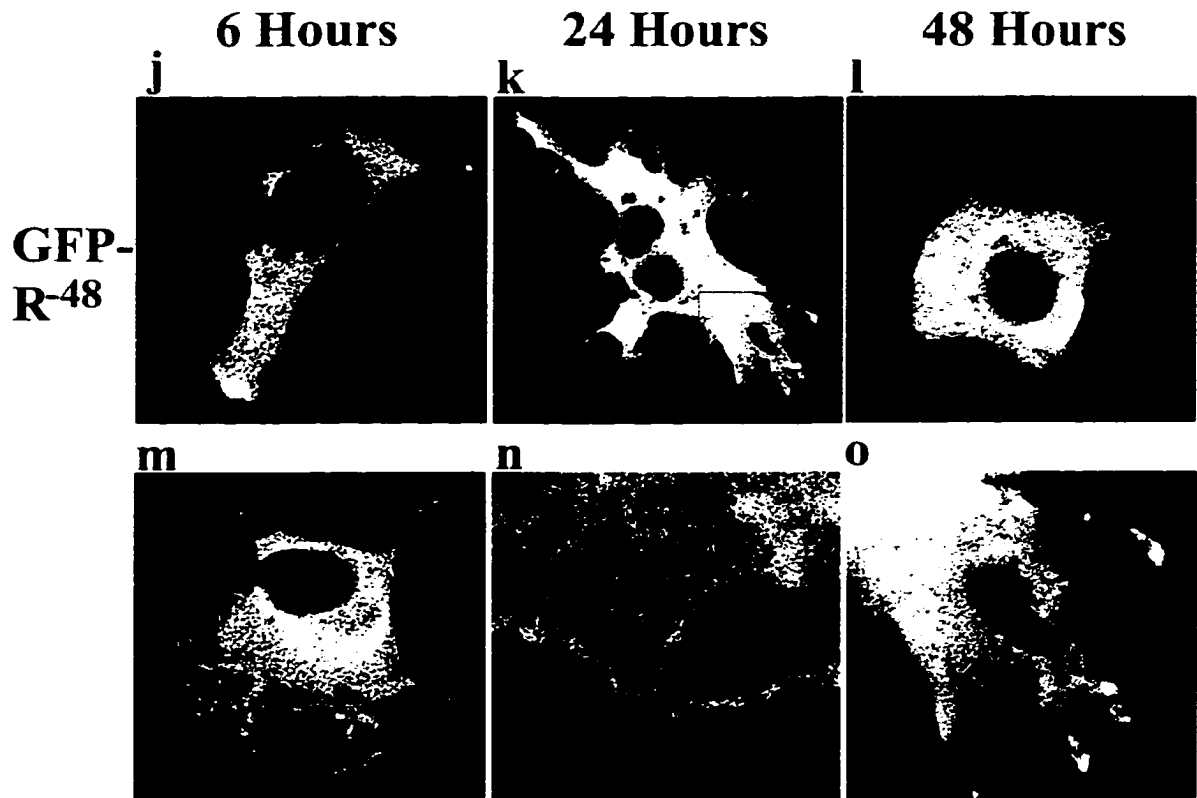
Figure 5.2 cont. GFP-RHAMM isoforms have different cellular distribution

patterns.

RHAMM^{FL}-transfected cells (Fig. 5.2d - f) was distinct compared with cells transfected with GFP plasmids. After 6 H of culture, GFP-RHAMM^{FL} was visible in transfected cells and had a diffuse, cytoplasmic staining pattern that was clearly absent from the nuclear region (Fig. 5.2d). After 24 H of culture, most transfected cells expressed greater quantities of GFP-RHAMM^{FL} diffusely distributed throughout the entire cell body including cell processes (Fig. 5.2e). In addition, some transfected cells had a fluorescent pattern suggesting a portion of the GFP-RHAMM^{FL} fusion protein was associated with the MT cytoskeleton. However, after 48 H of culture, all GFP-RHAMM^{FL}-transfected cells had a fluorescent pattern that was highly organized and appeared consistent with the majority of the fusion protein associating with the MT cytoskeleton throughout the cytoplasm and around the nucleus (Fig. 5.2f). A fraction of GFP-RHAMM^{FL} remained diffusely distributed in transfected cells even after 48 H of culture.

COS cells transfected with GFP-RHAMM^{-147} plasmid also had a lower level of transfection efficiency than GFP transfected cells as indicated by flow cytometric analysis (8 − 10% fluorescent cells). At all time points analyzed, GFP-RHAMM^{-147} fusion proteins had a tendency to associate with MTs (Fig. 5.2g - i). After 6 H of culture, the majority of fluorescence was in a MT-associated pattern throughout the cytoplasm while a minority of fusion protein was diffusely distributed in the cytoplasm (Fig. 5.2g). After 24 or 48 H of culture, GFP-RHAMM^{-147} fusion proteins were expressed throughout the cell body and along processes and virtually all fluorescing proteins were associated with the MT cytoskeleton (Fig. 5.2h & i). Recently, another group used confocal analysis to show endogenous RHAMM or GFP-RHAMM fusion proteins co-localize with tubulin in HeLa cells (Assmann et al., 1999). The sequence encoded by exon 4 of RHAMM was

required to mediate efficient binding of RHAMM to polymerized tubulin in an *in vitro* co-sedimentation assay, thus using a different model system, our results verify these observations.

GFP-RHAMM^{-48} transfectants had a diffuse staining pattern throughout the cytoplasm, absent from the nuclear region and not in a pattern indicating association with MTs at any time point (Fig. 5.2j – m). Flow cytometric analysis indicated 20 – 22% of cells were fluorescent. After 6 and 24 H of culture a portion of the fusion protein was localized at the tips of cell protrusions or lamellipodia and ruffled membranes (Fig. 5.2j, k, m). An enlarged view of Fig. 5.2k indicated GFP-RHAMM^{-48} was concentrated in discrete areas at the tips of lamellipodia that resemble focal complexes or focal adhesions (Fig. 5.2o). An enlarged view of Fig. 5.2m showed GFP-RHAMM^{-48} was clearly distributed along the ruffled membrane in proximity to or at the cell surface (Fig. 5.2n). Thus, GFP-RHAMM^{-48} was the only isoform of RHAMM clearly expressed in association with cell membranes. After 24 H of culture, a strong perinuclear distribution of RHAMM was apparent in some cells (Fig. 5.2m). After 48 H of culture, GFP-RHAMM^{-48} fusion proteins were diffusely distributed throughout the cell, but no longer demonstrated an association with the cell membrane (Fig. 5.2l).

5.3 RHAMM and GFP Epitopes Co-localize in Transfected COS Cells

GFP and GFP-RHAMM transfectants were stained with anti-RHAMM serum to ensure that fluorescing protein was comprised of GFP fused to RHAMM. COS cells transfected with GFP-RHAMM^{-48} (Fig. 5.3a – c) or GFP-RHAMM^{FL} (Fig. 5.3d – f) then

157
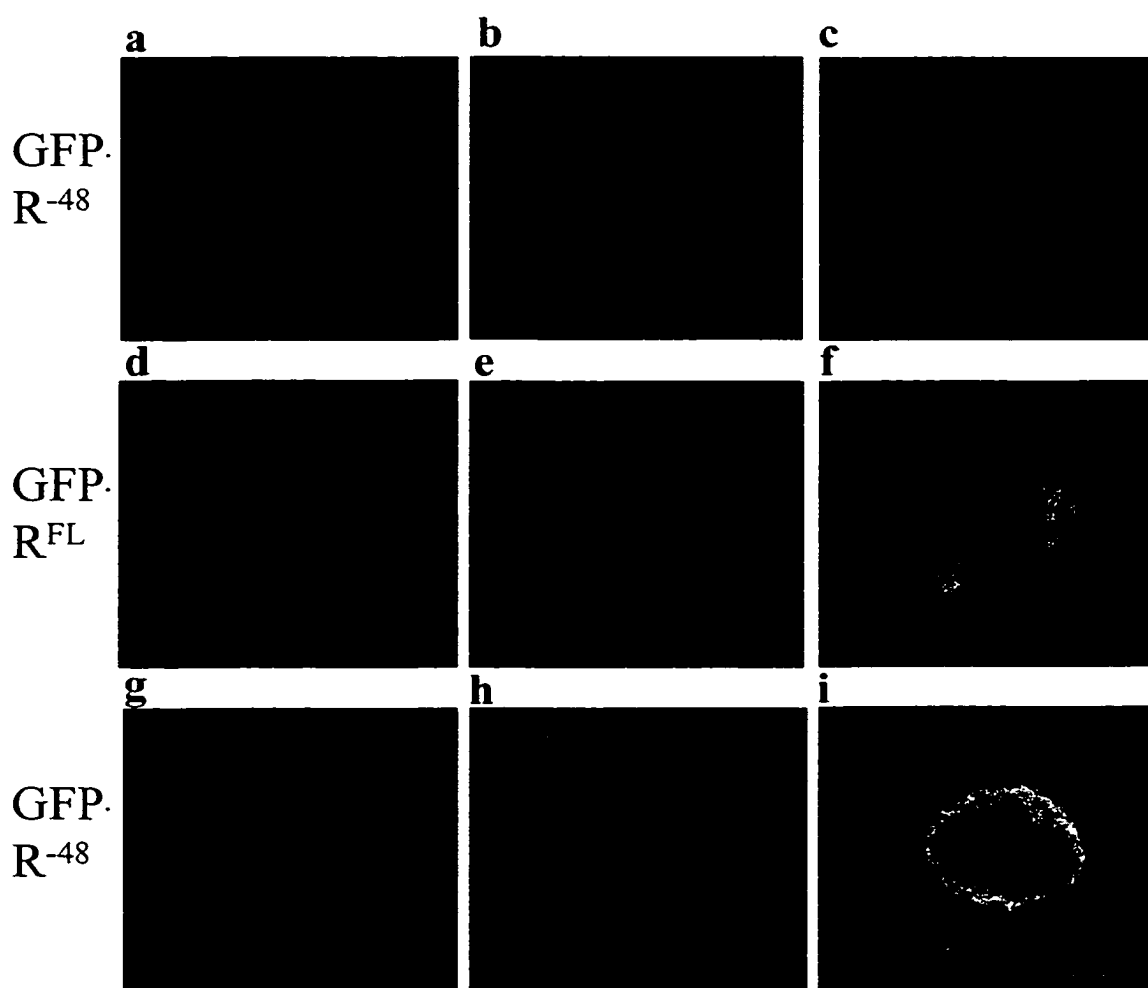
Figure 5.3 GFP-RHAMM transfected cells express RHAMM and GFP epitopes.

GFP-RHAMM^{-48} (a - c) or GFP-RHAMM^{FL} (d - f) transfected COS cells were stained

sequentially with anti-RHAMM serum followed by biotinylated goat anti-rabbit IgG

then streptavidin-QR or membranes of GFP-R^{-48} transfected COS cells were labeled

with PKH26 (g - i). Red depicts antibody or membrane staining (a, d, g), green

depicts GFP fluorescence (b, e, h) and areas of co-localization are yellow-orange(c, f,

i). Images were acquired on a Zeiss confocal LSM. The bars represent 10 μM.

stained with anti-RHAMM serum 48 H post transfection had a pattern of staining that co-localized with the distribution of GFP fluorophore indicating fluorescence was emitted from fusion proteins. Although anti-RHAMM staining did not delineate the MT association as clearly as did GFP fluorophore, this is likely due to the indirect method of staining. Confocal images of transfected cells stained with anti-GFP serum also indicated this staining protocol did not clearly delineate the MT association of GFP-RHAMM^{FL} or GFP-RHAMM^{-147}. Anti-RHAMM and anti-GFP sera also co-localized with GFP fluorophore in cells transfected with GFP-RHAMM^{-147}. Cells transfected with GFP plasmid also stained well with anti-GFP serum, but did not stain above background intensity when stained with anti-RHAMM serum. Anti-RHAMM mAbs 3T3-5 and 3T3-9 were also used to stain transfected cells, but detectable staining was not apparent in cells examined by flow cytometry or confocal microscopy (data not shown).

5.4 Cellular Distribution of Fusion Proteins is Altered when Cells are Rendered Non-adherent

To further examine whether GFP-RHAMM^{-48} fusion proteins were expressed at the cell surface, transfected COS cells were harvested and stained with the membrane dye PKH26 then examined by confocal microscopy. Transfected cells generally assumed a more rounded shape in suspension as indicated by membrane-stained images (Fig. 5.4a, d, g). The pattern of GFP-RHAMM distribution became diffuse for cells expressing either GFP-RHAMM^{FL} (Fig. 5.4a - c) or GFP-RHAMM^{-147} (Fig. 5.4d - f) suggesting these fusion proteins were no longer associated with the MT cytoskeleton or that the MT
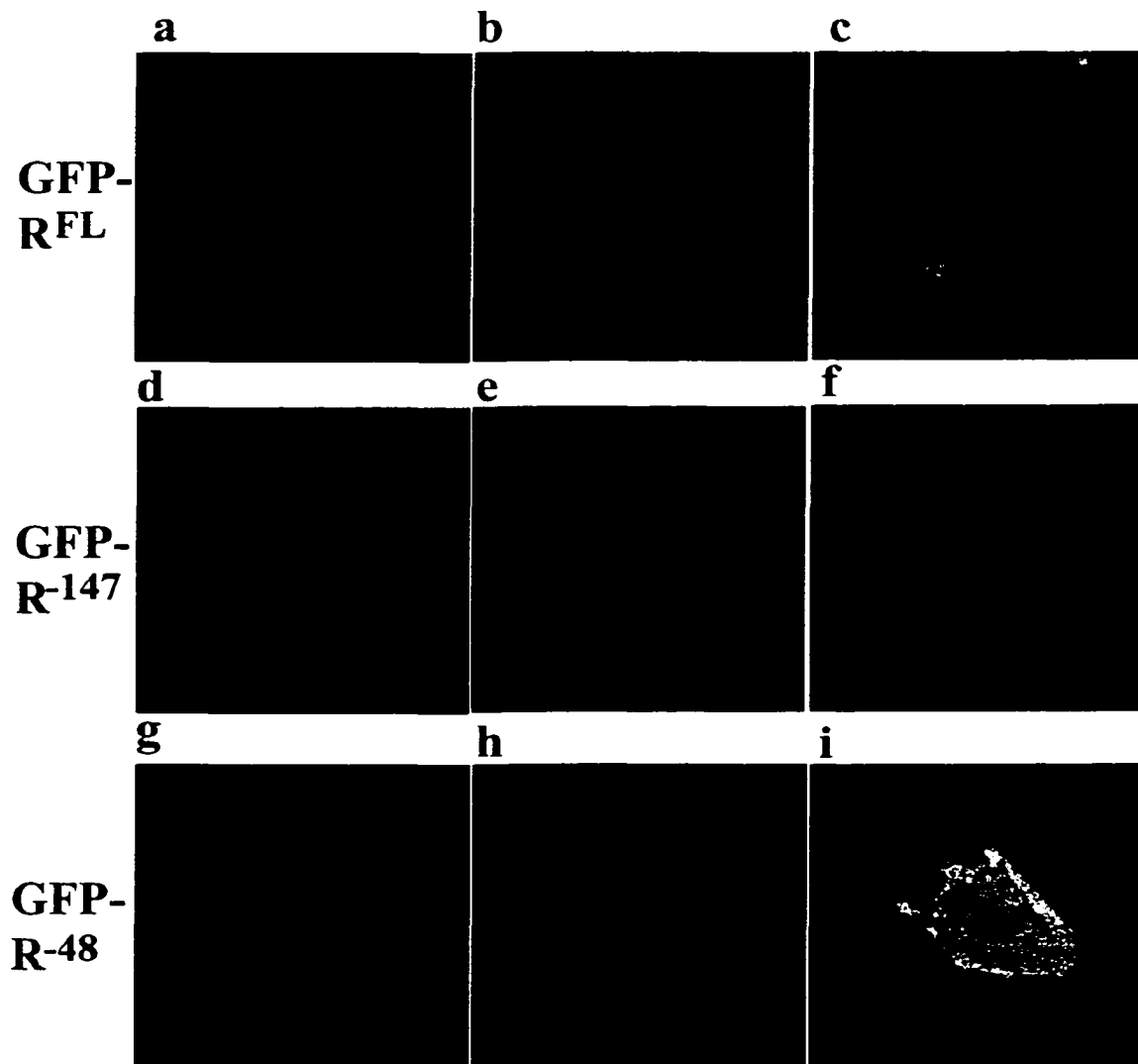
Figure 5.4 Non-adherent COS cells alter the distribution of GFP-RHAMM.

COS cells transfected with GFP-RHAMM^{FL} (a - c), GFP-RHAMM^{-147} (d - f) or GFP-RHAMM^{-48} (g - i) were harvested 48 H post-transfection and labeled with PKH26. Red images depict PKH26 staining (a, d, g), green images depict GFP fluorescence (b, e, h) and areas where the two fluorophores overlap are yellow (c, f, i). Images were acquired on a Zeiss confocal LSM. The bar represents 10 μm.

cytoskeleton was disassembled. Mid-section optical slices through transfected cells indicated GFP-RHAMM^{-147} fusion proteins remained intracellular (Fig. 5.4e) and there was little or no co-localization of GFP-RHAMM^{-147} with the cell membrane as indicated by the absence of yellow-orange staining in the composite confocal image (Fig. 5.4f). GFP-RHAMM^{FL} fusion proteins were also intracellular (Fig. 5.4b) and there were no or very minor associations with the stained membrane as indicated in the composite image (Fig. 5.4c).

GFP-RHAMM^{-48} transfected cells demonstrated strong co-localization of fusion protein with the stained membrane (Fig. 5.3g – i & 5.4g – i). An optical section of the outer cell surface demonstrated fusion proteins were distributed with the stained cell membrane as indicated by the yellow-orange color (Fig. 5.4i). Mid section optical slices of the same cell showed co-localization of fusion protein and stained membrane around the entire cell periphery (Fig. 5.3g – i). This suggested that for cells rendered non-adherent, GFP-RHAMM^{-48} was predominantly expressed in association with the cell membrane.

5.6 Summary: GFP-RHAMM Fusion Proteins Have Two Cellular Distribution Patterns

The GFP-RHAMM fusion constructs were prepared and used to transfect COS cells. This cell line proved to have the best transfection efficiency compared with Jurkat, CEM or 3T3 fibroblast cell lines. Biochemical analysis indicated each of the three different GFP-RHAMM fusion proteins was the expected size and was specifically detected by both anti-RHAMM and anti-GFP sera. Unfortunately, the anti-RHAMM

mAbs did not detectably precipitate nor blot any of the three GFP-RHAMM fusion proteins. The inability of mAbs 3T3-5 and 3T3-9 to precipitate RHAMM from lysates or blot precipitated RHAMM might reflect the low affinity of these mAbs. Recently, both mAbs detected purified fusion proteins in immunoblots, but a minimum of 6 μg of fusion protein was blotted before detection occurred (Pilarski et al., in press).

Confocal analysis of transfected cells indicated both GFP-RHAMM^{FL} and GFP-RHAMM^{-147} were distributed in a pattern suggesting association with the MT cytoskeleton. GFP-RHAMM^{-147} appeared to associate with MTs as early as 6 H post-transfection. GFP-RHAMM^{FL} was more diffusely distributed through the cytoplasm in most cells 6 H after transfection, but after 48 H of culture the majority of fusion proteins appeared to associate with the MT cytoskeleton.

GFP-RHAMM^{-48} was distributed in a pattern that indicated it did not associate with the MT cytoskeleton. The distribution pattern 6 and 24 H post-transfection was diffuse throughout the cytoplasm, with a strong perinuclear distribution present in some cells. A fraction of GFP-RHAMM^{-48} was also associated with the cell membrane in protrusions and along ruffled membranes. After 48 H of culture, GFP-RHAMM^{-48} was distributed through the cytoplasm with no obvious cell membrane distribution.

Another group recently reported similar results using GFP-RHAMM constructs to transfect HeLa cells except they observed intranuclear localization of GFP-RHAMM^{-48} (Assmann et al., 1999). Although the COS cell transfections have been repeated several times, nuclear localization of GFP-RHAMM^{-48} in COS cells was never observed; however, GFP transfected COS cells had detectable fluorescence localized to the nucleus. These experiments suggested exon 4, which is absent from RHAMM^{-48}, encodes all or

part of a MT binding domain. Using an *in vitro* tubulin binding assay, Assmann et al. (1999) confirmed RHAMM proteins bind to polymerized tubulin and the absence of the exon 4 encoded sequence decreases the efficiency of binding.

The transfected COS cells were stained using either anti-GFP or anti-RHAMM serum. Confocal analysis indicated co-localization of antibody staining and GFP fluorescence confirming both GFP and RHAMM epitopes were present on fusion proteins expressed by each of the three transfected cell lines. Anti-RHAMM mAbs 3T3-5 and 3T3-9 did not detectably stain any of the three different fusion proteins. This suggested the epitopes recognized by these two mAbs might be dependent on associations with other proteins. These mAbs were raised by immunizing mice with RHAMM (HABP) isolated from HA affinity columns suggesting these mAbs likely recognize conformation-dependent epitopes. This could also explain why the apparent binding affinity of the two mAbs to the RHAMM fusion protein was low.

To determine if GFP-RHAMM^{-48} fusion proteins were distributed to the cell membrane, tranfected COS cells were harvested and stained with a lipophilic membrane dye. Maintaining COS cells in suspension while staining the membranes altered cellular morphology and the MT association of GFP-RHAMM^{FL} and GFP-RHAMM^{-147} was no longer apparent. GFP-RHAMM^{-48} was distributed entirely to the cell membrane, although it was unclear if the fusion protein was redistributed to the cell surface. Whether intracellular RHAMM in thymocytes consisted of RHAMM^{FL}, RHAMM^{-48} or both could not be determined.

6 DISCUSSION

6.1 Integrins, ECM Components and RHAMM Guide Differentiating Thymocytes Through the Thymus

Ex vivo human and murine thymocytes adhere to and locomote on Fn-coated surfaces. This indicates thymocyte Fn-binding receptors are in constitutively active binding conformations suggesting they function *in vivo* as thymocytes differentiate. Thymocytes interact with stromal cells and migrate to different regions of the thymus as they undergo differentiation and selection and these activities are likely mediated by integrins. ECM components such as Fn have a restricted distribution pattern in the neonatal thymus that includes the subcortical cortex, the cortico-medullary junction and the medulla. Fn is sparsely distributed in the thymic cortex. These observations suggest differentiating thymocytes might modulate expression and function of Fn-binding integrins depending on the anatomic site in which cells are localized. Thus, patterns of β_1 integrin expression on different thymocyte subsets might have functional implications in regard to the anatomic sites supporting differentiation, positive and negative selection.

6.1.1   Integrin avidity promotes adhesion or motility for thymocytes

Flow cytometric analysis of α_4, α_5 and β_1 integrin expression on thymocytes indicated expression levels were relatively consistent among thymocytes of each subset, but varied between thymocyte subsets defined by CD4 and CD8 expression. This suggested integrin expression was modulated as thymocytes matured from DN cells to SP cells. Functional analyses using timelapse microscopy to record cell behavior indicated immature MN thymocytes were adhesive to Fn and utilized $\alpha_4\beta_1$ integrins to facilitate adhesion. $\alpha_4\beta_1$ integrins were also involved in locomotory activities of MN thymocytes.

MAbs to α_5 integrins did not have a significant effect on adhesion or motility when cell behavior was analyzed using timelapse microscopy. The data indicated interaction between $\alpha_4\beta_1$ integrins and Fn promoted either anchored behavior or promoted locomotion for cells among the MN subset.

The most mature SP thymocyte subsets had decreased expression levels of α_4 integrin chains and slightly increased expression of α_5 integrin chains. An equivalent fraction of this subset adhered to Fn compared with MN thymocytes, but unfractionated thymocytes contained twice as many Fn-adherent cells. Unfractionated thymocytes contained 85% $CD4^+8^+$ DP thymocytes and the two SP subsets constituted the majority of the remaining population. Thus, observations using unfractionated thymocytes strongly reflected the behavior of DP thymocytes. Since the unfractionated thymocytes contained a larger fraction of Fn-adherent cells than MN or SP subsets, this suggested the DP subset contained a larger proportion of cells at a stage of differentiation requiring anchored behavior.

$\alpha_4\beta_1$ integrins mediate adhesion to Fn or to VCAM-1 expressed on endothelial cells for many types of cells including thymocytes. VCAM-1 is expressed *in vivo* on cortical TECs and $\alpha_4\beta_1$ integrins on thymocytes mediate *in vitro* interactions with thymic epithelial cultures via interaction with VCAM-1 (Salomon et al., 1997). This suggests $\alpha_4\beta_1$ integrins mediate adhesion to cortical TECs as DP thymocytes undergo selection in the cortex. This is consistent with the observation that immature DP cells are relatively adhesive cells. Sessile behavior of this subset is consistent with the relatively high expression of α_4 integrins on DP thymocytes. The high number of Fn-adherent thymocytes among unfractionated thymocytes compared to MN or SP subsets is

consistent with the prediction that immature DP thymocytes are at a relatively sessile phase of differentiation.

Although mAbs to α_5 integrin did not significantly decrease the number of Fn-adherent cells among the unfractionated population, when these mAbs were added in combination with mAbs to α_4 integrins the number of Fn-adherent cells was significantly decreased. The decrease of adhesive cells was highly significant compared with samples treated only with mAbs to α_4 integrins. This suggested both α_4 and α_5 integrins facilitate interactions with Fn for the majority of thymocytes. When cell motility was assessed, both α_4 and α_5 integrins were required to mediate motility, since mAbs to either the α_4 or α_5 subunit significantly decreased the number of motile cells. This suggested Fn-binding integrins mediate interactions with Fn to maintain sessile behavior or promote motile behavior.

A substantial body of evidence suggests that DP thymocytes are positively selected in the cortex then migrate to the cortico-medullary junction and the medulla to undergo negative selection. Although the high expression levels of α_4 and β_1 subunits on DP thymocytes suggest $\alpha_4\beta_1$ integrins mediate high avidity interactions with ligand, the sparse distribution of Fn in the cortex suggests low avidity interactions between $\alpha_4\beta_1$ and Fn could occur in this region. Since low avidity interactions of integrins with their ligand promote motility, $\alpha_4\beta_1$ integrins could mediate migration through the cortex for DP thymocytes. Receptor occupancy of LFA-1 downregulates high affinity binding conformations of $\alpha_4\beta_1$ integrins and stimulates $\alpha_5\beta_1$-mediated migration of T lymphoblasts (Porter & Hogg, 1997). Thymocytes and TECs also express LFA-1 and

ICAM-1, respectively, suggesting this mechanism might enhance the motility of post-selection cortical thymocytes. Both our data and that of others indicated both $\alpha_4\beta_1$ and $\alpha_5\beta_1$ integrins mediated motility for the majority of motile thymocytes. Examination of the phenotype of migratory thymocytes indicates the majority of these thymocytes are SP thymocytes or have a 'post-selection' $CD3^{hi}4^{med}8^{med}69^+$ phenotype that presumably includes more mature DP thymocytes (Crisa et al., 1996) supporting the idea that positive selection stimulates thymocyte migration.

SP thymocytes have decreased expression of α_4 integrin chains and slightly increased expression of α_5 integrin chains suggesting the majority of these mature thymocytes might be motile. However, the proportion of $CD3^{hi}$ thymocytes was equivalent to the proportion of motile cells in the unfractionated population. This indicated purified $CD3^{hi}$ thymocytes did not contain a higher proportion of migratory cells than the unfractionated population. However, this subset cannot be examined *ex vivo* without first isolating the cells, raising the possibility that experimental manipulation might affect normal behavior. Both the cortico-medullary junction and the medulla contain high distribution levels of Fn and other ECM components. This might provide a migratory path for thymocytes to reach the medulla. These observations also suggest β_1 integrins in low affinity conformations are likely to support the low avidity interactions between β_1 integrins and Fn required to promote cell locomotion. Using an anti-β_1 integrin activating mAb to force β_1 integrins on unfractionated thymocytes into a high affinity binding conformation significantly enhanced the number of Fn-adhesive cells and caused a concomitant decrease in the number of motile cells. This suggested β_1 integrins in low affinity binding conformations promoted locomotion for migratory thymocytes.

6.1.2 Both β_1 integrins and RHAMM mediate motility for migratory

thymocytes

The motility receptor RHAMM mediates Fn-dependent motility for thymocytes (Pilarski et al., 1993). RHAMM was expressed at low density on fractions of thymocytes within each maturational subset except the most immature CD3$^-$ MN thymocytes (Gares & Pilarski, 1999). MAbs to RHAMM significantly decreased the number of motile cells among unfractionated and CD3^{hi} thymocytes. This indicated RHAMM along with $\alpha_4\beta_1$ and $\alpha_5\beta_1$ integrins functioned to mediate cell locomotion for the majority of motile thymocytes. The extent of inhibition of motility using mAbs to integrins or RHAMM was comparable. However, by recording cell behavior to quantitate motility a qualitative difference was detected in the inhibitory activity of the RHAMM mAbs versus the β_1 integrin mAbs. Anti-RHAMM mAbs inhibited motility, but adhesion to Fn was unaffected or increased. Function blocking mAbs to both α_4 and α_5 integrin components significantly decreased the number of adherent and motile cells. This suggested β_1 integrins were required by motile thymocytes to make weakly adhesive contacts with substrate, providing traction for locomoting cells. β_1 integrins were also required to mediate interactions with Fn that promoted anchorage. Anchored behavior is presumably promoted by higher avidity interactions between β_1 integrins and Fn.

Adhesion and motility may be viewed as opposing cellular behaviors in which adhesion receptors are operational while cells remain anchored to the substrate and are non-functional while cells are motile. However, these observations suggested β_1 integrins remained functional while cells were motile. One of the requirements for motility is to decrease the overall strength of adhesion and this can be achieved by

decreasing the binding affinity of integrin receptors. Binding affinity is a measure of the strength of binding between a receptor and its ligand. Affinity can be modulated by cross-talk between integrin receptors, ligand binding and ion binding (Imhof et al., 1997; Porter & Hogg, 1997; Weerasinghe et al., 1998). Integrins can also be forced into high affinity binding conformations by specific activating mAbs (Faull et al., 1994; Stewart & Hogg, 1996). Since cells express many integrin receptors, the overall avidity of interactions will determine the strength of cell adhesion to substrate. Motile behavior is dependent on weakly adhesive interactions between integrins and substrate that enable cell de-adhesion. Since β_1 integrins were highly expressed by thymocytes, this implied binding avidity might be modulated by alteration of the binding affinity of integrins. Thymocytes pre-treated with β_1 integrin activating mAbs were less motile and had a concomitant increase in adhesion. This suggested that high affinity interactions of integrins with Fn increased overall avidity and promoted sessile behavior (Fig. 6.1). When integrin binding avidity was increased, sessile behavior was dominent over RHAMM-mediated motility even in the presence of HA. This suggests that if RHAMM functions to de-adhere migratory cells, other factors might first be required to downregulate high avidity interactions between integrins and their ligands. In vivo, to stimulate motility of differentiating thymocytes, LFA-1 interactions with ICAM-1 might be required to downregulate high affinity binding conformations of β_1 integrins. Decreased expression of $\alpha_4\beta_1$ integrin as thymocytes mature might decrease the avidity of interactions between thymocytes and substrate.

β1 Integrins in High Affinity Conformations Promote Sessile Behavior

β1 Integrins in Low Affinity Conformations Promote Motile Behavior

High affinity α₄β₁ integrin

High affinity α₅β₁ integrin

Fn

HA

Low affinity α₄β₁ integrin

Low affinity α₅β₁ integrin

RHAMM
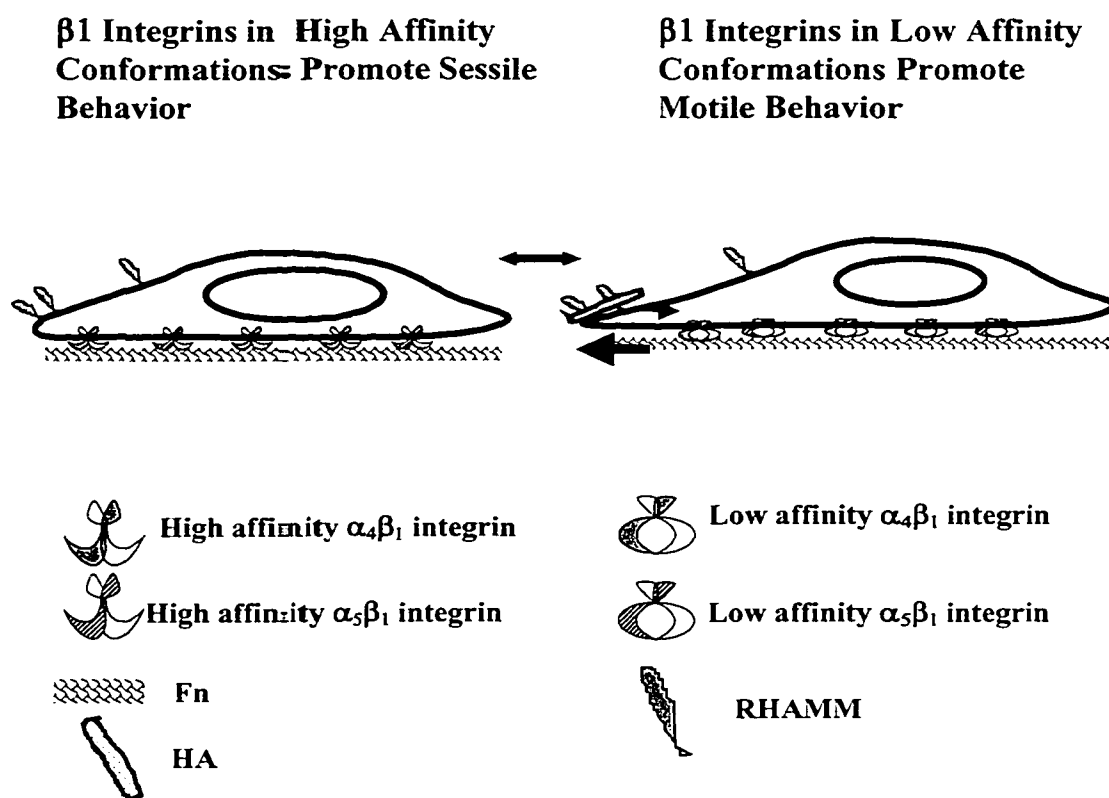
Figure 6.1 The balance between adhesion and motility is mediated by integrin avidity.

When $\alpha_4\beta_1$ and $\alpha_5\beta_1$ integrins are in high affinity binding conformations, the overall avidity of interactions with Fn is increased and sessile behavior predominates. β_1 integrins in low affinity binding conformations have decreased binding avidity that promotes motility. Thymocytes can revert to either behavior depending on the signals received from stromal cells or ECM components. HA binding to RHAMM might mediate de-adhesion and stimulate locomotion.

Once integrins interact with substrate at low avidity, HA interactions with RHAMM might stimulate cell de-adhesion and locomotion. HA is poorly adhesive for cells, supporting the idea that interactions between RHAMM and HA promote de-adhesion. The distribution of HA in the fetal and neonatal thymus is similar to the distribution of Fn. This is consistent with the view that Fn receptors and HA receptors have a functional relationship that promotes locomotory behavior. HA binding to RHAMM causes net de-phosphorylation of FAK and turns over focal adhesion in fibroblasts (Hall et al., 1994) and this could promote motility by decreasing the strength of adhesion.

6.1.3 The onset of RHAMM expression is dependent on receptor occupancy of β_1 integrins

The relationship between β_1 integrins and RHAMM was further characterized by examining expression and function of these receptors at an early point in differentiation prior to detectable RHAMM expression. MN thymocytes were purified using bead depletion or bead depletion in combination with cell sorting to remove $CD3^+4^+8^+19^+$ cells. Flow cytometric analysis of MN cells showed a lack of RHAMM expression, but moderate expression of α_4, α_5, α_6 and β_1 integrin subunits (Gares & Pilarski, 1999). Timelapse microscopy indicated of all the MN thymocytes that interacted with Fn, more than 50% were locomotory while the remaining thymocytes were anchored cells. This observation suggested the MN subset contains a mixture of cells with respect to their behavior on Fn. $\alpha_4\beta_1$ integrins mediate high affinity or avidity interactions with Fn that promote anchorage to Fn for a portion of the subset. $\alpha_4\beta_1$ integrins also mediate lower

affinity or avidity interactions that promote locomotion for a different population within the MN subset. These two behavioral types of MN cells might revert between anchored behavior and migratory behavior (Fig. 6.2).

MN thymocytes were cultured on uncoated or Fn-coated tissue culture wells over a period of several days and expression of RHAMM and integrin subunits was monitored over time (Gares & Pilarski, 1999). MN thymocytes cultured *in vitro* for two days upregulated expression of the β_1 integrin subunits and RHAMM in the presence or absence of Fn. This suggested thymocytes undergoing *in vitro* differentiation became migratory and likely used RHAMM to mediate migratory behavior at this point in development. Although Fn was not required to upregulate short term RHAMM expression, thymocytes cultured for longer periods maintained RHAMM expression only in the presence of Fn. This implied prolonged RHAMM expression might be dependent upon integrin-mediated signaling. Alternatively, RHAMM might interact directly or indirectly with Fn to maintain expression. To test whether high avidity interactions of integrins affected RHAMM expression, MN thymocytes were cultured in Fn-coated wells containing immobilized mAbs to α_4, α_5, or β_1 integrins. The immobilized mAbs inhibited prolonged RHAMM expression (Gares & Pilarski, 1999). Control mAbs or anti-RHAMM mAbs did not affect the prolonged expression of RHAMM. This data indicated high avidity ligand binding (emulated by integrin binding to immobilized mAbs) mediated by $\alpha_4\beta_1$ and $\alpha_5\beta_1$ integrins was not only dominant over RHAMM-mediated motility, but modulated the expression of this motility receptor.

MN Thymocytes Use Integrins to Promote Adhesion or Motility

CD3/TCR⁺ Thymocytes Use Integrins and RHAMM to Mediate Motility

No Differentiation

CD3⁻

Affinity or Avidity Modulation

?

CD3⁺

Differentiation

CD3⁻

High affinity $\alpha_4\beta_1$ integrin

Low affinity $\alpha_4\beta_1$ integrin

Fn

RHAMM

HA
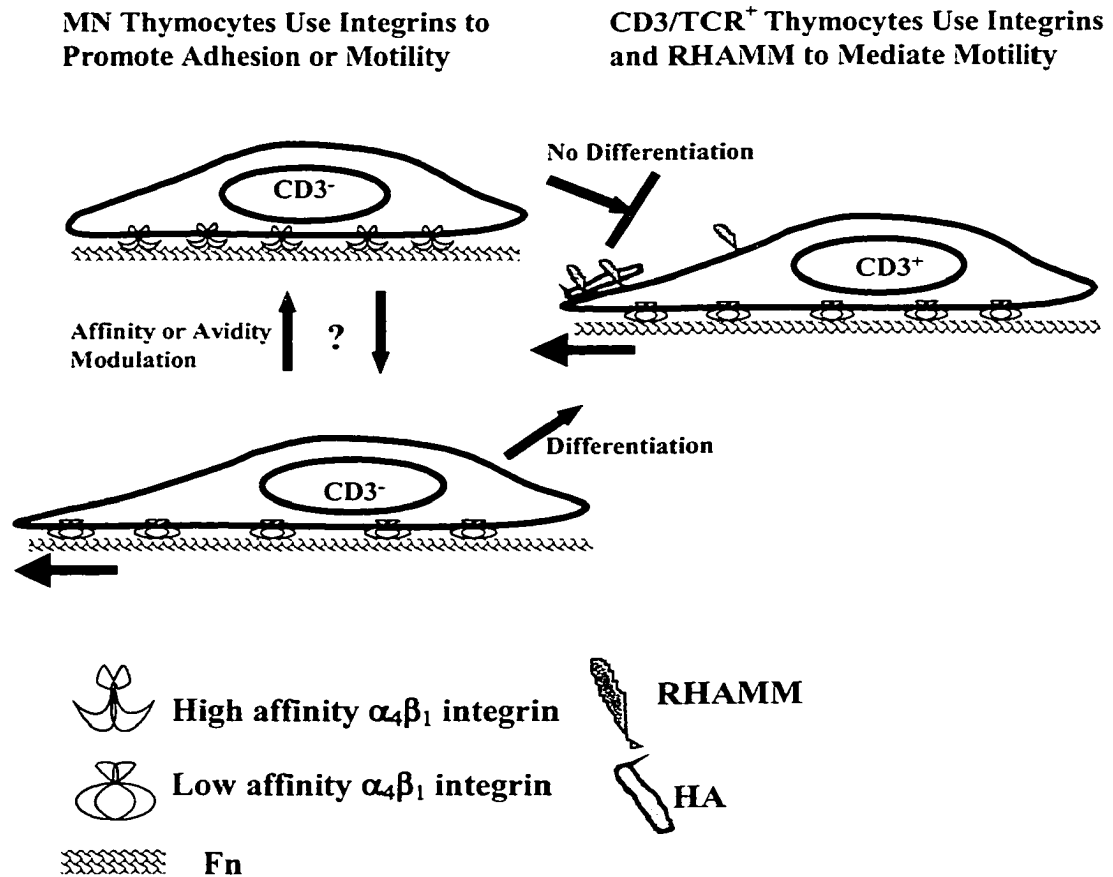
Figure 6.2 Differentiation of MN thymocytes correlates with decreased binding avidity of $\alpha_4\beta_1$ integrins and the onset of RHAMM expression.

High avidity binding of $\alpha_4\beta_1$ and $\alpha_5\beta_1$ integrins maintain sessile behavior for MN thymocytes by mediating stong binding to Fn or stromal cells. $\alpha_4\beta_1$ integrins also mediate motility for MN thymocytes by mediating weaker adhesive contacts with Fn. Highly adhesive MN thymocytes might be at a different developmental stage. As MN thymocytes differentiate and express CD3, they begin to express RHAMM which also mediates motility.

To determine if RHAMM expressed by cultured MN thymocytes functioned to promote thymocyte motility, cell behavior was assessed. After two days of culture on Fn the number of motile cells increased compared with *ex vivo* MN thymocytes. Motility became RHAMM-dependent, since anti-RHAMM mAbs decreased the proportion of motile cells and increased the number of Fn-adherent cells (Fig. 6.2). By day 2 of culture, thymocytes also expressed CD3/TCR, indicating that differentiation of thymocytes correlated with RHAMM expression and function (Gares & Pilarski, 1999). These experiments suggested β_1 integrins functioned very early in thymocyte differentiation to promote anchored or motile behavior. They also suggested β_1 integrin signaling might inhibit the expression of RHAMM when integrins are held in high avidity binding conformations (Fig. 6.2).

6.2 HA Promotes Motility by Redistributing Intracellular RHAMM to the Cell Surface

RHAMM expression on thymocyte subsets was analyzed using two different anti-RHAMM mAbs. Only 15 to 20% of thymocytes stained with mAb 3T3-5 had weak surface staining while approximately 30 to 60% of thymocytes treated with mAb 3T3-9 were stained with weak intensity. RHAMM was required by migratory thymocytes for locomotion, since anti-RHAMM mAbs significantly decreased the number of motile cells among unfractionated or $CD3^{hi}$ thymocytes. To begin to characterize the cellular localization of RHAMM in thymocytes, these two anti-RHAMM mAbs were used for further analysis.

Binding patterns of the two anti-RHAMM mAbs indicated mAb 3T3-9 preferentially bound to an epitope expressed by surface RHAMM while mAb 3T3-5 preferentially bound to an epitope expressed by intracellular RHAMM, which we have termed RHAMM-9 and RHAMM-5, respectively. Both anti-RHAMM mAbs showed similar binding to a RHAMM fusion protein. Confocal analysis of anti-RHAMM/HA-FITC stained cells indicated co-localization of surface RHAMM-9 expression and bound HA. This suggested RHAMM-9 was an HA binding receptor for human thymocytes. Few sites of CD44 expression co-localized with sites of HA binding suggesting that on human thymocytes, CD44 is not in an activated, HA-binding state. To determine if HA affected RHAMM expression, thymocytes were pre-treated with HA then stained with anti-RHAMM mAbs. Pre-treatment of thymocytes with HA strongly increased surface expression of RHAMM-5 as indicated by an increased staining intensity as well as an increase in the number of RHAMM-5$^+$ cells. The HA-induced increase in RHAMM-5 expression was abrogated by sodium azide indicating that metabolic energy was required. RHAMM-5 might be a conformation-dependent epitope revealed when HA binds to RHAMM-9. However, the slight increase of RHAMM-9 expression following HA pre-treatment suggested the HA-induced expression of RHAMM-5 could be a result of redistribution of RHAMM from another cellular compartment.

Confocal analysis of permeabilized thymocytes confirmed RHAMM-5 was predominantly intracellular. There was also a minor co-localization of RHAMM staining with cell surface CD45 staining suggesting RHAMM-5 was expressed at the cell surface at very low density. To investigate whether binding of HA stimulated mobilization of the intracellular RHAMM-5 to the cell surface, we used PLC to cleave RHAMM from the

cell surface followed by addition of exogenous HA. PLC treatment decreased surface RHAMM-5 expression, but did not remove RHAMM-9. This suggested the low density of RHAMM-5 was susceptible to cleavage by PLC, while RHAMM-9 was impervious. When PLC-treated thymocytes were exposed to HA and subsequently stained, surface RHAMM-5 expression was greater than could be caused by an HA-induced conformational change of surface RHAMM-9. This suggested exogenous HA increased mobilization of intracellular RHAMM-5 to the cell surface. This also suggested RHAMM-5 was expressed at the cell surface in association with a gpi-anchored protein.

To determine whether redistributed RHAMM-5 was a functional mediator of motility for thymocytes, motility assays were done. Of the total thymocyte population, approximately 16% of cells were motile on Fn-coated wells in the presence or absence of HA. In the absence of exogenous HA, mAb 3T3-9 significantly decreased the number of motile cells while mAb 3T3-5 decreased the proportion of motile cells to a lesser, but significant, extent. This suggested that even in the absence of exogenous HA, RHAMM-9 was capable of promoting motility for human thymocytes while RHAMM-5 played a minor role. This observation also suggested RHAMM-mediated motility occurred in the absence of ligand. However, hyaluronidase treatment of thymocytes significantly decreased the number of motile cells suggesting HA was required to stimulate locomotion (Gares et al., 1998). Addition of exogenous HA to motility assays restored motility of hyaluronidase-treated thymocytes indicating HA was essential for RHAMM-mediated motility and suggested thymocytes might synthesize endogenous HA. The observation that thymocytes have the potential to synthesize their own HA is provocative and suggests

differentiating thymocytes do not just respond to their microenvironment, but participate in creating a microenvironment likely to promote RHAMM-mediated motility.

The observation that either anti-RHAMM mAb inhibited motility in conditions when both RHAMM-9 and RHAMM-5 were optimally expressed at the cell surface indicated both RHAMM-9 and RHAMM-5 were required to mediate locomotion. Sequence analysis indicates RHAMM contains coiled coil domains that could support dimerization or oligomerization of RHAMM (Assmann et al., 1999). RHAMM molecules might form multimeric complexes at the cell surface that mediate motility. Removal of surface RHAMM by PLC treatment of thymocytes significantly inhibited cell motility. However, when PLC-treated thymocytes were exposed to HA, motility was restored, as expected if RHAMM-5 was mobilized from an intracellular pool to the cell surface by HA. The requirement for *both* RHAMM-9 and RHAMM-5 to mediate motility was emphasized by the PLC treatment, since motility was abrogated even though PLC did not affect surface expression of RHAMM-9.

Localization of RHAMM to different cellular compartments suggested thymocytes expressed distinct isoforms of RHAMM. RHAMM variants consist of a full length isoform containing all encoding exons, an isoform with a 48 bp deletion that correlates to the excision of exon 4 and a downstream 147 bp deletion that correlates to excision of exon 13 (Crainie et al., 1999; Assmann et al., 1999). RT-PCR characterization of RHAMM mRNA from three different thymocyte preparations showed expression of three distinct RHAMM transcripts. RHAMM^{FL} and RHAMM^{-48} were readily detectable, whereas RHAMM^{-147} was expressed at barely detectable levels of only two thymocyte preparations from five separate donors. RHAMM proteins of two

different apparent molecular weights were also detected in thymocyte lysates. The molecular weight of two of the bands was consistent with the predicted molecular weight of RHAMM^{FL} and RHAMM^{-48}. Therefore, molecular and biochemical data indicated thymocytes expressed two different RHAMM isoforms. To determine if the two different RHAMM isoforms expressed the RHAMM-5 and RHAMM-9 epitopes, thymocyte lysates were precipitated with anti-RHAMM mAbs 3T3-5 and 3T3-9. The mAbs were also used for immunodetection of blots containing RHAMM precipitated with anti-RHAMM serum. However, neither mAb detectably precipitated nor blotted RHAMM proteins.

6.2.1 Do anti-RHAMM mAbs detect two RHAMM isoforms?

The mAb binding patterns indicated the epitopes detected by each mAb, RHAMM-9 and RHAMM-5, localized to the cell surface and an intracellular site, respectively, in untreated *ex-vivo* thymocytes. This suggested thymocytes expressed two isoforms of RHAMM that might perform different functions for cells. Thymocytes expressed mRNA for both RHAMM^{FL} and RHAMM^{-48} and proteins of the appropriate molecular weights for each isoform could be precipitated using anti-RHAMM serum. However, anti-RHAMM mAbs did not bind detectably to denatured proteins in western blots. Thus, it could not be determined if the RHAMM-5 and RHAMM-9 epitopes were expressed by RHAMM^{FL}, RHAMM^{-48} or both. RHAMM-9 and RHAMM-5 could be genetically identical and occur in two cellular compartments as a consequence of receptor recycling. RHAMM-mediated endocytosis of HA has been reported (Masellis-Smith et al., 1996; Collis et al., 1998) and internalized RHAMM-9 could contribute to the intracellular pool of RHAMM identified as RHAMM-5 or vice versa. Anti-RHAMM

mAbs 3T3-5 and 3T3-9 did bind with apparently low affinity to a GST-RHAMM fusion protein. The fusion protein contains a partial RHAMM sequence that is downstream of the sequence encoded by exon 4 suggesting the mAbs recognize epitopes that are likely expressed by both RHAMM^{FL} and RHAMM^{-48}. However, the relatively low binding affinity of each mAb to the fusion protein suggested the recombinant protein was not in a conformation that allowed optimal mAb binding. Conformation-dependent epitopes can be dependent on intra- or inter-molecular interactions that might be unique to each RHAMM isoform. Although each anti-RHAMM mAb likely binds to a domain common to RHAMM^{FL} and RHAMM^{-48}, the distant domains unique to each isoform might influence the overall shape of the common domains. These data neither confirms nor refutes that the two anti-RHAMM mAbs recognize epitopes expressed by one or two different RHAMM isoforms.

Although different cellular distribution patterns were suggestive of the existence of two different RHAMM proteins, the mAb binding patterns could conceivably be a result of one RHAMM isoform. The cellular localization of RHAMM might influence the protein conformation and the availability of mAb-specific epitopes. 'Intracellular' conformations presumably reveal the RHAMM-5 epitope while 'cell surface' conformations reveal the RHAMM-9 epitope. At the cell surface, RHAMM might associate with other surface molecules and assume a conformation hiding the 3T3-5 binding epitope while preserving the 3T3-9 epitope. This would result in negligible binding to cell surface RHAMM by mAb 3T3-5. MAb 3T3-5 did bind to RHAMM that was presumably redistributed to the cell surface, but redistributed RHAMM might interact with alternate cell surface proteins than does RHAMM-9 when it is initially

redistributed to the cell surface. This would maintain RHAMM-5, at least transiently, in a conformation that reveals the 3T3-5 epitope and hides the 3T3-9 epitope. Although it is enticing to assume the two mAbs bind to different isoforms of RHAMM, there is no definitive data to support this view.

6.2.2 How does RHAMM function to mediate motility?

MAb binding profiles provided suggestive but inconclusive evidence for the presence of two distinct RHAMM isoforms in different compartments. The motility analyses suggested RHAMM-9 and RHAMM-5 cooperated to mediate locomotion, since mAb binding to either epitope significantly decreased the number of motile cells. These observations are difficult to reconcile without assuming intracellular RHAMM was redistributed to the cell surface. Thymocytes treated with hyaluronidase are not motile indicating HA is absolutely required by thymocytes to mediate motility (Gares et al., 1998). The requirement for HA suggested HA binding to RHAMM-9 mediated motility, generated signals and/or redistributed RHAMM-5 to the cell surface (Fig. 6.3). Redistributed RHAMM-5 then mediated motility alone or in combination with RHAMM-9. MAb 3T3-9 inhibited motility in this assay system, but we do not know if motility is inhibited directly or whether upstream events are inhibited by mAb binding to RHAMM-9. Anti-RHAMM mAbs might interfere with interactions between RHAMM-9 and other proteins required to generate signals or mediate motility. HA binding to RHAMM results in net de-phosphorylation of FAK (Hall et al., 1995), thus HA binding might mediate signals through RHAMM-9 or perhaps other surface molecules. This signaling cascade might maintain low affinity binding conformations of integrins required to promote
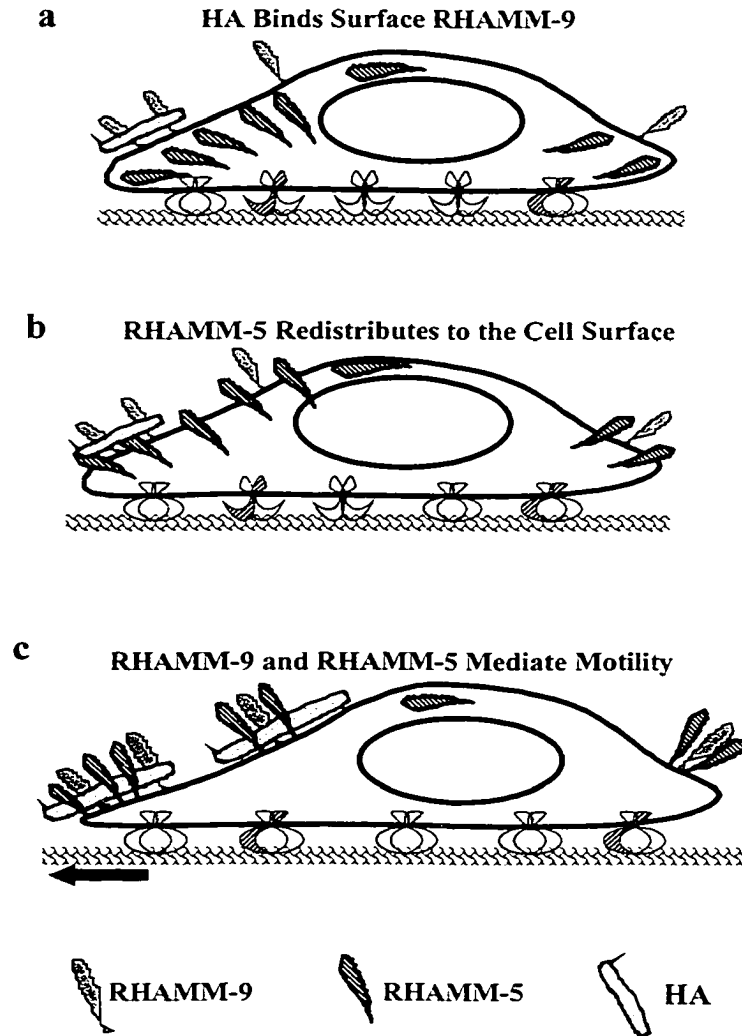
Figure 6.3 RHAMM-5 redistributed to the cell surface participates in motility.

Thymocytes express a low density of surface RHAMM-9 and a higher density of intracellular RHAMM-5 (a). HA binding to RHAMM might initiate signals that result in a redistribution of RHAMM-5 to the cell surface (b). At the cell surface RHAMM-5 associates with RHAMM-9 to form complexes that mediate motility and might enhance HA binding (c). Low avidity binding by β_1 integrins mediate weak adhesive contacts with Fn that provide traction for locomoting thymocytes.

motile behavior (Fig. 6.3). For RHAMM-5 to participate in locomotion it was presumably redistributed to the cell surface, perhaps in response to HA interactions with RHAMM-9 (Fig. 6b). But if both RHAMM-9 and RHAMM-5 are required, how did cells locomote in the absence of exogenous HA? Synthesis of endogenous HA during the period of mAb pre-treatment (without exogenous HA), which is at 4°C, must be insufficient to mobilize RHAMM-5 to the cell surface in the quantities required for mAbs to bind. Thus, in the absence of exogenous HA, only a low density of RHAMM-5 is available for mAb binding during the pre-treatment. However, while cells are equilibrating at 37°C, endogenous HA synthesis must be sufficient to mediate redistribution of intracellular RHAMM-5 to the cell surface where it then mediates motility.

The ability of both mAbs to decrease the number of motile cells indicated both RHAMM epitopes had a functional role in the motile process. This suggested RHAMM-9 and RHAMM-5 might combine to form multimers at the cell surface and these multimers function to mediate motility (Fig. 6.3C). There is evidence suggesting RHAMM receptors associate in multimeric complexes to mediate motility. A RHAMM gene truncated to remove the HA binding domains behaves as a dominant suppressor of RHAMM function when transfected into tumorigenic cells (Hall et al., 1995). The transfected cells become less motile and form large stable focal adhesions indicating RHAMM function is downregulated. These cells express wild-type RHAMM as well as mutant RHAMM, yet mutant RHAMM dominates in mediating cellular behavior. This suggests wild-type RHAMM and mutant RHAMM are unable to form multimers or form

multimers that are unable to function normally because they lack the full complement of HA binding domains. Consistent with the idea that RHAMM mediates motility when it forms a multimeric complex, mAb binding to either epitope of RHAMM might interfere with the ability of RHAMM-9 and RHAMM-5 to associate. Expression of RHAMM in a multimeric complex is likely to increase ligand binding avidity since HA is a relatively linear, polymeric molecule. Only multimers of the basic HA dimer mediate motility (Turley, 1992), therefore, a multimeric association of RHAMM-5 and RHAMM-9 might be required to bind HA and mediate motility.

6.3 GFP-RHAMM Isoforms Have Different Cellular Distributions

To examine the cellular distribution of each different RHAMM isoform, plasmids were constructed containing the GFP gene fused to the sequence encoding each RHAMM isoform. These plasmids were used to transfect COS cells. The COS cell line was efficiently transfected by the GFP plasmids compared with three other cell lines. Transfected COS cells expressed GFP-RHAMM fusion proteins with the expected molecular weights. Based on the deduced amino acid sequences of RHAMM^{FL}, RHAMM^{-147} and RHAMM^{-48}, their respective molecular weights are 84.2, 78.4 and 82.3 Kd. GFP-RHAMM^{FL}, GFP-RHAMM^{-147} and GFP-RHAMM^{-48} had apparent molecular weight of 108, 100 and 104 Kd respectively, thus were approximately the expected size. Biochemical analysis using anti-GFP and anti-RHAMM polyclonal sera confirmed each fusion protein contained GFP and RHAMM epitopes. Anti-RHAMM mAbs did not detectably precipitate fusion proteins.

Confocal microscopic analysis of transfected cells showed the three different GFP-RHAMM fusion proteins were distributed in two distinct patterns. When transfected cells were examined by confocal microscopy 48 H after transfection, the distribution patterns of GFP-RHAMM^{FL} and GFP-RHAMM^{-147} suggested both fusion proteins associated with the MT cytoskeleton. This staining pattern was consistent with other work (Assmann et al., 1999). At earlier time points, GFP-RHAMM^{FL} was diffusely distributed throughout the cytoplasm suggesting GFP-RHAMM^{FL} did not associate with MTs when cells were actively spreading and dividing. In contrast, GFP-RHAMM^{-147} tended to associate with MTs as early as 6 H after transfection. Cells transfected with GFP-RHAMM^{-48} plasmids had a diffuse pattern of cytoplasmic fluorescence at each time point and no apparent association with MTs. This confirmed that the sequence encoded by exon 4, which was absent from the RHAMM^{-48} isoform, expressed a MT binding domain (Assmann et al., 1999). Six and 24 H after transfection, GFP-RHAMM^{-48} fusion protein was also observed at the tips of cell protrusions and ruffled membranes demonstrating this fusion protein associated with cell membranes. At these earlier time points there was also a strong perinuclear distribution of GFP-RHAMM^{-48}. This model system demonstrated RHAMM isoforms exhibited two distinct distribution patterns with the majority of RHAMM expressed intracellularly and a small percentage, consisting of GFP-RHAMM^{-48}, in contact with cell membranes or at the cell surface. This correlated with our observations in thymocytes, therefore, provided evidence that the distribution patterns of RHAMM-5 and RHAMM-9 in thymocytes might reflect expression of two isoforms of RHAMM, RHAMM^{FL} and RHAMM^{-48}.

Each transfected cell line was stained with anti-RHAMM or anti-GFP serum to ensure GFP fluorescence correlated with expression of GFP-RHAMM fusion proteins. Antibody staining was co-localized with the fluorescence pattern of GFP indicating transfected COS cells were expressing fusion proteins. Anti-RHAMM mAbs were also used to stain GFP-RHAMM transfectants, but no detectable mAb staining was observed when the stained COS cells were examined by flow cytometry and confocal microscopy.

To further assess the association of GFP-RHAMM^{-48} with the cell membrane, transfected COS cells were harvested at 48 H, labeled with the membrane dye PKH26 then examined by confocal microscopy. The membrane labeling procedure was done with the cells in suspension, so cells were considered 'non-adherent'. In non-adherent COS cells, GFP-RHAMM^{FL} and GFP-RHAMM^{-147} fusion proteins did not appear to associate with MTs, perhaps because the MT cytoskeleton was disassembled while cells were in suspension. The cells assumed a rounded shape and fluorescence was diffusely distributed throughout the cytoplasm. Neither GFP-RHAMM^{-147} nor GFP-RHAMM^{FL} demonstrated substantial co-localization with the stained cell membrane. In contrast, virtually all GFP-RHAMM^{-48} fusion protein was co-localized with cell membranes, although it was not clear if the fusion proteins were at the cell surface. The distribution patterns of GFP-RHAMM in non-adherent cells suggested distribution of RHAMM isoforms might be dependent on many different factors including cell type and microenvironmental conditions.

These observations suggested that migratory cells such as lymphocytes, that radically reorganize the MT cytoskeleton as they initiate migration (Ratner et al., 1997), distribute RHAMM in patterns distinct from the patterns observed for strongly adherent

cell lines in which the MT cytoskeleton is maintained in a radial distribution. Furthermore, the distribution patterns of GFP-RHAMM^{FL} and GFP-RHAMM^{-48} in transfected cells 6 and 24 H post-transfection differed from the distribution patterns at 48 H when cells had formed a confluent monolayer. At early time points, distribution patterns of RHAMM fusion proteins are more likely to reflect the functional response of RHAMM in motile cells.

The membrane association of GFP-RHAMM^{-48} differs from a recent report by Assmann et al., 1999; however, we observed this distribution pattern at early time points not examined by this group. They also reported intranuclear expression of GFP-RHAMM^{-48} in tranfected cells, whereas we observed intranuclear expression only of GFP controls. This could reflect the use of a different cell line or different methods; however, they did not stain cells with antibody to RHAMM to verify that intranuclear staining consisted of fusion protein.

The GFP-RHAMM^{FL} and GFP-RHAMM^{-147} fusion proteins had similar distribution patterns, but GFP-RHAMM^{-147} demonstrated an earlier cytoskeletal association than did GFP-RHAMM^{FL}. This suggests the tubulin binding sequence encoded by exon 4 dominates RHAMM isoform distribution at quiescence, but that sequence (s) encoded by exon 13 might be dominant at earlier stages of cell growth. Examination of exon 13 indicates the first two amino acids of a YVRM sequence are encoded by the last 6 nucleotides of this 147 bp exon. Therefore, excision of exon 13 destroys this motif. The YXXϕ motif interacts with adaptor proteins used by clathrin-coated pits and vesicles involved in protein trafficking (Zhang & Allison, 1997). The phosphorylation state of the YXXϕ motif affects interaction of this sequence with these

adaptor proteins as well as signaling molecules (Schneider et al., 1995), thus if this is a functional sequence for RHAMM^{FL} and RHAMM^{-48}, RHAMM distribution patterns are likely to be affected by cellular activities while adherent cells are spreading.

Maintaining intracellular stores of a motility receptor would enable cells to promptly adapt to changes in their microenvironment by enabling rapid redistribution of receptors to the cell surface to mediate motile behavior. Receptors are also sequestered from ubiquitously expressed ECM components until appropriate conditions or events signal a need for increased surface expression. This strategy seems particularly suitable for cells such as thymocytes that continually adjust their behavior between adhesion and motility as they mature in the thymus. PMNs maintain an intracellular pool of the gpi-anchored protein CD14 in secretory vesicles that enables PMNs to rapidly increase surface expression of these endotoxin receptors when stimulated by bacterial products (Detmers et al., 1995). Internalization has also been reported for gpi-anchored proteins such as CD59 and 5-methyltetrahydrofolate and this endocytic path is associated with signal transduction activities (Smart et al., 1994; Deckert et al, 1996; Parolini et al., 1996). The gpi-anchored cellular prion protein (PrP^c) is internalized via this path and recycles back to the cell surface through endosomes (Shyng et al., 1993; Chen et al., 1995). Recycling of integrins involved with motile behavior has also been observed. $\alpha_5\beta_1$ and $\alpha_v\beta_3$ integrins mediate motility on Fn and vitronectin, respectively, and both integrins might be endocytosed at the rear of locomoting neutrophils then cycled back to the cell front by endocytic vesicles (Lawson & Maxfield, 1995; Pierini et al., 2000). This process is postulated to de-adhere locomoting cells. RHAMM might also function in de-adhesion of locomoting cells. RHAMM^{FL} and RHAMM^{-147} clearly associated with MTs

in transfected COS cells and in HeLa cells (Assmann et al., 1999). HA binding domains resemble ERM binding domains suggesting intracellular RHAMM might also interact with ERM proteins. Migratory T cells redistribute ERM proteins, the MT cytoskeleton and cell adhesion receptors such as CD44, and ICAMs to the uropod. Intracellular RHAMM interacting with MTs or ERM proteins might be redistributed to the cell surface at the rear of migrating lymphocytes to participate in de-adhesion. Alternatively, cell surface RHAMM might be endocytosed at the cell rear similar to recycling integrins.

In conclusion, weakly adhesive interactions between β_1 integrins and Fn are required by migratory thymocytes and these interactions presumably provide traction for locomoting cells. RHAMM is also involved in the motile process and interaction with HA is required for cells to locomote. HA stimulates redistribution of intracellular RHAMM-5 to the cell surface suggesting the mechanism involved in RHAMM-mediated motility is receptor cycling. The association of RHAMM[FL] with MTs and the redistribution of MTs to the uropods of locomoting T cells suggests RHAMM[FL] could be distributed to the uropod to facilitate cell de-adhesion.

7. REFERENCES

Aepfelbacher, Martin, Franz Vauti, Peter C. Weber and John A. Glomset. 1994. Spreading of differentiating human monocytes is associated with a major increase in membrane-bound Cdc42. *PNAS* 91:4263-4267.

Allen, William E., Daniel Zicha, Anne J. Ridley and Gareth E. Jones. 1998. A role for Cdc42 in macrophage chemotaxis. *J. Cell Biol.* 141:1147-1157.

Allen, William E., Gareth E. Jones, Jeffrey W. Pollard and Anne J. Ridley. 1997. Rho, Rac and Cdc42 regulate actin organization and cell adhesion in macrophages. *J. Cell Science* 110:707-720.

Amsen, Derk and Ada M. Kruisbeek. 1998. Thymocyte selection: not by TCR alone. *Immunol. Rev.* 165:209-229.

Anderson, D. C., B. J. Hughes, L. J. Wible, G. J. Perry, C. W. Smith and B. R. Brinkley. 1984. Impaired motility of neonatal PMN leukocytes: relationship to abnormalities of cell orientation and assembly of microtubules in chemotactic gradients. *J. Leuk. Biol.* 36:1-15.

Anderson, Graham, Nel C. Moore, John J. T. Owen and Eric J. Jenkinson. 1996. Cellular interactions in thymocyte development. *Annu. Rev. Immunol.* 14:73-99.

Andrew, David P., Lusijah S. Rott, Peter J. Kilshaw and Eugene C. Butcher. 1996. Distribution of $\alpha_4\beta_7$ and $\alpha_E\beta_7$ integrins on thymocytes, intestinal epithelial lymphocytes and peripheral lymphocytes. *Eur. J. Immunol.* 26:897-905.

Arroyo, Alicia, Joy T. Yang, Helen Rayburn and Richard Hynes. 1996. Differential requirements for α_4 integrins during fetal and adult hematopoiesis. *Cell* 85:997-1008.

Assmann, Volker, David Jenkinson, John F. Marshall and Ian R. Hart. 1999. The intracellular hyaluronan receptor RHAMM/IHABP interacts with microtubules and actin filaments. *J. Cell Science* 112:3943-3954.

Assmann, Volker, John F. Marshall, Christina Fieber, Martin Hofmann and Ian R. Hart. 1998. The human hyaluronan receptor RHAMM is expressed as an intracellular protein in breast cancer cells. *J. Cell Science* 111:1685-1694.

Azzarà, Antonio. 1997. Evaluation of neutrophil motility by image analysis. *Ann. NY Acad. Sci.* 832:29-52.

Benoist, Christophe and Diane Mathis. 1989. Positive selection of the T cell repertoire: where and when does it occur? *Cell* 58:1027-1033.

Bernard, Ghislaine, Didier Zoccola, Michel Ticchioni, Jean-Philippe Breittamayer, Claude Aussel and Alain Bernard. 1994. Engagement of the CD45 molecule induces homotypic adhesion of human thymocytes through a LFA-1/ICAM-1-dependent pathway. *J. Immunol.* 152:5161-5170.

Berrih, S., W. Savino, and S. Cohen. 1985 Extracellular matrix of the human thymus: immunofluorescence studies on frozen sections and cultured epithelial cells. *J. Histochem. Cytochem.* 33:655-664.

Blom, Bianca, Martie C. M. Verschuren, Mirjam H. M. Heemskerk, Arjen Q. Bakker, Ellen J. van Gastel-Mol, Ingrid L. M. Wolvers-Tettero, Jacques J. M. van Dongen and Hergen Spits. 1999. TCR gene rearrangement and expression of the pre-T cell receptor complex during human T-cell differentiation. *Blood* 93:3033-3043.

Borland, G., J. A. Ross and K. Guy. 1998. Forms and functions of CD44. *Immunol.* 93:139-148.

Boudreau, Nancy, Eva Turley and Marlene Rabinovitch. 1991. Fibronectin, hyaluronan and hyaluronan binding protein contribute to increased ductus arteriosus smooth muscle cell migration. *Dev. Biol.* 143:235-247.

Boyd, Richard L. and Patrice Hugo. 1991. Towards an integrated view of thymopoiesis. *Immunol. Today* 12:71-78.

Brabb, Thea, Eric S. Huseby, Todd M. Morgan, Derek B Sant'Angelo Jacqueline Kirchner, Andrew G. Farr and Joan Goverman. 1997. Thymic stromal organization is regulated by the specificity of T cell receptor/major histocompatibility complex interactions. *Eur. J. Immunol.* 27:136-146.

Bretscher, Anthony. 1999. Regulation of cortical structure by the ezrin-radixin-moesin protein family. *Curr. Opin. Cell Biol.* 11:109-116.

Bretscher, Mark and Carmen Aguado-Velasco. 1998. Membrane traffic during cell locomotion. *Curr. Opin. Cell. Biol.* 10:537-541.

Bretscher, Mark S. 1996. Getting membrane flow and the cytoskeleton to cooperate in moving cells. *Cell* 87:601-606.

Bretscher, Mark. 1992. Circulating integrins: $\alpha5\beta1$, $\alpha6\beta1$ and Mac-1, but not $\alpha3\beta1$, $\alpha4\beta1$ or LFA-1. *EMBO J.* 11:405-410.

Campbell, James J., Ellen F. Foxman and Eugene C. Butcher. 1997. Chemoattractant receptor cross talk as a regulatory mechanism in leukocyte adhesion and migration. *Eur. J. Immunol.* 27:2571-2578.

Campbell, James J., Shixin Qin, Kevin B. Bacon, Charles R. Mackay and Eugene Butcher. 1996. Biology of chemokine and classical chemoattractant receptors:

differential requirements for adhesion-triggering versus chemotactic responses in lymphoid cells. *J. Cell Biol.* 134:255-266.

Carlow, Douglas A., Nicolai S. C. van Oers, Soo-Jeet Teh and Hung-Sia Teh. 1992. Deletion of antigen-specific immature thymocytes by dendritic cells requires LFA-1/ICAM-1 interactions. *J. Immunol.* 148:1595-1603.

Cepek, Karyn, Sunil K. Shaw, Christina M. Parker, Gary J. Russel, Jon S. Morrow, David L. Rimm and Michael B. Brenner. 1994. Adhesion between epithelial cells and T lymphocytes mediated by E-cadherin and the $\alpha_E\beta_7$ integrin. *Nature* 372:190-196.

Chan, Susan, Margarida Correia-Neves, Christophe Benoist and Diane Mathis. 1998. CD4/CD8 lineage commitment: matching fate with competence. *Immunol. Rev.* 165:195-207.

Chang, Andrew C., Scott Wadsworth and John E. Coligan 1993. Expression of merosin in the thymus and its interaction with thymocytes. *J. Immunol.* 151:1789-1801.

Chen, Hui, Barbara W. Bernstein and James R. Bamburg. 2000. Regulating actin filament dynamics *in vivo*. *Trends Biochem. Science* 25:19-23.

Chen, S. G., D. B. Teplow, P. Parchi, J. K. Teller, P. Gambetti and L. Autilio-Gambetti. 1995. Truncated forms of the human prion protein in normal brain and in prion diseases. *J. Biol. Chem.* 270:19173-19180.

Clark, Edwin A., Warren G. King, Joan S. Brugge, Marc Symons and Richard O. Hynes. 1998. Integrin-mediated signals regulated by members of the Rho family of GTPases. *J. Cell Biol.* 142:573-586.

Coates, Thomas D., Raymond G. Watts, Raymond Hartman and Thomas H. Howard. 1992. Relationship of F-actin distribution to development of polar shape in human polymorphonuclear neutrophils. *J. Cell Biol.* 117:765-774.

Collis, L., C. Hall, L. Lange, M. Ziebell, R. Prestwich and E. A. Turley. 1998. Rapid hyaluronan uptake is associated with enhanced motility: implications for an intracellular mode of action. *FEBS Letters* 440:444-449.

Condeelis, John, Joan Jones and Jeffrey E. Segall. 1992. Chemotaxis of metastatic tumor cells: clues to mechanisms from the Dictyostelium paradigm. *Cancer and Meta. Rev.* 11:55-68.

Cook, Tiffani A., Takayuki Nagsaki and Gregg G. Gundersen. 1998. Rho guanosine triphosphatase mediates *the selective stabilization of microtubules induced by* lysophosphatidic acid. *J. Cell Biol.* 141:175-185.

Cox, Dianne, Peter Chang, Qing Zhang, P. Gopal Reddy, Gary M. Bokoch and Steven Greenberg. 1997. Requirements for both Rac1 and Cdc42 in membrane ruffling and phagocytosis in leukocytes. *J. Exp. Med.* 186:1487-1494.

Crainie, Mary, Andrew R. Belch, Michael J. Mant and Linda M. Pilarski. 1999. Overexpression of the receptor for hyaluronan-mediated motility (RHAMM) characterizes the malignant clone in multiple myeloma: identification of three distinct RHAMM variants. *Blood.* 93:1684-1696.

Cramer, Louise P., Margaret Siebert and Timothy J. Mitchison. 1997. Identification of novel graded polarity actin filament bundles in locomoting heart fibroblasts: implications for the generation of motile force. *J. Cell Biol.* 136:1287-1305.

Crisa, Laura, Vincenzo Cirulli, Mark H. Ellisman, Jennifer K. Ishii, Mariano J. Elices and Daniel R. Salomon. 1996. Cell adhesion and migration are regulated at distinct stages of thymic T cell development: The roles of fibronectin, VLA4 and VLA5. *J. Exp. Med.* 184:215-228.

Cronstein, Bruce N., Yair Molad, Joan Reibman, Edmond Balakhane, Richard I. Levin and Gerald Weissmann. 1995. Colchicine alters the quantitative and qualitative display of selectins on endothelial cells and neutrophils. *J. Clin. Invest.* 96:995-1002.

Cunningham, C. Casey. 1992. Actin structural proteins in cell motility. *Cancer Metastasis Rev.* 11:69-77.

Dairaghi, Daniel J., Karin Franz-Bacon, Eleni Callas, James Cupp, Thomas J. Schall, Susan A. Tamraz, Stefan A. Boehme, Naomi Taylor and Kevin B. Bacon. 1998 Macrophage inflammatory protein-1β induces migration and activation of human thymocytes. *Blood* 91:2905-2913.

Damsky, Caroline H. and Zena Werb. 1992. Signal transduction by integrin receptors for extracellular matrix: cooperative processing of extracellular information. *Curr. Biol.* 4:772-781.

Dardenne, Mireille and Wilson Savino. 1994. Control of thymus physiology by peptidic hormones and neuropeptides. *Immunol. Today* 11:518-523.

Deckert, Marcel, Michel Ticchioni and Alain Bernard. 1996. Endocytosis of GPI-anchored proteins in human lymphocytes: Role of glycolipid-based domains, actin cytoskeleton and protein kinases. *J. Cell Biol.* 133:791-799.

De Mello-Coelho, Valéria, Wilson Savino, Marie-Catherine Postel-Vinay and Mireille Dardenne. 1998. Role of prolactin and growth hormone on thymus physiology. Dev. Immunol. 6:317-323.

Dianzani, Umberto and Fabio Malavasi. 1995. Lymphocyte adhesion to endothelium. *Crit. Rev. Immunol.* 15:167-200.

del Pozo, Miguel Angel, Leo S. Price, Nazilla B. Alderson, Xiang-Dong Ren and Martin Alexander Schwartz. 2000. Adhesion to the extracellular matrix regulates the coupling of the small GTPase Rac to its effector PAK. *EMBO J.* 19:2008-2014.

del Pozo, Miguel Angel, Miguel Vicente-Manzanares, Reyes Tejedor, Juan Manuel Serrador and Francisco Sánchez-Madrid. 1999. Rho GTPases control migration and polarization of adhesion molecules and cytoskeletal ERM components in T lymphocytes. *Eur. J. Immunol.* 29:3609-3620.

del Pozo, Miguel Angel, Carlos Cabañas, María C. Montoya, Ann Ager, Paloma Sanchez-Mateos and Francisco Sánchez-Madrid. 1997. ICAMs redistributed by chemokines to cellular uropods as a mechanism for recruitment of T lymphocytes. *J. Cell Biol.* 137:493-508.

del Pozo, Miguel, Paloma Sánchez-Mateos, Marta Nieto and Francisco Sánchez-Madrid. 1995. Chemokines regulate cellular polarization and adhesion receptor redistribution during lymphocyte interaction with endothelium and extracellular matrix. Involvement of cAMP signaling pathway. *J. Cell Biol.* 131:495-508.

Detmers, Patricia A., Dahua Zhou, Darius Powell, Henri Lichenstein, Michael Kelley and Rossitza Pironkova. 1995. Endotoxin receptors (CD14) are found with CD16

(FcγRIII) in an intracellular compartment of neutrophils that contains alkaline phosphatase. *J. Immunol.* 155:2085-2095.

Dowthwaite, Gary P., Jo C. W. Edwards and Andrew A. Pitsillides. 1998. An essential role for the interaction between hyaluronan and hyaluronan binding proteins during joint development. *J. Histochem. Cytochem.* 46:641-651.

D'Souza-Schorey, Benjamin Boettner and Linda van Aelst. 1998. Rac regulates integrin-mediated spreading and increased adhesion of T lymphocytes. *Mol. Cell. Biol.* 18:3936-3946.

Dunon, Dominique, Luca Piali and Beat A. Imhof. 1996. To stick or not to stick: the new leukocyte homing paradigm. *Curr. Opin. Cell Biol.* 8:714-723.

Dunon, Dominique and Beat A. Imhof. 1993. Mechanisms of thymus homing. *Blood* 81:1-8.

Eddy, Robert J., Lynda M. Pierini, Fumio Matsumura and Frederick R. Maxfield. 2000. Ca2+-dependent myosin II activation is required for uropod retraction during neutrophil migration. *J. Cell Science* 113:1287-1298.

Ellmeier, Wilfred, Shinichiro Sawada and Dan R. Littman. 1999. The regulation of CD4 and CD8 coreceptor gene expression during T cell development. *Annu. Rev. Immunol.* 17:523-554.

Entschladen, Frank, Matthias Gunzer, Chi Mi Scheuffele, Bernd Niggemann and Kurt S. Zänker. 2000. T lymphocytes and neutrophil granulocytes differ in regulatory signaling and migratory dynamics with regard to spontaneous locomotion and chemotaxis. *Cell. Immunol.* 199:104-114.

Entschladen, Frank, Bernd Niggemann, Kurt Zänker and Peter Friedl. 1997. Differential requirement of protein tyrosine kinases and protein kinase C in the regulation of T cell locomotion in three-dimensional collagen matrices. *J. Immunol.* 159:3203-3210.

Entwistle, Joycelyn, Christine L. Hall and Eva A. Turley. 1996. HA receptors: regulators of signaling to the cytoskeleton. *J. Cell. Biochem.* 61:569-577.

Euteneuer, Ursula and Manfred Schliwa. 1984. Persistent, directional motility of cells and cytoplasmic fragments in the absence of microtubules. Nature 310:58-61.

Faull, Randall J., Nichols L. Kovach, John M. Harlan and Mark Ginsberg. 1994. Stimulation of integrin-mediated adhesion of T lymphocytes and monocytes: two mechanisms with divergent biological consequences. *J. Exp. Med.* 179:1307-1316.

Fieber, Christina, Ria Plug, Jonathon Sleeman, Peter Dall, Helmut Ponta and Martin Hofmann. 1999. Characterization of the murine gene encoding the intracellular hyaluronan receptor IHABP (RHAMM). *Gene* 226:41-50.

Fine, Jay S. and Ada M. Kruisbeek. 1991. The role of LFA-1/ICAM-1 interactions during murine T lymphocyte development. *J. Immunol.* 147:2852-2859.

Franz-Bacon, Karin, Daniel J. Dairaghi, Stefan A. Boehme, Susan K. Sullivan, Thomas J. Schall, Paul J. Conlon, Naomi Taylor and Kevin B. Bacon. 1999. Human thymocytes express CCR-3 and are activated by eotaxin. *Blood* 10: 3233-3240.

Fraser, J. R. E., T. C. Laurent and U. B. G. Laurent. 1997. Hyaluronan: its nature, distribution, functions and turnover. *J. Internal Med.* 242:27-33.

Friedl, Peter, Frank Entschladen, Christoph Conrad, Bernd Niggemann and Kurt S. Zänker. 1998. CD4$^+$ T lymphocytes migrating in three-dimensional collagen lattices lack focal adhesions and utilize β1 integrin-independent strategies for polarization, interaction with collagen fibers and locomotion. *Eur. J. Immunol.* 28:2331-2343.

Friedl, Peter, Peter B. Noble and Kurt S. Zänker. 1995. T lymphocyte locomotion in a three-dimensional collagen matrix. *J. Immunol.* 154:4973-4985.

Galy, Anne, Sunita Verma, Alicia Bárcena and Hergen Spits. 1993. Precursors of CD3$^+$CD4$^+$CD8$^+$ cells in the human thymus are defined by expression of CD34. Delineation of early events in human thymic development. *J. Exp. Med.* 178:391-401.

Gares, Sheryl L. and Linda M. Pilarski. 1999. Beta$_1$-integrins control spontaneous adhesion and motility of human progenitor thymocytes and regulate differentiation-dependent expression of the receptor for hyaluronan-mediated motility. *Scand. J. Immunol.* 50:626–634.

Gares, Sheryl L., Nadia Giannakopoulos, Donna MacNeil, Randall J. Faull and Linda M. Pilarski. 1998. During human thymic development, β1 integrins regulate adhesion, motility and the outcome of RHAMM/hyaluronan engagement. *J. Leuk. Biol.* 64:781–790.

Garnotel, Roselyne, Jean-Claude Monboisse, Alain Randoux, Bernard Haye and Jacques Paul Borel. 1995. The binding of type I collagen to lymphocyte function-associated antigen (LFA) 1 integrin triggers the respiratory burst of human polymorphonuclear neutrophils. *J. Biol. Chem.* 270:27495-27503.

Hall, Alan. 1998. Rho GTPases and the actin cytoskeleton. *Science* 279:509-514.

Hall, C. L., L. A. Lange, D. A. Prober, S. Zhang and E. A. Turley. 1996. pp60$^{c\text{-src}}$ is required for cell locomotion regulated by the hyaluronan receptor RHAMM. *Oncogene.* 13:2213-2224.

Hall, Christine L., Baihua Yang, Xuiwei Yang, Shiwen Zhang, Maureen Turley, Shanti Samuel, Laurie Lange, Chao Wang, Genevieve D. Curpen, Rashmin Savani, Arnold H. Greenberg and Eva A. Turley. 1995. Overexpression of the hyaluronan receptor RHAMM is transforming and is also required for H-*ras* transformation. *Cell.* 82:19-28.

Hall, Christine L., Chao Wang, Laurie A. Lange and Eva A. Turley. 1994. Hyaluronan and the hyaluronan receptor RHAMM promote focal adhesion turnover and transient tyrosine kinase activity. *J. Cell Biol.* 126:575-588.

Halvorson, Mark J., William Magner and John E. Coligan. 1998. α4 and α5 integrins costimulate the CD3-dependent proliferation of fetal thymocytes. *Cell. Immunol.* 189:1-9.

Hardwick, C., K. Hoare, R. Owens, H. P. Hohn, M. Hook, D. Moore, V. Cripps, L. Austen, D. M. Nance and E. A. Turley. 1992. Molecular cloning of a novel hyaluronan receptor that mediates tumor cell motility. *J. Cell Biol.* 117:1343-1350.

Harlow, E. and D. Lane. 1988. Antibodies: a laboratory manual. Cold Spring Harbor Laboratory, Cold Spring Harbor, NY. pp 298-299.

Harris H. and M. Miyasaka. 1995. Reversible stimulation of lymphocyte motility by cultured high endothelial cells: mediation by L-selectin. *Immunol.* 85:47-54.

Haynes, Barton F. and Laura P. Hale. 1998. The human thymus. *Immunol. Res.* 18:175-192.

Haynes, Barton F. 1986. The role of the thymic microenvironment in promotion of early stages of human T cell maturation. *Clin. Res.* 34:422-431.

Haynes, Barton F. 1984 The human thymic microenvironment. *Adv. Immunol.* 36:87-141.

Hirsch, Emilio, Antonio Iglesias, Alexandre J. Potocnik, Ursula Hartmann and Reinhard Fassler. 1996. Impaired migration but not differentiation of haematopoietic stem cells in the absence of $\beta 1$ integrins. *Nature* 380:171-175.

Hofmann, Martin, Christina Fieber, Volker Assmann, Martin Göttlicher, Jonathon Sleeman, Ria Plug, Norma Howells, Oliver von Stein, Helmut Ponta and Peter Herrlich. 1998. Identification of IHABP, a 95 kda intracellular hyaluronate binding protein. *J. Cell Science.* 111:1673-1684.

Hollander, Georg A., Baoping Wang, Aliki Nichogiannopoulou, Peter Paul Platenburg, Willem van Ewijk Steven J. Burakoff, Jose-Carlos Gutierrez-Ramos and Cox Terhorst. 1995. Developmental control point in the induction of thymic cortex regulated by a subpopulation of prothymocytes. *Nature* 373:350-353.

Hotchin, Neil A. and Alan Hall. 1995. The assembly of integrin adhesion complexes requires both extracellular matrix and intracellular rho/rac GTPases. *J. Cell Biol.* 131:1857-1865.

Imhof, Beat A., Dheepika Weerasinghe, Eric J. Brown, F. Lindberg, P. Hamel, L. Perali, M. Dressing, and Ronald H. Gisler. 1997. Crosstalk between $\alpha v \beta 3$ and $\alpha 4 \beta 1$

integrin regulates lymphocyte migration on vascular cell adhesion molecule 1. *Eur. J. Immunol.* 27:3242-3252.

Kaverina, Irena, Klemens Rottner and J. Victor Small. 1998. Targeting, capture, and stabilization of microtubules at early focal adhesions. *J. Cell Biol.* 142:181-190.

Killeen, Nigel, Bryan A. Irving, Susanne Pippig and Kurt Zingler. 1998. Signaling checkpoints during the development of T lymphocytes. *Curr. Opin. Immunol.* 10:360-367.

Kisielow, Pawel and Harald von Boehmer. 1995. Development and selection of T cells: facts and puzzles. Adv Immunol. 58:87-209.

Klewes, Ludger, Eva A. Turley and Peter Prehm. 1993. The hyaluronate synthase from a eukaryotic cell line. *Biochem J.* 290:791-795.

Knudson, Cheryl B. and Warren Knudson. 1993. Hyaluronan-binding proteins in development, tissue homeostasis and disease. *FASEB J.* 7:1233-1241

Kornovski, Barbara S., John McCoshen, Jeremy Kredentser and Eva Turley. 1994. The regulation of sperm motility by a novel hyaluronan receptor. *Fertil. Steril.* 61:935-940

Kraft, Daniel L., Irving L. Weissman and Edmund K. Waller. 1993 Differentiation of CD3⁻4⁻8⁻ human fetal thymocytes in vivo: characterization of a CD3⁻4⁺8⁻ intermediate. *J. Exp. Med.* 178:265-277.

Kuntz, Rebecca M. and Mark Saltzman. 1997. Neutrophil motility in extracellular matrix gels: mesh size and adhesion affect speed of migration. *Biophys. J.* 72:1472-1480.

Kyewski, Bruno A. 1987. Seeding of thymic microenvironments defined by distinct thymocyte-stromal cell interactions is developmentally controlled. *J. Exp. Med.* 166:520-538.

Lafrenie, Robert M. and Kenneth Yamada. 1996. Integrin-dependent signal transduction. *J. Cell. Biochem.* 61:543-553.

Lagrota-Cândido, Jussara M., Déa Maria Serra Villa-Verde, Flavio H. Vanderlei Jr. and Wilson Savino. 1996. Extracellular matrix components of the mouse thymus microenvironment. V. Interferon-γ modulates thymic epithelial cell/thymocyte interactions via extracellular matrix ligands and receptors. *Cell. Immunol.* 170:235-244.

Lannes-Vieira Joseli, Mireille Dardenne and Wilson Savino. 1991. Extracellular matrix components of the mouse thymus microenvironment: ontogenetic studies and modulation by glucocorticoid hormones. *J. Histochem. Cytochem.* 39:1539-1546.

Laudanna, Carlo, James J. Campbell and Eugene C. Butcher. 1996. Role of Rho in chemoattractant-activated leukocyte adhesion through integrins. *Science* 271:981-983.

Lauffer, Terri M., Jennifer DeKoning, Jay S. Markowitz, David Lo and Laurie Glimcher. 1996. Unopposed positive selection and autoreactivity in mice expressing class II MHC only on thymic cortex. *Nature* 383:81-85.

Lauffenburger, Douglas A. and Alan F. Horwitz. 1996. Cell migration: a physically integrated process. *Cell* 84:359-369.

Laurent, Torvard C., Ulla B. G. Laurent and J. Robert E. Fraser. 1996. The structure and function of hyaluronan. *Immunol. Cell Biol.* 74:A1-A7.

Lawson, Moira A. and Frederick R. Maxfield. 1995. Ca^{2+} and calcineurin-dependent recycling of an integrin to the front of migrating neutrophils. Nature 377:75-79.

Lee, M. G., S. O. Sharrow, A. G. Farr, A. Singer and M. C. Udey. 1994. Expression of the homotypic adhesion molecule E-cadherin by immature murine thymocytes and thymic epithelial cells. *J. Immunol.* 152:5653.

Legg, James W. and Clare M. Isacke. 1998. Identification and functional analysis of the ezrin-binding site in the hyaluronan receptor CD44. *Curr. Biol.* 8:705-708.

Lesley, Jayne, Nicole Howes, Astrid Perschl and Robert Hyman. 1994. Hyaluronan binding function of CD44 is transiently activated on T cells during an *in vivo* immune response. *J. Exp. Med.* 180:383-387.

Lesley, Jayne, Paul W. Kincade and Robert Hyman. 1993. Antibody-induced activation of the hyaluronan receptor function of CD44 requires multivalent binding by antibody. *Eur. J. Immunol.* 23:1902-1909.

Mackay, Deborah J. G., Fred Esch, Heinz Furthmayr and Alan Hall. 1997. Rho- and Rac-dependent assembly of focal adhesion complexes and actin filaments in permeabilized fibroblasts: an essential role for ezrin/radixin/moesin proteins. *J. Cell Biol.* 138:927-938.

Mandeville, John T. H., Moira A. Lawson and Frederick R. Maxfield. 1997. Dynamic imaging of neutrophil migration in three dimensions: mechanical interactions between cells and matrix. *J. Leuk. Biol.* 61:188-200.

Masellis-Smith, A., A. R. Belch, M. J. Mant, E. A. Turley and L. M. Pilarski. 1996. Hyaluronan- dependent motility of B cells and leukemic plasma cells in blood, but

not of bone marrow plasma cells, in multiple myeloma: alternate use of receptor for hyaluronan-mediated motility (RHAMM) and CD44. *Blood* 87:1891-1899.

Mermall, Valerie, Penny L. Post and Mark S. Mooseker. 1998. Unconventional myosins in cell movement, membrane traffic, and signal transduction. *Science* 279:527-532.

Mitchison, T. J. and L. P. Cramer. 1996. Actin-based cell motility and cell locomotion. *Cell* 84:371-379.

Mojcik, Christopher F., Daniel R. Salomon, Andrew C. Chang and Ethan M. Shevach. 1995. Differential expression of integrins on human thymocyte subpopulations. *Blood* 86:4206-4217.

Nabi, Ivan R. 1999. The polarization of the motile cell. *J. Cell Science.* 112:1803-1811.

Nagy, J., I. J. Hacking, U. N. Frankenstein and E. A. Turley. 1995. Requirement of the hyaluronan receptor RHAMM in neurite extension and motility as demonstrated in primary neurons and neuronal cell lines. *J. Neuroscience.* 15:241-252.

Niggli, Verena. 1999. Rho-kinase in human neutrophils: a role in signaling for myosin light chain phosphorylation and cell migration. *FEBS Letters* 445:69-72.

Nieto, Marta, José M. R. Frade, David Sancho, Mario Mellado, Carlos Martinez-A and Francisco Sánchez-Madrid. 1997. Polarization of chemokine receptors to the leading edge during lymphocyte chemotaxis. *J. Exp. Med.* 186:153-158.

Nikolai, G., B. Niggemann, M. Werner and K. S. Zanker. 1999. Colcemid but not taxol modulates the migratory behavior of human T lymphocytes within 3-D collagen lattices. *Immunobiol.* 201:107-119.

Nobes, Catherine D. and Alan Hall. 1995. Rho, Rac, and Cdc42 GTPases regulate the assembly of multimolecular focal complexes associated with actin stress fibers, lamellipodia and filopodia. *Cell* 81:53-62.

Oehen, S., L. Feng, Y. Xia, C. D. Suh and S. M. Hedrick. Antigen compartmentation and T helper cell tolerance induction. *J. Exp. Med.* 183:2617-2626.

Palacek, Sean P., Joseph C. Loftus, Mark H. Ginsberg, Douglas Lauffenburger and Alan F. Horwitz. 1997. Integrin-ligand binding properties govern cell migration speed through cell-substratum adhesiveness. *Nature.* 385:537-540.

Parent, Carole A. and Peter N. Devreotes. 1999. A cell's sense of direction. *Science* 284:765-770.

Parolini, I., M. Sargiacomo, M. P. Lisanti and C. Peschle. 1996. Signal transduction and glycophosphatidylinositol-linked proteins (LYN, LYK, CD4, CD45, G proteins and CD55) selectively localize in triton-insoluble plasma membrane domains of human leukemic cell lines and normal granulocytes. *Blood.* 87:3783-3794.

Patel, Dhavalkumar D., Laura P. Hale, Leona P. Whichard, Gilbert Radcliff, Charles R. Mackay and Barton F. Haynes. 1995. Expression of CD44 molecules and CD44 ligands during human thymic fetal development: expression of CD44 isoforms is developmentally regulated. *Int. Immunol.* 7:277-286.

Perschl, Astrid, Jayne Lesley, Nicole English, Ian Trowbridge and Robert Hyman. 1995. Role of CD44 cytoplasmic domain in hyaluronan binding. *Eur. J. Immunol.* 25:495-501.

Pierini, Lynda M., Moira A. Lawson, Robert J. Eddy, Bill Hendey and Frederick R. Maxfield. 2000. Oriented endocytic recycling of $\alpha5\beta1$ in motile neutrophils. *Blood* 95:2471-2481.

Pilarski, L. M., S. L. Gares, E. Pruski, D. Paine and J. Wisniak. 7th Human Leukocyte Differentiation Antigen Workshop. In Press.

Pilarski, Linda M., Eva Pruski, Juanita Wisniak, Darlene Paine, Karen Seeberger, Michael J. Mant, Chris B. Brown and Andrew R. Belch. 1999. Potential role for hyaluronan and the hyaluronan receptor RHAMM in mobilization and trafficking of hematopoietic progenitor cells. *Blood* 93:2918-2927.

Pilarski, Linda M., Helena Miszta and Eva A. Turley. 1993. Regulated expression of a receptor for hyaluronan-mediated motility on human thymocytes and T cells. *J. Immunol.* 150:4292-4302.

Pilarski, Linda M. 1993a. Adhesive interactions in thymic development: does selective expression of CD45 isoforms promote stage-specific microclustering in the assembly of functional adhesive complexes on differentiating T lineage lymphocytes? *Immunol. Cell Biol.* 71:59-69.

Pilarski, Linda M. 1993b. Antigen-independent adhesive interactions in thymic development: implications for cell type-specific function. *In*: Lymphocyte Adhesion Molecules. Ed. Y. Shimizu. R. G. Landes Co. Austin, TX. Pp221-248

Porter, Joanna C. and Nancy Hogg. 1997. Integrin cross talk: activation of lymphocyte function-associated antigen-1 on human T cells alters $\alpha4\beta1$- and $\alpha5\beta1$-mediated function. *J. Cell Biol.* 138:1437-1447.

Ratner, Stuart, Wilbert S. Sherrod and Darcy Lichlyter. 1997. Microtubule retraction into the uropod and its role in T cell polarization and motility. *J. Immunol.* 159:1063-1067.

Ratner, Stuart. 1992. Lymphocyte migration through extracellular matrix. *Invasion Metastasis* 12:82-100.

Reinhardt, Paul H., Christopher A. Ward, Wayne R. Giles and Paul Kubes. 1997a. Emigrated rat neutrophils adhere to cardiac myocytes via $\alpha4$ integrin. *Circ. Res.* 81:196-201.

Reinhardt, Paul H., John F. Elliott and Paul Kubes. 1997b. Neutrophils can adhere via $\alpha_4\beta_1$-integrin under flow conditions. *Blood* 89:3837-3846.

Res, Pieter and Hergen Spits. 1999. Developmental stages in the human thymus. *Sem. Immunol.* 11:39-46.

Reya, Tannishtha, Hamid Bassiri, Renée Biancaniello and Simon Carding. 1998. Thymic stromal-cell abnormalities and dysregulated T-cell development in IL2-deficient mice. *Dev. Immunol.* 5:287-302.

Ritter, Mary A. and Richard L. Boyd. 1993. Development in the thymus: it takes two to tango. *Immunol. Today.* 14:462-469.

Rodewald, Hans-Reimer and Hans Jörg Fehling. 1998 Molecular and cellular events in early thymocyte development. *Adv. Immunol.* 69: 1-112.

Rudzki, Z. and S. Jothy. 1997. CD44 and the adhesion of neoplastic cells. *Mol. Pathol.* 50:57-71.

Salomon, Daniel R., Laura Crisa, Christopher F. Mojcik, Jennifer K. Ishii, George Klier and Ethan M. Shevach. 1997. Vascular cell adhesion molecule-1 is expressed by

cortical thymic epithelial cells and mediates thymocytes adhesion, implications for the function of α4β1 (VLA4) integrin in T cell development. *Blood* 89:2461-2471.

Salomon, Daniel R., Christopher F. Mojcik, Andrew C. Chang, Scott Wadsworth, David H. Adams, John E. Coligan and Ethan M. Shevach. 1994. Constitutive activation of integrin α4β1 defines a unique stage of human thymocyte development. *J. Exp. Med.* 179:1573-1584.

Salomon, D. 1991. Labeling antibody with fluorescein isothiocyanate (FITC). *In* Current Protocols in Immunology. J. E. Coligan, A. M. Kruisbeek, D. H. Margulies, E. M. Shevach and W. Strober, editors. Greene Publishing & Wiley-Interscience, New York. 5.3.2, Supplement 1

Samuel, Shanti K., Robert A. R. Hurta, Maureen A. Spearman, Jim A. Wright, Eva A. Turley and Arnold H. Greenberg. 1993. TGF-β$_1$ stimulation of cell locomotion utilizes the hyaluronan receptor RHAMM and hyaluronan. *J. Cell Biol.* 123:749-758.

Sánchez-Madrid, Francisco and Miguel Angel del Pozo. 1999. Leukocyte polarization in cell migration and immune interactions. *EMBO J.* 18:501-511.

Savani, Rashmin C., Chao Wang, Baihua Yang, Shiwen Zhang, Michael G. Kinsella, Thomas N. Wight, Robert Stern, Dwight M. Nance and Eva A. Turley. 1995. Migration of bovine aortic smooth muscle cells after wounding injury: The role of hyaluronan and RHAMM. *J. Clin. Invest.* 95:1158-1168.

Savino, Wilson, Déa Maria Serra Villa-Verde, Luiz Anastácio Alves and Mireille Dardenne. 1998. Neuroendocrine control of the thymus. *Ann. NY Acad Sci.* 840:470-479.

Savino, Wilson. 1996. The conveyer belt model for intrathymic T-cell migration. *Immunol. Today.* 17:97-98.

Savino, Wilson, Déa Maria S. Villa-Verde and Joseli Lannes-Vieira. 1993. Extracellular matrix proteins in intrathymic T-cell migration and differentiation? *Immunol. Today.* 14:158-161.

Sawada, Motoyuki, Jun Nagamine, Kiyoshi Takeda, Keiroh Utsumi, Atsushi Kosugi, Yoichi Tatsumi, Toshiyuki Hamaoka, Kensuke Miyake, Kiichiroh Nakajima, Takushi Watanabe, Shumpei Sakakibara and Hiromi Fujiwara. 1992. Expression of VLA-4 on thymocytes: maturation stage-associated transition and its correlation with their capacity to adhere to thymic stromal cells. *J. Immunol.* 149:3517-3524.

Schmid-Alliana, Annie, Lionel Menou, Serge Manié, Heidy Schmid-Antomarchi, Marie-Ange Millet, Sylvie Giuriato, Bernard Ferrua and Bernard Rossi. 1998. Microtubule integrity regulates src-like and extracellular signal-related kinase activities in human pro-monocytic cells. *J. Biol. Chem.* 273:3394-3400.

Schneider, Helga, K. V. S. Prasad, Steven E. Shoelson and Christopher E. Rudd. 1995. CTLA-4 binding to the lipid kinase phosphatidylinositol 3-kinase in T cells. *J. Exp. Med.* 181:351-355.

Sebzda, Eric, Sanjeev Mariathasan., Toshiaki Ohteki, Russell Jones, Martin F. Bachmann and Pamela S. Ohashi 1999. Selection of the T cell repertoire. *Annu. Rev. Immunol.* 17:829-874

Seipel, Katja, Quintus G. Medley, Nancy L. Kedersha, Xin A. Zhang, Stephen P. O'Brien, Carles Serra-Pages, Martin E. Hemler and Michel Streuli. 1999. Trio amino-terminal guanine nucleotide exchange factor domain expression promotes actin cytoskeleton reorganization, cell migration and anchorage-independent cell growth. *J. Cell Science* 112:1825-1834.

Serrador, Juan M., Marta Nieto, José L. Alonso-Lebrero, Miguel del Pozo, Javier Calvo, Heinz Furthmayr, Reinhard Schwartz-Albiez, Francisco Lozano, Roberto González-Amaro, Paloma Sánchez-Mateos and Francisco Sánchez-Madrid. 1998. CD43 interacts with moesin and ezrin and regulates its redistribution to the uropods o f T lymphocytes at the cell-cell contacts. *Blood* 12:4632-4644.

Serrador, Juan M., José L. Alonso-Lebrero, Miguel del Pozo, Heinz Furthmayr, Reinhard Schwartz-Albiez, Javier Calvo, Francisco Lozano and Francisco Sánchez-Madrid. 1997. Moesin interacts with the cytoplasmic region of intercellular adhesion molecule-3 and is redistributed to the uropod of T lymphocytes during cell polarization. *J. Cell Biol.* 138:1409-1423.

Servant, Guy, Orion D. Weiner, Paul Herzmark, Tamás Balla, John W. Sedat and Henry R. Bourne. 2000. Polarization of chemoattractant receptor signaling during neutrophil chemotaxis. *Science* 287:1037-1040.

Singer, Kay H., Stephen M. Denning, Leona P. Whichard and Barton F. Haynes. 1990. Thymocyte LFA-1 and thymic epithelial cell ICAM-1 molecules mediate binding

of activated human thymocytes to thymic epithelial cells. J. Immunol. 144:2931-2939.

Sherman, L., J. Sleeman, P. Herrlich and H. Ponta. 1994. Hyaluronate receptors: key players in growth, differentiation, migration and tumor progression. *Curr. Opin. Cell Biol.* 6:726-733.

Shortman Ken and Li Wu. 1996. Early T lymphocyte progenitors. *Annu. Rev. Immunol.* 14:29-47.

Shyng, Show-Ling, Mary T. Huber and David A. Harris. 1993. A prion protein cycles between the cell surface and an endocytic compartment in cultured neuroblastoma cells. *J. Biol. Chem.* 21:15922-15928.

Sleeman, Jonathan, Wolfgang Rudy, Martin Hofmann, Jürgen Moll, Peter Herrlich and Helmut Ponta. 1996. Regulated clustering of variant CD44 proteins increases their hyaluronate binding capacity. *J. Cell Biol.* 135:1139-1150.

Small, J. Victor, Irina Kaverina, Olga Krylyshkina and Klemens Rottner. 1999a. Cytoskeleton cross-talk during cell motility. *FEBS letters* 452:96-99.

Small, J. Victor, Klemens Rottner and Irina Kaverina. 1999b. Functional design of the actin cytoskeleton. *Curr. Opin. Cell Biol.* 11:54-60.

Smart, Eric J., David C. Foster, Yun-Shu Ying, Barton A. Kamen and Richard G. W. Anderson. 1994. Protein kinase C activators inhibit receptor -mediated potocytosis by preventing internalization of caveolae. *J. Cell Biol.* 124:307-313.

Smilenov, Lubomir B. Alexei Mikhailov, Robert J. Pelham Jr., Eugene E. Marcantonio and Gregg G. Gundersen. 1999. Focal adhesion motility revealed in stationary fibroblasts. Science 286:1172-1174.

Southern, C., P. C. Wilkinson, K. M. Thorp, L. K. Henderson, M. Nemec and N. Matthews. 1995. Inhibition of protein kinase C results in a switch from a non-motile to a motile phenotype in diverse human lymphocyte populations. *Immunol.* 84:326-332.

Springer, Timothy A. 1994. Traffic signals for lymphocyte recirculation and leukocyte emigration: the multistep paradigm. *Cell* 76:301-314.

Springer, Timothy A. 1990. Adhesion receptors of the immune system. *Nature* 346:425-434.

Stewart, Mairi and Nancy Hogg. 1996. Regulation of leukocyte function: affinity vs avidity. *J. Cell. Biochem.* 61:554-561.

Stossel, Thomas P. 1993. On the crawling of animal cells. *Science* 269:1086-1094.

Stowers, Lisa, Deborah Yelon, Leslie J. Berg and John Chant. 1995. Regulation of the polarization of T cells toward antigen-presenting cells by ras-related GTPase CDc42. *Proc. Natl Acad. Sci.* 92:5027-5031.

Surh, Charles D. and Jonathon Sprent. 1994. T-cell apoptosis detected *in situ* during positive and negative selection. T-cell apoptosis detected *in situ* during positive and negative selection. *Nature* 372:100-103.

Suzuki, Gen, Hirofumi Sawa, Yoshiyasu Kobayashi, Yukiko Nakata, Ken-ichi Nakagawa, Akiko Uzawa, Hisako Sakiyama, Shizuko Kakinuma, Kazuya Iwabuchi and Kazuo Nagashima. 1999. Pertussis toxin-sensitive signal controls the trafficking of thymocytes across the corticomedullary junction in the thymus. *J. Immunol.* 162:5981-5985.

Takahaishi, Kenji, Takuya Sasakü, Takaki Kameyama, Sachiko Tsukita, Shoichiro Tsukita and Yoshimi Takai. 1995. *Oncogene* 11:39-48.

Terstappen, Leon W. M. M., Shian:g Huang and Louis J. Picker. 1992. Flow cytometric assessment of human T-cell differentiation in thymus and bone marrow. *Blood* 79:666-677.

Toole, B. P. 1997. Hyaluronan in morphogenesis. *J. Int. Med.* 242:35-40.

Turley, E. A., L. Austen, D. Moore and K. Hoare. 1993. *Ras*-transformed cell express both CD44 and RHAMM hyaluronan receptors: only RHAMM is essential for hyaluronan-promoted locomotion. *Exp. Cell Res.* 207:277-282.

Turley, E. A. 1992. Hyaluronan and cell locomotion. *Cancer Metastasis. Rev.* 11:21-30.

Turley, E. A., L. Austen, K. Vanıdeligt and C. Clary. 1991. Hyaluronan and a cell-associated hyaluronan binding protein regulate the locomotion of *ras*-transformed cells. *J. Cell Biol.* 112:1041–1047.

Turley, E. A., P. Brassel and D. Moore. 1990. A hyaluronan-binding protein shows a partial and temporally regulated codistribution with actin on locomoting chick heart fibroblasts. *Exp. Cell Res.* 187:243-249.

Turley, E. and N. Auersperg. 1989. A hyaluronate binding protein transiently codistributes with p21^{k-ras} in cultured cell lines. *Exp. Cell Res.* 182:340-348.

Turley, E. A. 1989. The role of a cell-associated hyaluronan-binding protein in fibroblast behavior. *In* The biology of Îhyaluronan. Ciba Foundation Symposium pp. 121-137

Turley, E. A., D. Moore and L. J. Hayden. 1987. Characterization of hyaluronate binding proteins isolated from 3T3 and murine sarcoma virus transformed 3T3 cells. *Biochem.* 26:2997-3005.

Turley, E. A. and J. Torrance. 1985. Localization of hyaluronate and hyaluronate-binding protein on motile and non-motile fibroblasts. *Exp. Cell Res.* 161:17-28.

Utsumi, Keioh, Motoyuki Sawada, Seiji Narumiya, Jun Nagamine, Tsuneaki Sakata, Shoji Iwagami, Yasumichi Kita, Hiroshi Teraoka, Hideyasu Hirano, Masato Ogata, Toshiyuki Hamaoka and Hiromi Fujiwara. 1991. Adhesion of immature thymocytes to thymic stromal cells through fibronectin molecules and its significance for the induction of thymocyte differentiation. *Proc. Natl. Acad. Sci.* 88:5685-5689.

Vachula, Mona and Dennis E. van Epps. 1992. In vitro models of lymphocyte transendothelial migration. *Invasion Metastasis* 12:66-81.

van Ewijk, W., Shores, E. W. and Singer, A. 1994. Crosstalk in the mouse thymus. *Immunol. Today* 15:214-217.

Vasiliev, J. M. 1991. Polarization of pseudopodial activities: cytoskeletal mechanisms. *J. Cell Science* 98:1-4.

Volkov, Yuri, Aideen Long and Dermot Kelleher. 1998. Inside the crawling T cell: leukocyte function-associated antigen-1 cross-linking is associated with microtubule-directed translocation of protein kinase C isoenzymes $\beta(I)$ and δ. *J. Immunol.* 161:6487-6495.

von Boehmer, Harald. 1990. Developmental biology of T cells in T cell receptor transgenic mice. *Annu. Rev. Immunol.* 8:531-553.

Wadsworth, Scott, Mark J. Halvorson and John E. Coligan. 1992. Developmentally regulated expression of the $\beta 4$ integrin on immature mouse thymocytes. *J. Immunol.* 149:421-428.

Wang, Chao, Ann D. Thor, Dan H. Moore II, Yong Zhao, Russell Kerschmann, Robert Stern, Peter H. Watson and Eva. A. Turley. 1998. The overexpression of RHAMM, a hyaluronan-binding protein that regulates ras signaling, correlates with overexpression of mitogen-activated protein kinase and is a significant parameter in breast cancer progression. Clin. Cancer Res. 4:567-576.

Wang, Chao, Joycelyn Entwistle, Guangpei Hou, Quan Li and Eva A. Turley. 1996. The characterization of a human RHAMM cDNA: conservation of the hyaluronan-binding domains. *Gene.* 174:299-306.

Waterman-Storer Clare M. and E. D. Salmon. 1999. Positive feedback interactions between microtubule and actin dynamics during cell motility. *Curr. Opin Cell Biol.* 11:61-67.

Watt, Suzanne M., J. Alero Thomas, Andrew J. Edwards, Sarah J. Murdoch and Michael Horton. 1992. Adhesion receptors are differentially expressed on developing thymocytes and epithelium in human thymus. *Exp. Hematol.* 20:1101-1111.

Weber, Christian and Timothy A. Springer. 1998. Interaction of very late antigen-4 with VCAM-1 supports transendothelial chemotaxis of monocytes by facilitating lateral migration. *J. Immunol.* 161:6825-6834.

Weber, Kim S. C., Lloyd B. Klickstein, Peter C. Weber and Christian Weber. 1998. Chemokine-induced monocyte transmigration requires Cdc-42-mediated cytoskeletal changes. *Eur. J. Immunol.* 28:2245-2251.

Weber, Christian, Ronen Alon, Bernhard Moser and Timothy A. Springer. 1996. Sequential regulation of $\alpha 4\beta 1$ and $\alpha 5\beta 1$ integrin avidity by CC chemokines in

monocytes: implications for transendothelial chemotaxis. *J. Cell Biol.* 134:1063-1073.

Weerasinghe, Dheepika, Kevin P. McHigh, Frederick P. Ross, Eric J. Brown, Roland H. Gisler and Beat A. Imhof. 1998. A role for the $\alpha v \beta 3$ integrin in the transmigration of monocytes. *J. Cell Biol.* 142:595-607.

Werr, Joachim, Joakim Johansson, Einar E. Eriksson, Per Hedqvist, Erkki Ruoslahti and Lennart Lindbom. 2000. Integrin $\alpha 2 \beta 1$ (VLA-2) is a principal receptor used by neutrophils for locomotion in extravascular tissue. *Blood* 95:1804-1809.

Werr, Joachim, Xun Xie, Per Hedqvist, Erkki Ruoslahti and Lennart Lindbom. 1998. $\beta 1$ integrins are critically involved in neutrophil locomotion in extravascular tissue in vivo. *J. Exp. Med.* 187:2091-2096.

Wilkinson, P. C. 1998. Assays of leukocyte locomotion and chemotaxis. *J. Immunol. Methods* 216:139-153.

Williams, Mark A. and Joseph S. Solomkin. 1999. Integrin-mediated signaling in human neutrophil functioning. *J. Leuk. Biol.* 65:725-736.

Yang, Baihua, Bing Luo Yang, Rashmin C. Savani and Eva A. Turley. 1994. Identification of a common hyaluronan binding motif in the hyaluronan binding proteins RHAMM, CD44 and link protein. *EMBO J.* 13:286-296.

Yang, Baihua, Liying Zhang and Eva A. Turley. 1993. Identification of two hyaluronan-binding domains in the hyaluronan receptor RHAMM. *J. Biol. Chem.* 268:8617-8623.

Zaballos, Ángel, Julio Gutiérrez, Rosa Varona, Carlos Ardavín and Gabriel Márquez. 1999. Identification of the orphan chemokine receptor GPR-9-6 as CCR9, the receptor for the chemokine TECK. *J. Immunol.* 162:5671-5675.

Zaitseva, Marina B., Shirley Lee, Ronald L. Rabin, H. Lee Tiffany, Joshua M. Farber, Keith W. C. Peden, Philip M. Murphy and Hana Golding. 1998. CXCR4 and CCR5 on human thymocytes: Biological function and role in HIV-1 infection. *J. Immunol.* 161:3103-3113.

Zhang, Wei V., Yi Yang, Randal W. Berg, Euphemia Leung and Geoffrey W. Krissansen. 1999. The small GTP-binding proteins Rho and Rac induce T cell adhesion to the mucosal addressin MAdCAM-1 in a hierarchal fashion. *Eur. J. Immunol.* 29:2875-2885.

Zhang, Shiwen, Michael C. Y. Chang, Danuta Zylka, Stefanie Turley, Rene Harrison and Eva A. Turley. 1998. The hyaluronan receptor RHAMM regulates extracellular-regulated kinase. *J. Biol. Chem.* 273:11342-11348.

Zhang, Y. and J. P. Allison. 1997. Interaction of CTLA-4 with AP50, a clathrin-coated pit adaptor protein. *Proc. Nat. Acad. Sci.* 94:9273-9278.

Zigmond, Sally H., Hyam I. Levitsky and Barbara J. Kreel. 1981. Cell polarity: an examination of its behavioral expression and its consequences for polymorphonuclear leukocyte chemotaxis. *J. Cell Biol.* 89:585-592.